The copyright of this thesis vests in the author. No quotation from it or information derived from it is to be published without full acknowledgement of the source. The thesis is to be used for private study or non-commercial research purposes only.

Published by the University of Cape Town (UCT) in terms of the non-exclusive license granted to UCT by the author.

University of Cape Town

Metal sulphide precipitation: effect of operational parameters on particle characteristics and process efficiency

A thesis submitted to the University of Cape Town in fulfilment of the requirements for the degree of

Doctor of Philosophy

by

Thebe Phillip Mokone

University of Cape Town
Yunivesithi yaseKapa • Universiteit van Kaapstad

Department of Chemical Engineering
University of Cape Town

September 2010

This work is dedicated to:

My late father, my mother and four sisters

"Ke leboha lerato, kutluisiso le lithapelo tseo ba ntshehelitseng ka tsona hore ke fihle boemong bona."

University of Cape Town

Acknowledgements

I would like to extend my sincere gratitude towards the following people who all contributed directly or indirectly to the preparation of this thesis.

First and foremost, God Almighty for His guidance and gracious love that carried me up to this point in my life.

Professor Alison Lewis for her supervision and the opportunity she afforded me to be part of this exciting field of research. Dr Rob van Hille, as my co-supervisor for his leadership and his willingness to share his profound expertise. Completion of this work would never have been possible without his inspiring and enthusiastic contribution. I am very grateful for the example he set me in scientific thinking.

Prof Janusz Lawskoski, from University of British Columbia, for the helpful discussions that helped shaped the direction of this study. The Analytical Laboratory staff (past and present) in the Department for the many analyses they helped with. Miranda Waldron from Electron Microscopy Unit at UCT for all the micro-structural analysis. All my fellow postgraduate colleagues and support stuff (past and present) in the Crystallization and Precipitation Unit and the Department of Chemical Engineering. Their support and encouragement kept me going when times where tough. Ms Fran Pocock for always been available to lend an ear when I needed to offload.

My parents, sisters, nephews and nieces for all their love, understanding, patience and support. My beautiful fiancée (Malebo), Palesa and Mokhethoa for always putting a smile on my face and standing by me. I appreciate all the sacrifices they made to help me realise this dream. I would especially like to thank my family as a whole and friends for always believing in me and my dreams.

Last but not least, I wish to thank the National Research Foundation, Water Research Commission and the Department of Labour for their financial support.

University of Cape Town

List of publications

T. P. Mokone, R. P. van Hille, A. E. Lewis (2010) Effect of solution chemistry on particle characteristics during metal sulphide precipitation. *Journal of Colloid and Interface Science*, 351, 10 – 18.

Mokone, T. P., van Hille, R. P., Lewis, A. E. (2009) Mechanisms responsible for particle formation during metal sulphide precipitation process, *International Mine Water Conference*, Pretoria, South Africa.

Mokone, T. P., van Hille, R. P., Lewis, A. E. (2008) Effect of surface properties on solid-liquid separation characteristics of metal sulphides, *Mineral Processing Conference*, Cape Town, South Africa.

Mokone, T. P., van Hille, R. P., Lewis, A. E. (2007) An investigation into the feasibility of metal sulphide precipitation in a seeded fluidised bed reactor and zinc sulphide precipitation using H_2S gas in a bubble column, *Mineral Processing Conference*, Cape Town, South Africa.

University of Cape Town

Abstract

Acid mine drainage (AMD) is one of the major, long-term environmental challenges facing the minerals processing industry. Uncontrolled discharges have polluted thousands of kilometres of rivers, as well as surface and groundwater bodies with acidic effluents high in dissolved metals and sulphate. Conventional treatment technologies rely on oxidation, neutralisation and precipitation. While these may be effective they are expensive and not sustainable in the long term. Several biological treatment technologies, based on the activity of sulphate reducing bacteria (SRB), have been successfully developed and applied at both laboratory and industrial scale. The SRB uses sulphate as the terminal electron acceptor and with a suitable electron donor produce bicarbonate alkalinity and sulphide. These can be used to neutralise acidic effluents and effect precipitation of dissolved metal ions as metal sulphides. However, a number of challenges exist around the precipitation step, particularly where the recovery of valuable metals is desired. Metal sulphide precipitation reactions are inherently driven by extremely high levels of supersaturation. As a result, metal sulphide precipitation reactions are difficult to control and a large number of small particles are formed during the process. This leads to significant technical challenges with respect to solid-liquid separation and subsequent recovery of the precipitate. Despite the theoretically high metal removal, related to the low solubility of metal sulphides, practical efficiency is often significantly lower.

Previous studies have shown that metal precipitation reactions require controlled physico-chemical conditions and the control of high levels of supersaturation to achieve optimum efficiency. The objective of this study was to extend this approach to metal suphide systems. Initial data indicated that conventional techniques to manage supersaturation were not effective and subsequent work focused on characterising the effect of reaction conditions on particle properties and investigating downstream processing options. The intention of this research was to bridge the gap between highly fundamental studies and practical application of sulphide precipitation technologies.

University of Cape Town

To achieve the objectives, precipitation of copper and zinc ions from solution using an aqueous mixture containing sulphide and bicarbonate ions was studied. Initial studies compared metal precipitation using biogenic (generated in SRB reactors) reagents, in the presence and absence of cells and particulate matter, with synthetic (sulphide and bicarbonate salts) solutions. These showed no significant difference so subsequent work was performed using synthetic solutions. Experiments were performed in a laboratory scale, seeded fluidised bed reactor (FBR). Experiments were conducted using two (2FP) and six (6FP) reagent feed points, which had previously been used to manage local supersaturation levels in metal carbonate systems, to investigate the effect on process efficiency and particle characteristics. The results showed that the amount of metal ions precipitated from solution was enhanced due to the buffering effect of the bicarbonate ions. However, the enhanced metal precipitation was obtained at the expense of particle characteristics. Almost 100% of the dissolved zinc ions were precipitated from solution but most of the precipitated metal salt (> 90%) left the reactor in the effluent stream as fine particles. In the case of copper, the amount of dissolved metal ion removed from solution was low (around 40%) due to the formation of very small copper sulphide particles (i.e. mean particle size of ± 0.01 μm). A decrease in the level of supersaturation due to an increase in the amount of reagent feed points was found to have no significant effect on fine particle removal. The amount of zinc sulphide fines recovered from suspension was reduced by ± 10% when 6FP was used in place of 2FP. Under quiescent conditions, the zinc sulphide fines could be effectively recovered from suspension by settling while the copper sulphide fines remained stable in suspension. The copper sulphide particles were found to be highly charged (–50 mV) with a mean particle size of ± 0.01 μm. The zinc sulphide fines, on the other hand, had a mean particle size of ± 5 μm and the charge on the surface of the particles was around –11 mV. The high surface charge on the copper sulphide particles was attributed to an instantaneous reaction between copper and sulphide which resulted in rapid nucleation of a large number of particles that adsorbed the free sulphide available near the reagent inlet points before proper mixing was achieved. The change in recirculation flow rate was found to have a slight effect on the process efficiency, pH and the charge on the surface of the particles. The process efficiency was increased by ± 5% when 120 mL min^{-1} was used for recirculation instead of 300 mL min^{-1}, the pH was increased from pH 7.5 to just above

University of Cape Town

pH 8 and the magnitude of the negative zeta potential was increased from – 10 mV to – 25 mV. An increase in pH and the charge on the surface of the particles was attributed to an increase in free sulphide due to a decrease in the extent to which the reagents were mixed at low flow rate.

To develop a more fundamental understanding into the effect of processing conditions on particle characteristics, copper and zinc sulphide precipitation was conducted in a 900 mL CSTR. Solution characteristics, metal recovery and particle size distribution were monitored over time. These parameters stabilised after 30 minutes, after which the reactor was considered to be in pseudo steady state. Subsequent analyses were performed during this "steady state". The effect of sulphide concentration and speciation on particle characteristics was investigated by varying the stoichiometric metal to sulphide molar ratio and operational pH. A large number (> 1 x 10^{19} particles per m^3) of small copper sulphide particles, with highly negatively charged surfaces (–50 mV) and poor settling characteristics were formed in the presence of a stoichiometric excess of sulphide at pH 6. When the precipitation process was conducted below pH 6, the size and settling characteristics of the particles were significantly improved, while the number of particles and the magnitude of their zeta potential decreased. By comparison, for zinc sulphide, a small change in the number and size of the particles was observed for all metal to sulphide molar ratios and tested operating pH values. Precipitates generated at pH 6 had the most negative zeta potential (– 40 mV), while operating at pH lower than pH 6 reduced the magnitude of the negative surface charge (from – 40 mV to – 25 mV) and improved the settling and dewatering characteristics of the precipitate. The data indicates that the amount of sulphide available in solution and its pH dependent speciation determine the surface charge and nature of particles. The data also suggest there is a threshold potential (i.e. – 40 mV) below which particle aggregation is suppressed and a stable colloidal suspension is obtained.

To investigate the option of downstream processing, copper and zinc precipitates were prepared by sulphide precipitation in a 2 L batch reactor. Characterisation of the produced metal precipitate by XRD and EDAX showed that a mixed precipitate comprising of ± 60% covellite and ± 37 % copper hydroxysulphate was formed

University of Cape Town

during copper sulphide precipitation reaction. The precipitate produced by zinc sulphide precipitation reaction was found to be highly amorphous but contained only zinc sulphide particles. The metal precipitates were suspended in 750 mL of background electrolyte solution (KCl) with concentrations ranging between 1 mM – 100 mM. The effect of suspension pH and the addition of sulphide, a divalent (Ca^{2+}) and trivalent (Al^{3+}) cation on particle characteristics (i.e. surface charge, mean particle size and surface area) was studied. An increase in suspension pH, from pH 6 to pH 11 resulted in an increase in the magnitude of the negative charge on the surface of the particles for both copper and zinc precipitates. This was generally more substantial for zinc, although the magnitude was lower in the 100 mM electrolyte solution due to compression of the electrical double layer at high ionic strength. At pH values below pH 6, the surface charge on the zinc particles tended toward zero, with the point of zero charge around pH 3. For the copper precipitate, reducing the pH below pH 7 had little effect on the zeta potential, which remained between – 25 mV and – 30 mV.

Addition of a small amount of sulphide to the zinc precipitate was found to result in a significant decrease in the zeta potential of the particles, a slight decrease in the mean particle size, and an increase in the surface area of the particles. The magnitude of the negative zeta potential was reduced by ± – 10 mV when 100 mM molar background electrolyte solution was used. In the case of copper, the amount of sulphide which resulted in a significant increase in surface charge was slightly higher due to the consumption of the initially added sulphide by the copper hydroxysulphate component of the precipitate. The significant change in the magnitude of the negative zeta potential was attributed to the adsorption of the negatively charged sulphide species onto the particle surfaces.

The addition of a divalent cation (Ca^{2+}) to the suspension had little effect on the surface charge of the particles and did not result in a substantial change in particle size or surface area. However, addition of a small amount (0.5 mM) of Al^{3+} ions to the copper and zinc precipitate suspensions resulted in a significant change in the zeta potential of the particles, from – 30 to – 10 mV in the case of copper and from – 23 mV to – 5 mV in the case of zinc. This was attributed to the formation of aluminium hydroxy complexes on the surface of the particles.

University of Cape Town

The information presented in this study shows that the characteristics of the particles produced during metal sulphide precipitation processes are strongly affected by the conditions under which the particles are produced. In the case of copper sulphide, the reaction proceeds extremely rapidly, resulting in a large number of very small particles. These form before the sulphide reagent has dispersed and, if sufficient sulphide is present, the negatively charged sulphide species adsorb onto the surface of the particles. This imparts a large negative charge and the particles remain stable in suspension. In the case of zinc, there is an induction time prior to the appearance of discrete particles. The result is more effective dispersal of reagents and less sulphide adsorption to the particles. As a result, zinc sulphide particles carry a lower surface charge and are more likely to aggregate and settle. However, primary nucleation remains the dominant mechanism and little precipitation onto seed material was observed in the FBR. This study has provided a deeper level of understanding to previously reported empirical observations and will help to inform the design and operation of AMD treatment systems.

University of Cape Town

Table of contents

University of Cape Town

University of Cape Town

University of Cape Town

University of Cape Town

List of figures

University of Cape Town

University of Cape Town

University of Cape Town

University of Cape Town

List of tables

University of Cape Town

CHAPTER 1
INTRODUCTION

1. Background

Many industrial processes, especially the mining and metallurgical process industries, produce acidic effluents containing significant amounts of metals. When these metal contaminated wastewaters are exposed to the environment they can cause serious and sometimes permanent ecological damage (Micera and Dessi, 1988). Acid mine drainage (AMD) has been identified as one of the most important environmental problems facing the minerals industry globally (Ribet et al, 1995). AMD is caused by chemical or biologically catalysed oxidation of sulphide minerals upon exposure to atmospheric oxygen and moisture. It is characterised by low pH and elevated concentrations of dissolved heavy metals and sulphate.

Several technologies have been developed for remediation of metal contaminated wastewater (both industrial effluents and AMD) prior to discharge into the environment (Johnson and Hallberg, 2005). Traditionally, chemical precipitation by addition of lime is employed as the primary method for metal removal and acid neutralisation. Although this process in its basic concept is a low technology approach that provides a cost effective solution to treatment of acidic and metal laden effluents, there are a number of problems associated with it (Coulton et al, 2003). The precipitates produced are sensitive to pH and large volumes of sludge are often produced during the process (Bhattacharyya et al, 1981).

In recent years the use of biological treatment processes, based on the activity of sulphate reducing bacteria (SRB), have become more prominent. In these treatment processes, sulphate reducing bacteria generate sulphide and bicarbonate ions through the oxidation of a suitable electron donor and carbon source. The bicarbonate ions are used to neutralise acidic effluents while the sulphide ions are used to effect precipitation of the dissolved metal ions as metal sulphides (Bhagat et al, 2004). Thus far, a substantial amount of work has been devoted to developing a detailed understanding of the biological sulphate reduction process (Dvorak et al, 1992; Chang

University of Cape Town

et al, 2000; Hao et al, 2007; Kaksonen et al, 2003; Oyekola et al, 2009). Several novel treatment technologies, based on the sulphate reduction process, have been successfully developed and implemented at industrial scale (Rowley et al, 1997; Dvorak et al, 1992; Rose et al, 2000; Hulshoff Pol et al, 2001; van Houten et al, 2006; Huismann et al, 2006). However, a number of challenges exist around the precipitation step, particularly where the recovery of valuable metals is desired.

Due to the low solubility of metal sulphides and the high affinity between the reactants, metal sulphide precipitation reactions are inherently driven by very high levels of supersaturation. Consequently, metal sulphide precipitation reactions are difficult to control and a large number of small particles are formed during the process. This leads to significant technical challenges with respect to solid-liquid separation and subsequent recovery of the precipitate. Thus, despite the theoretically high metal removal, due to the low solubility of the resulting metal precipitate, the practical efficiency is often significantly lower. Furthermore, the mechanisms involved in particle formation during metal sulphide precipitation are not well understood and this makes it difficult to relate the effect of processing conditions to product characteristics. According to Demopolous (2009), the correlation between the processing conditions and the product characteristics during precipitation processes is determined and controlled by the solid-liquid equilibria, precipitation kinetics, colloid-surface chemistry and the reactor selection and design. Thus, all these factors need to be considered when studying any precipitating system.

Previous studies have shown that metal precipitation reactions require controlled physico-chemical conditions and effective control of the high levels of supersaturation to produce precipitates with desirable particle characteristics (Franke and Mersmann, 1995; Taty Costodes and Lewis, 2006; Zhou et al, 1999; Seckler et al, 1996). Veeken and coworkers (2003a) studied zinc sulphide precipitation in a continuously stirred tank reactor using controlled sulphide addition at pH 6.5. The study showed that the amount of zinc precipitated from solution and the particle size of the resulting zinc sulphide precipitate were affected by the sulphide concentration present in solution. Al-Tarazi (2004) studied the effect of operating conditions on the particle rate processes involved during metal sulphide precipitation under different regimes of pH, metal to sulphide molar ratio and residence time using a mixed-suspension mixed-

University of Cape Town

product removal (MSMPR) method. The study showed that all these factors had an effect on the particle rate processes, but it was concluded that the MSMPR method was not suitable for studying the particle rate processes involved due to the fast reaction kinetics. Al-Tarazi (2004) also showed that the reactor type, mass transfer and the initial metal concentration have a considerable influence on the morphology of the particles produced. Peters et al (1984), on the other hand, studied metal sulphide precipitation under different operating conditions and tried to model the active particle rate processes using population balance models, which assume only nucleation and growth. The model was found to be unsuitable for this purpose and it was concluded that particle aggregation played an important role in particle size enlargement during the process. Although these studies provide important information regarding the effect of process conditions on efficiency and particle characteristics during metal sulphide precipitation, their relationship is still relatively poorly understood. In addition, the studies conducted on metal sulphide precipitation to date have not taken into account the colloidal nature of the particles produced during the process. Consequently, the effect of colloid-surface chemistry on particle-particle interactions and solid-liquid separation characteristics has not been comprehensively investigated.

To develop a better understanding of the precipitation process and to define the conditions necessary for effective metal precipitation and precipitate recovery, a fundamental study into the relationship between operational conditions and the characteristics of the resulting precipitates is necessary. In the present work, the effect of operating conditions on metal sulphide precipitation efficiency and the characteristics of the particles produced are presented. To provide a comprehensive understanding into the relationship between operational conditions and product characteristics, copper and zinc sulphide precipitation was studied using different sulphide sources, operating pH and metal to sulphide molar ratio. The efficiency of metal precipitation and the characteristics of the particles (i.e. particle size distribution, surface properties and settling characteristics) were used to characterise the process. The option of downstream processing was also investigated by studying the effect of post-precipitation conditions on the surface properties of colloidal particles produced by metal sulphide precipitation.

University of Cape Town

1.1. Thesis outline

This thesis is divided into seven chapters. **Chapter 2** presents a review of the relevant literature and the theory on which this study is based. The chapter starts by highlighting acid mine drainage as an important source of metal contamination and discusses the methods most commonly used to treat metal contaminated wastewater. This is followed by an overview of the crystallization theory of precipitation and the surface chemistry aspects of colloidal particles. The chapter concludes with an extensive review of metal sulphide precipitation, focusing especially on the chemistry of precipitate formation and the factors affecting the process. The experimental methods and materials used in this work are covered in **Chapter 3**. The results of an investigation into the effect of supersaturation control on process efficiency and particle characteristics are presented and discussed in **Chapter 4**. **Chapter 5** describes and discusses an investigation into the effect of reaction conditions on the nature and settling characteristics of the particles produced during metal sulphide precipitation. The study of the effect of post-precipitation conditions on the surface properties of colloidal particles produced by metal sulphide precipitation is presented in **Chapter 6**. The overall conclusions and the areas requiring further investigation are discussed in **Chapter 7**.

University of Cape Town

CHAPTER 2
LITERATURE REVIEW

2. Background

This literature review provides a detailed background to previous work and reviews the theory on which this study is based. The chapter highlights acid mine drainage (AMD) as an important source of metal contamination. AMD generation is described and the methods most commonly used to treat metal contaminated wastewater are briefly reviewed. The crystallization theory of precipitation is reviewed extensively in the context of sparingly soluble compounds, such as metal sulphides. The role of supersaturation in precipitation, different particle rate processes associated with precipitation and the population balance methods used to determine the active particle rate processes in continuous precipitation systems are discussed. The role of surface properties on the suspension stability of colloidal particles is also reviewed. Metal sulphide precipitation is extensively reviewed in the context of effluent treatment, focusing especially on the chemistry of metal sulphide formation and the factors affecting the formation of metal sulphide precipitates.

University of Cape Town

2.1. Acid mine drainage

Acid mine drainage (AMD) refers to acidic water, containing high levels of sulphate and dissolved heavy metals, draining from areas where sulphide bearing minerals have been exposed to atmospheric oxygen and moisture. Due to the high levels of dissolved iron and sulphur, AMD is typically characterised by a rich red-orange or yellow colour. AMD is a major environmental problem for both closed and operational mines where the mining activities have exposed a significant amount of sulphide-bearing minerals. The characteristic composition of AMD (i.e. low pH, high heavy metal concentration and salinity) is detrimental to the environment and its resident life. If discharged untreated, AMD can result in major environmental degradation, human health problems and reduce the quality of fresh water streams (Ledin and Pedersen, 1996).

Reports indicate that AMD affects over 700 km of streams and rivers in Great Britain (Jarvis and Younger, 2000) and over 3000 km in the United States (Hedin, 1997). In South Africa, the full impact of AMD contamination is yet to be experienced. Although the activities of coal mining in the Witbank Coalfield have led to AMD contamination of ground and surface water, this has tended to be localised and on a relatively small scale (Bell et al, 2001). The South African gold industry represents the most immediate threat of a high volume, uncontrolled AMD discharge. The gold mining industry in the Witwatersrand area has been a major part of the South African economy for many years. However, potable water resources in and around the Witwatersrand Mining basin are under increasing threat of contamination from AMD due to the 400 km^2 of tailing dams and 6 billion tonnes of pyrite left by many years of gold mining in the area (EarthLife Africa Jhb, 2009). In certain parts of the basin, the underground acid mine water is already rising by up to one meter per day and the mining companies in the area are currently pumping up to 175 mega litres per day of underground acid mine water (EarthLife Africa Jhb, 2009). It is estimated that the first decant will be experienced within the next two years and this will not only have a tremendous effect on the water resources in the area but it will also compromise the structural integrity of the entire city of Johannesburg.

University of Cape Town

2.1.1. Acid mine drainage generation

Acid mine drainage is caused by chemical or biologically catalyzed oxidation of sulphide minerals upon exposure to oxygen and water. This process may occur in operating and abandoned mines, where sulphide minerals are exposed to the atmosphere, as well as in the waste rock piles and tailings generated by the processing of the mined ore (Johnson, 2003).

Pyrite is the most common sulphide mineral responsible for acid generation and metal solubilisation. The reactions involved in pyrite oxidation and AMD formation can be summarized according to the following reactions (Johnson, 2003):

Initiator reaction:

$$2FeS_2 + 7O_2 + 2H_2O \leftrightarrow 2Fe^{2+}{}_{(aq)} + 4SO_4{}^{2-}{}_{(aq)} + 4H^+{}_{(aq)} \quad 2.1$$

Propagation reaction:

$$4Fe^{2+}{}_{(aq)} + O_{2(g)} + 4H^+{}_{(aq)} \leftrightarrow 4Fe^{3+}{}_{(aq)} + 2H_2O_{(l)} \quad 2.2$$

The reaction for ferrous ion oxidation (Equation 2.2) is catalysed by the different types of naturally occurring bacteria (Christensen et al, 1996; Benner et al, 2000). The ferric ion formed through this reaction can undergo hydrolysis to form the red-orange precipitate [$Fe(OH)_3$] characteristic of AMD discharge (Equation 2.3). Alternatively, the ferric ions can react with more pyrite to regenerate the ferrous ions (Equation 2.4).

Hydrolysis:

$$Fe^{3+}{}_{(aq)} + 3H_2O_{(l)} \leftrightarrow 2Fe(OH)_{3(s)} + 3H^+{}_{(aq)} \quad 2.3$$

Further oxidation of pyrite:

$$FeS_{2(s)} + 14Fe^{3+}{}_{(aq)} + 8H_2O_{(l)} \leftrightarrow 15Fe^{2+}{}_{(aq)} + 2SO_4{}^{2-}{}_{(aq)} + 16H^+{}_{(aq)} \quad 2.4$$

The regeneration of ferrous ions is the key step in promoting the ongoing oxidation of the mineral. According to the reaction schemes shown in Equation 2.1 to 2.4, a ferric hydroxide precipitate and four moles of hydrogen ion acidity are generated for every mole of pyrite oxidized. Hence, AMD is characterised by low pH (< 4), suspended solids and high sulphate concentration. Equation 2.5 shows the overall reaction responsible for pyrite oxidation.

University of Cape Town

Net reaction:

$$4FeS_{2(s)} + 15O_{2(g)} + 14H_2O_{(l)} \leftrightarrow 4Fe(OH)_{3(s)} + 8SO_4{}^{2-}{}_{(aq)} + 16H^+{}_{(aq)} \quad 2.5$$

At low pH values, the ferric ions produced by bacterial oxidation of sulphide minerals can also oxidize other metal sulphides (MS) and cause dissolution of other metal ions, as shown by Equation 2.6.

$$3Fe^{3+}{}_{(aq)} + MS_{(s)} \leftrightarrow 2Fe^{2+}{}_{(aq)} + M^{2+}{}_{(aq)} + S^0{}_{(s)} \quad 2.6$$

However, the leaching of other metal ions from their corresponding sulphide minerals may not lead to acidity production (Younger et al, 2002). Table 2.1 demonstrates the variability in the composition of AMD streams from five different mines in South Africa.

University of Cape Town

Table 2.1: Chemical composition of a typical AMD stream for different South African Mines. All the concentrations are in mg L^{-1}.

	Highveld[1]	**Grootvlei**[1, 2]	**West Rand**[1]	**Klipsruit**[1]	**Vaal Barrage**[3]
pH	1.51 - 2.91	6.3	2.4	2.6	2.3 - 3.8
Fe	0.25 - $6.3x10^3$	$1.9x10^2$	$6.7x10^3$	-	1.24 - $5.99x10^3$
Zn	-	0.01	-	-	0.59 - $1.22x10^2$
Cu	-	-	-	-	-
Cd	-	-	-	-	-
As	-	-	-	-	-
Al	-	0.3	-	-	0.91 - $1.8x10^3$
Mn	0.3 - $2.4x10^2$	4.1	-	-	0.42 - $1.33x10^2$
Mg	0.4 - $2.8x10^3$	$1.97x10^2$	-	-	1.64 - $2.02x10^3$
Ca	-	$4.22x10^2$	-	-	2.0 - $6.5x10^2$
Na	0.4 - $4.1x10^3$	$2.9x10^2$	$0.8x10^2$	$1.9x10^3$	-
K	11 - 52.6	$0.13x10^2$	-	-	4.6 - 14.[3]
SO_4^-	6.16 - $14.9x10^3$	$2.2x10^3$	$2.3x10^4$	$8.1x10^3$	1.78 - $4.1x10^4$
NO_3^-	0.4 - $1.6x10^2$	-	-	-	-

The concentration of iron and sulphate is high in all cases and the characteristic heavy metal composition is beyond the recommended limits for domestic use and aquatic life (WHO, 2006).

University of Cape Town

2.2. Treatment options for metal removal and AMD remediation

Several treatment techniques have been developed for remediation of metal contaminated wastewater, both industrial effluents and AMD, prior to discharge into the environment (Johnson and Hallberg, 2005). These may be applied as passive or active treatment processes. In passive treatment processes, the removal of metals is accomplished by the use of naturally occurring geochemical and biological processes

[1] Walmsley Environmental, 1995
[2] Oryx Environmental and Jones & Wagener Consulting Engineers, 2003
[3] Steffen, 1989

in the absence of active control. Wetlands and anoxic limestone drains (ALDs) are typical examples of passive treatment systems (Johnson, 2006). Active treatment processes, on the other hand, require ongoing inputs of energy and/or (bio)chemical reagents (Younger et al, 2002). Active treatment processes are typified by more rapid kinetics and enhanced control in comparison with the passive treatment systems.

The choice of the treatment technique for remediation of heavy metal contaminated wastewater is dependent on the nature, the extent of contamination, and the proposed use of the treated water (Gazea et al, 1996).

2.2.1. Chemical treatment

Heavy metal removal techniques that are classified as chemical or partially chemical include coagulation-flocculation, precipitation, adsorption, ion exchange, reverse osmosis and electrolysis. The method most widely used to treat large volumes of acidic metal contaminated effluents is the active treatment process involving the addition of a chemical neutralising reagent (Coulton et al, 2003). In this treatment method, a chemical neutralising reagent is added to the acidic water to raise the pH and cause many of the metals present in solution to precipitate (Hammack et al, 1994). Although a number of different neutralising reagents are readily available, acid neutralisation and metal precipitation is most commonly achieved by addition of lime ($Ca(OH)_2$) or limestone ($CaCO_3$). These reagents offer the additional advantage of sulphate removal, to the saturation point for gypsum, when treating sulphate laden wastewater like AMD. Equations 2.7 and 2.8 shows the reaction that takes place when lime and limestone, respectively, are added to metal and sulphate laden wastewater.

$$Ca(OH)_{2(s)} + Me^{2+}{}_{(aq)} + SO_4{}^{2-}{}_{(aq)} \rightarrow Me(OH)_{2(s)} + CaSO_{4(s)} \qquad 2.7$$

$$CaCO_{3(s)} + Me^{2+}{}_{(aq)} + SO_4{}^{2-}{}_{(aq)} \rightarrow MeCO_{3(s)} + CaSO_{4(s)} \qquad 2.8$$

The active chemical treatment process by addition of a neutralising reagent is a low technology approach that provides a cost effective solution for the treatment of AMD.

University of Cape Town

However, there are a number of associated problems. The optimum pH required for minimum metal solubility varies for the different metal species and the different precipitation processes. Therefore, multiple stage precipitation processes are often required to reduce all the metals to acceptable discharge concentrations. Furthermore, the precipitates produced by neutralising reagents can be gelatinous and difficult to dewater. Settled sludge concentrations of between 2 and 5% solids are frequently achieved when separating the solids from the treated water using conventional solid-liquid separation techniques such as filtration and sedimentation (Bhattacharyya et al, 1981; Zhou et al, 1999). Consequently, the cost of multiple stage process design and sludge disposal can represent a significant proportion of the overall process cost. There have been a number of refinements aimed at improving the efficiency of the process and reducing the problems associated with the bulky sludge produced. The high density sludge (HDS) process has been successfully used to improve the settled sludge concentration of conventional precipitation processes by up to 50% (Kostenbader and Haines, 1970; Bosman et al, 1983). In this process, sludge recirculation is used to promote metal precipitation onto the surface of the pre-existing sludge, and thus minimising homogeneous nucleation. The HDS process has also been shown to decrease the cost of conventional precipitation processes by decreasing the amount of the chemical reagents required for precipitation (Coulton et al, 2003).

University of Cape Town

2.2.2. Biological treatment

The basis for bioremediation of metal contaminated wastewater is the ability of certain micro-organisms to generate alkalinity and immobilize metals. Microbial processes that generate alkalinity are typically reductive and include denitrification, methanogenesis, sulphate reduction, and iron and manganese reduction (Johnsonn and Hallberg, 2005). Although some of these processes are of minor importance in AMD-impacted environments, due to relative scarcity of the necessary materials, both ferric ions and sulphate tend to be abundant in AMD. Thus, biological sulphate reduction has substantial potential in the management of AMD-impacted environments.

Sulphate reduction may occur as an assimilatory or dissimilatory process. Assimilatory sulphate reduction is a biosynthetic process in which sulphate is reduced

to sulphide by bacteria, fungi or plants for synthesis of certain amino acids and metabolism (Widdel et al, 1988; Cooney et al, 1996). Dissimilatory sulphate reduction, on the other hand, is the process whereby sulphate reduction is catalysed by sulphate reducing bacteria (SRB) in the presence of a suitable organic substrate which acts as an electron donor. In this process, the sulphate acts as an electron acceptor for the degradation of the organic substrate (Brüser et al, 2000). As a result, simultaneous carbon transformation and liberation of bicarbonate alkalinity and sulphide ions take place during the process (Equation 2.9).

$$\text{Electron donor} + SO_4^{2-}{}_{(aq)} \xrightarrow{\text{SRB}} HS^-{}_{(aq)} + HCO_3^-{}_{(aq)} \qquad 2.9$$

Various organic substrates have been used as electron donors (Dvorak et al, 1992; Christensen et al, 1996; Chang et al, 2000; Hao et al, 2007; Oyekola et al, 2009). The ratio of the bicarbonate alkalinity to aqueous sulphide generated depends on the carbon source and the composition of the microbial consortium (Gibson, 1990). The bicarbonate alkalinity can be used to neutralise acidic effluents while sulphide ions can be used to effect the precipitation of dissolved metal ions as metal sulphides (Kaksonen et al, 2006). The pH neutralization reaction and the reaction that takes place between the sulphide ions and the dissolved metal ions can be summarised as shown in Equations 2.10 and 2.11, respectively.

$$HCO_3^-{}_{(aq)} + H^+{}_{(aq)} \rightarrow H_2O_{(l)} + CO_{2(g)} \qquad 2.10$$

$$Me^{2+}{}_{(aq)} + HS^-{}_{(aq)} \rightarrow MeS_{(s)} + H^+{}_{(aq)} \qquad 2.11$$

The metal sulphide precipitates formed are significantly less soluble than their hydroxide counterparts (even at low pH), resulting in the potential for lower residual metal concentrations in the treated effluent (Hammack et al, 1994).

Over the past two decades a number of novel treatment technologies, based on SRB mediated sulphate reduction for treatment of metal contaminated effluents and AMD remediation, have been successfully developed and applied at industrial scale (Brown et al, 2002). The Thiopaq® process was developed in the Netherlands by Paques B. V.

University of Cape Town

and has been successfully implemented at Budelco zinc refinery (Netherlands), Kennecott Bingham copper mine (USA) and the synthetic fibre production plant of Akzo Nobel (Netherland) (Boonstra et al, 1999; Hulshoff Pol et al, 2001; van Houten et al, 2006; Huisman et al, 2006). The BioSulphide® process developed by BioteQ Environmental Technologies Inc has also been successfully implemented at mine sites in Canada, USA, Mexico, Australia and China (Rowley et al, 1997; Lopez et al, 2009). The Rhodes BioSURE® process was developed in South Africa and links the treatment of AMD and sewage sludge disposal (Rose et al, 2000; Whittington-Jones et al, 2006). This system consists of a falling sludge bed reactor in which the macromolecules of the sewage sludge are degraded to provide electrons for the SRB. A new plant using this technology was commissioned at the Ancor Sewage Works in South Africa, but is not currently operational.

To reduce metal toxicity to the SRB, most of these treatment systems are designed with the sulphate reduction stage separate from the metal precipitation step. Thus, while the reactive species may be of biological origin, the precipitation process is essentially the same as that which occurs in the chemically based treatment systems.

University of Cape Town

2.3. Precipitation theory

Precipitation generally refers to a relatively fast crystallization process whereby the formation of an insoluble phase is brought about by a chemical reaction. Thus, precipitation is often referred to as "reactive crystallisation". The chemical reaction may involve two liquids, a liquid and a solid or a liquid and a gas (Söhnel and Garside, 1992). Due to the fast reaction kinetics and the sparingly soluble nature of most precipitating compounds, precipitation processes are characterised by high levels of supersaturatiton, high nucleation rates and production of a large number of particles (i.e. > 10^{11} particles per m^3) with small particle size (i.e. < 10 μm) (Söhnel and Garside, 1992).

Precipitation processes are of great importance in the chemical and process industries. Many consumer products, such as paint and pharmaceuticals, are produced via precipitation processes (Söhnel and Garside, 1992). Precipitation can also be used to

separate a metal or a group of metals from others, either for the purpose of removing impurities or minor metallic constituents (Jackson, 1986). In waste and wastewater treatment, precipitation is used as a scavenging process to recover dissolved metal ions from wastewater prior to discharge. The properties (i.e. particle size, morphology and surface area) of the precipitates are of key importance in most practical applications and can have a major impact on the post-precipitation processing, such as solid-liquid separation, drying, bulk density, etc (Söhnel and Garside, 1992). Therefore, it is important to develop precipitation processes that produce precipitates with appropriate particle characteristics.

2.3.1. Supersaturation

Supersaturation is the thermodynamic driving force behind every precipitation process and the level of supersaturation in the precipitating system governs the rate of particle rate processes such as nucleation, crystal growth, Ostwald ripening, aggregation and breakage. According to Mersmann (2001), supersaturation represents the difference in the chemical potential between the fluid and the crystal phase. The chemical potential can be described by the following relation:

$$\mu = \mu^0 + N_A kT \ln \alpha \qquad 2.12$$

where μ represent the chemical potential (J mol^{-1}), μ^0 is the standard chemical potential (J mol^{-1}), N_A is Avogadro's number (mol^{-1}), k is the Boltzmann's constant (J K^{-1}) and T the temperature (K) (Mersmann, 2001). For a crystallization system where a crystallizing compound results from an ionic solution, such as precipitation, the change in chemical potential ($\Delta\mu$) is described by Equation 2.13,

$$\Delta\mu = N_A kT \ln\left(\frac{\alpha_\pm}{\alpha_\pm^*}\right) \qquad 2.13$$

where $\alpha_\pm$ is the general expression for a solute in an aqueous solution and $\alpha_\pm^*$ is the general expression for a solute at equilibrium (Mersmann, 2001). For an ionic

University of Cape Town

reaction, given in Equation 2.14, the solubility product, K_{sp}, can be formulated from the activities and is described according to Equation 2.15

$$xA^{z+} + yB^{z-} \leftrightarrow A_xB_y \qquad 2.14$$

$$K_{spa} = (a^*_A)^x (a^*_B)^y \qquad 2.15$$

In Equation 2.14, z is the valency number of the ions.

The supersaturation, S_a, based on activities is thus given as shown in Equation 2.16 (Mersmann, 2001).

$$S_a = \left(\frac{(a_A)^x (a_B)^y}{K_{sp}} \right)^{1/(x+y)} \qquad 2.16$$

Therefore, the change in the chemical potential of a precipitating system is related to supersaturation according to Equation 2.17.

$$\Delta\mu = N_A kT \ln S_a \qquad 2.17$$

For the precipitating system where the ionic activity coefficient is close to unity, the solubility product, can be described in terms of the ion concentrations, C, and is represented by Equation 2.18, where C_{eq} represents the equilibrium concentration of the reagents. For such a system, the supersaturation, S, is described by Equation 2.19.

$$K_{sp} = (C_{eq\,A})^x (C_{eq\,B})^y \qquad 2.18$$

$$S = \left(\frac{(C_A)^x (C_B)^y}{K_{sp}} \right)^{1/(x+y)} \qquad 2.19$$

University of Cape Town

The effect of anion and cation concentration on supersaturation can be illustrated as shown in Figure 2.1 (Nielsen, 1979).

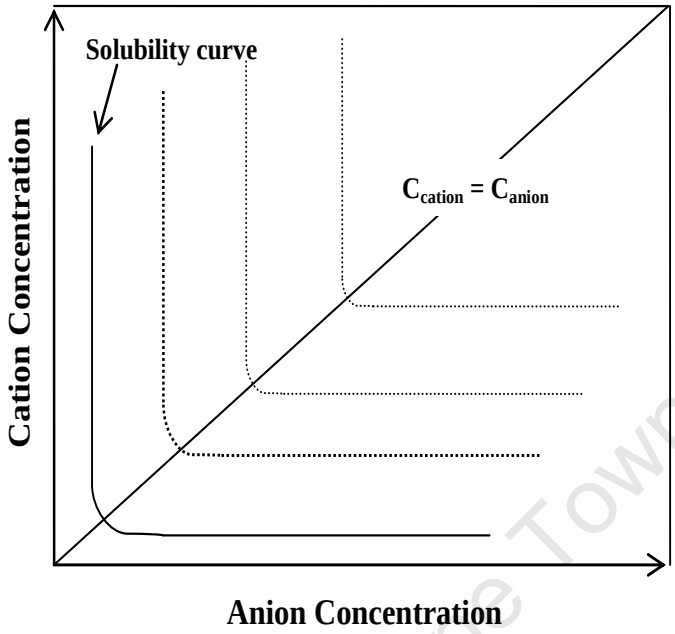

Figure 2.1: The effect of anion and cation concentrations on supersaturation (adapted from Nielsen, 1979)

The position of the solubility curve depends on the solubility of the resulting product. If the solubility of the product is very high, the position of the curve will be further away from the axis and the concentration of the reagents required to produce the level of supersaturation necessary for precipitation will be much higher. If the precipitation process results in the formation of a sparingly soluble compound, high levels of supersaturation are produced even at low reagent concentrations. Table 2.2 shows the solubility products of different metal sulphides (Rickard and Luther, 2006). The solubilities are presented both in molal (m) and parts per million (ppm) of total dissolved metal. The data in Table 2.2 were modified for $pK_2 = 18$ and the values were calculated for pure water at 25^0C, 1.013 bars total pressure, pH 7, Eh = – 0.2 V, total S(-II) = 10^{-3} M (sulphides). The Davies equation was used to compute the activity.

University of Cape Town

Table 2.2: Solubility products (K_{sp}) of various metal sulphides (Rickard and Luther, 2006)

Metal sulphide	***m***	***ppm***
CuS	5×10^{-19}	3×10^{-14}
CdS	1×10^{-18}	4×10^{-13}
PbS	4×10^{-17}	1×10^{-13}
ZnS	1×10^{-13}	8×10^{-9}
CoS	1×10^{-10}	5×10^{-3}
NiS	3×10^{-10}	2×10^{-5}
FeS	2×10^{-6}	6×10^{-2}
MnS	1×10^{-4}	6×10^{0}

Most metal sulphides are sparingly soluble and thus the level of supersaturation produced during metal sulphide precipitation is very high, even at low reagent concentrations. Seckler (1994) suggested the use of a seeded fluidised bed reactor (FBR) with multiple reagent feed points to reduce the high levels of supersaturation created during precipitation of sparingly soluble compounds. This strategy was successfully used by Taty Costodes and Lewis (2006) to control the amount of fine particles generated during nickel carbonate precipitation. Mishra and Kapoor (1978) and later Oktaybaş et al (1994) proposed the use of a gaseous precipitating reagent for precipitation of sparingly soluble compounds to reduce the high levels of supersaturation by exploiting the gas-liquid mass transfer limitation. Al-Tarazi (2004) used this approach for copper and zinc sulphide precipitation in a bubble column with gaseous H_2S and concluded that the morphology of the metal sulphide precipitate produced using gaseous hydrogen sulphide were more favourable than that of the precipitate produced using aqueous sulphide source.

2.3.2. Particle Rate Processes

Particle rate processes refer to the kinetic processes of nucleation, growth, aggregation and breakage which are responsible for the evolution of the particle size distribution during the precipitation process.

University of Cape Town

2.3.2.1. Nucleation

Nucleation refers to the formation of the smallest thermodynamically stable solid phase from a supersaturated solution (Jones, 2002). According to the classical theory of nucleation (Nielsen, 1964; Kaschiev, 2000), solute molecules collide with each other at a certain frequency due to Brownian motion. After the creation of a driving force for precipitation, these collisions lead to the formation of clusters of solute molecules. The driving force for the creation of these clusters is the decrease in the chemical potential of the molecules leaving the solution due to a decrease in the Gibbs free energy, ΔG, between the two bulk phases.

The work of formation for an n-sized cluster, W (J), can be approximated by the following equation:

$$W(n) = -nkT\ln S + \gamma A_c(n) \qquad 2.20$$

where n is the number of molecules in the cluster of a critical nucleus, k is the Boltzmann constant (J K^{-1}), T is the temperature (K), γ is the interfacial energy (J m^{-2}) and $A_c(n)$ is the cluster surface area (m^2). The work of formation of a cluster will at first increase with an increasing number of molecules, until a maximum is reached. At this point the critical cluster size, n^*, is reached and the flux of the solute molecules attaching to the cluster is equal to the flux of the molecules detaching from the cluster. The cluster of size n^* is referred to as the supercritical cluster or nucleus while the corresponding free energy is called the Gibbs free energy of nucleation, ΔG^* (J). Above n^*, clusters grow with each addition of a molecule while the free energy decreases. Clusters with size less than n^*, i.e. embryos or subcritical nucleus, dissolve because their free energy is less negative than that corresponding to n^*. Figure 2.2 shows an illustration of the change in free energy as a function of nucleus size denoted by the cluster radius, r.

University of Cape Town

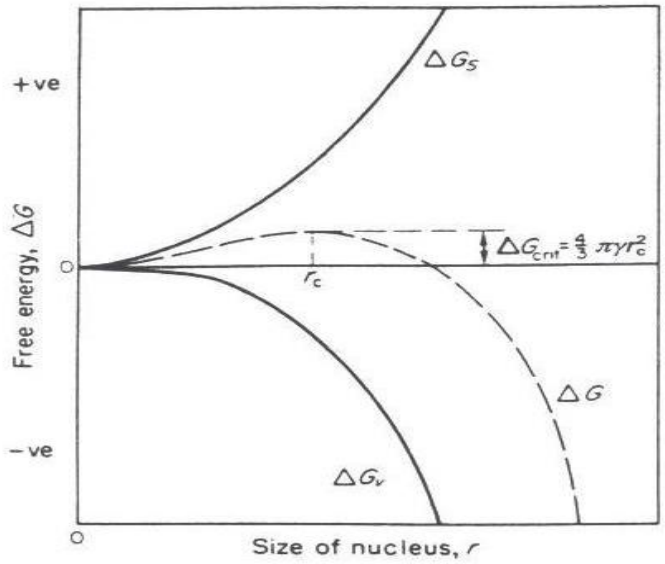

Figure 2.2: Free energy change as a function of nucleus size (source: Mullin, 2001).

According to Söhnel and Garside (1992), the various mechanisms responsible for formation or birth of the nuclei can be schematically represented as shown below.

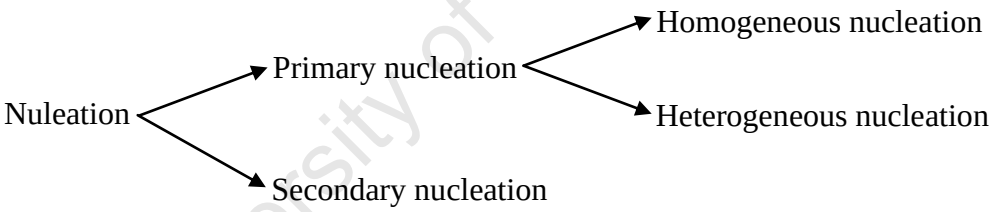

The mechanism which is most important in any given system depends on both the specific condition during nucleation and the physical properties of the system. In primary nucleation, the formation of a new solid phase is not influenced by the presence of the solid phase being formed. Secondary nucleation, on the other hand, refers to the birth of nuclei at the interface of the parent crystal and/or crystal fragments. This type of nucleation is very rare during precipitation of sparingly soluble compounds (Söhnel and Garside, 1992).

University of Cape Town

2.3.2.1.1. Homogeneous nucleation

Jones (2002) describes homogeneous nucleation as spontaneous nucleation from clear solution. The rate of homogeneous nucleation, J (# m^{-3} s^{-1}), from a solution of a certain volume can be defined as the change in the number of supercritical clusters within a certain time period and can be represented according to Equation 2.21,

$$J(t) = \frac{1}{V}\frac{dN^*}{dt} \qquad 2.21$$

where V is the volume of the solution (m^3), N^* is the number of supercritical clusters and t is the time period (s). Under stationary conditions, when the driving force is constant, the rate of homogeneous nucleation is defined as the time-independent frequency of transformation of the nucleus into the smallest super-nucleus according to Equation 2.22;

$$J = zf^* C_n^* \qquad 2.22$$

where z is the Zeldovich factor, f^* is the attachment frequency (s^{-1}) and C_n^* is the concentration of the nuclei (m^{-3}). The Zeldovich factor corrects for the fact that not all supernuclei grow out to macroscopically large sizes. The factor is a constant with a value between 0.01 and 1, and it can be calculated using Equation 2.23 (Kaschiev, 2000). The attachment frequency is the product of the incoming flux of monomers to the nucleus surface and the nucleus area.

$$z = \left(\frac{\Delta G^*}{3\pi kTn^{*2}} \right)^{\frac{1}{2}} \qquad 2.23$$

For homogeneous nucleation, the concentration of the nuclei can be approximated with a Boltzmann type formula, as shown in Equation 2.24 (Söhnel and Garside, 1992);

University of Cape Town

$$C_n^* = C_0 \exp\left(-\frac{\Delta G^*}{kT}\right) \quad 2.24$$

where C_0 is the concentration of the nucleation sites and k is the Boltzmann constant (k = 1.38 x 10^{-23} J K^{-1}). The concentration of the nucleation sites is equal to the molecular volume, $1/v_0$, because the nucleus can be formed anywhere in the supersaturated solution.

The rate of homogeneous nucleation, thus, can be rewritten according to Equation 2.25.

$$J = zf^* C_0 \exp\left(-\frac{\Delta G^*}{kT}\right) \quad 2.25$$

Substituting for ΔG^* according to the Gibbs-Thomson equation, Equation 2.26 for the rate of homogeneous nucleation is obtained (Söhnel and Garside, 1992).

$$J_{homo} = A_{homo} \exp\left(-\frac{16\pi v_0^{\,2}\gamma^3}{3(kT)^3 \ln^2 S}\right) \quad 2.26$$

In this equation, A_{homo} is the pre-exponential kinetic parameter (m^{-3} s^{-1}) which can be estimated from the attachment frequency of the two possible mechanisms, i.e. volume-diffusion control and interface-transfer control.

2.3.2.1.2. Heterogeneous nucleation

The formation of nuclei from homogeneous nucleation in practice is a rare event. In most cases, the formation of new crystals is induced by the presence of an interface different from that of the solute. Apart from the interface between the cluster and the solution, two additional interfaces are created when nucleation takes place in the presence of a heterogeneous surface area. The one interface is created between the heterogeneous surface and the solution, and the other interface is created between the heterogeneous surface and the cluster (Söhnel and Garside, 1992). The interplay

University of Cape Town

between the different interfacial energies results in an effective interfacial energy, γ_{eff} (J m^{-2}). Thus, the Gibbs free energy for heterogeneous nucleation would be expressed according to Equation 2.27 (Söhnel and Garside, 1992).

$$\Delta G^*_{hetero} = \left(\frac{16\pi v_0^{\,2} \gamma_{eff}^{\,3}}{3(kT)^3 \ln^2 S} \right) \qquad 2.27$$

For heterogeneous nucleation, the effective interfacial energy, γ_{eff}, is less than the interfacial energy, γ. The Gibbs free energy for the formation of supernuclei in the presence of a heterogeneous surface area is substantially smaller than the Gibbs free energy for homogeneous nucleation (Kaschiev, 2000). Substituting ΔG^*_{hetero} in Equation 2.26, the rate of heterogeneous nucleation can be obtained using Equation 2.28.

$$J_{hetero} = A_{hetero} \exp\left(-\frac{16\pi v_0^{\,2} \gamma_{eff}^{\,3}}{3(kT)^3 \ln^2 S} \right) \qquad 2.28$$

The pre-exponential kinetic parameter for heterogeneous nucleation, A_{hetero} (m^{-3} s^{-1}), is much lower than the pre-exponential kinetic parameter for homogeneous nucleation, A_{homo}, since the concentration of the active sites in the presence of heterogeneous surfaces is much smaller than the molecular volume. The attachment frequency is also lower for the formation of a nucleus on a substrate.

Mersmann (2001) developed a way for determining the rates for homogeneous and heterogeneous nucleation as a function of the dimensionless driving force, i.e supersaturation. At lower supersaturation, the effect of the exponential term in Equations 2.26 and 2.28 dominates and the rate of heterogeneous nucleation is greater than the rate of homogeneous nucleation. At much higher supersaturation, the kinetic pre-exponential term takes over and the rate of heterogeneous nucleation is smaller than the rate of homogeneous nucleation. Figure 2.3 shows the effect of solubility and supersaturation on the nucleation mechanisms (Mersmann, 2001).

University of Cape Town

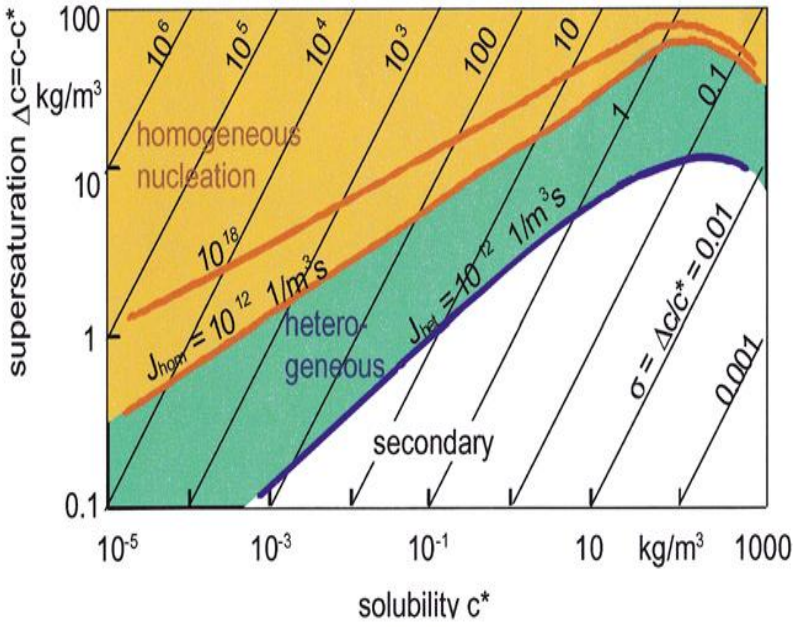

Figure 2.3: A simplified diagram showing the effect of solubility and supersaturation on the nucleation mechanism (source: Kind, 2002 as adopted from Mersmann, 2001).

2.3.2.2. Growth

Crystal growth is the process by which the initially formed primary particles grow into larger particles by the deposition of solute molecules (growth units) into the crystal face from a supersaturated solution. The growth units in this case can be molecules, ions, monomers, clusters, etc. The rate at which the crystal face on the crystal grows determines the shape of the crystal and, together with the growth mechanisms, it also determines the crystal surface structure and the purity of the crystal.

The growth rate of a particular crystal face is mostly described by its linear growth rate, G_r or R_{lin} (m s^{-1}), which refers to the rate of growth of that face in the direction normal to the face (Söhnel and Garside, 1992).

Since a crystal is mostly terminated by more than one crystallographically different crystal face, an overall linear growth rate is defined in relation to the increase in the mass of the crystal according to Equation 2.29 (Mullin, 2001);

University of Cape Town

$$\frac{1}{A}\frac{dm}{dt} = \frac{\rho k_v}{k_a L^2}\frac{dL^3}{dt} = 3\frac{k_v}{k_a}\rho G_r = 6\frac{k_v}{k_a}\rho \overline{R}_{lin} \qquad 2.29$$

where m is the mass of the crystal (kg), L is the volumetric diameter of the crystal (m), A is the surface area of the crystal (m^2), k_a is the area shape factor, k_v is the volume shape factor and ρ is the density of the crystal (kg m^{-3}).

The growth of the crystals is usually considered to be a two step process which involves the transport of the growth units from the bulk of the solution to the surface of the crystal and the incorporation of those growth units into the crystal lattice (Mersmann, 2001). Thus, the crystal growth process can be controlled by either diffusion or surface integration.

Figure 2.4 illustrates the reaction steps involved in crystal growth. Here, C_b is the bulk concentration (mol m^{-3}), C_i is the concentration at the interface (mol m^{-3}) and C^* is the concentration at the crystal surface (mol m^{-3}).

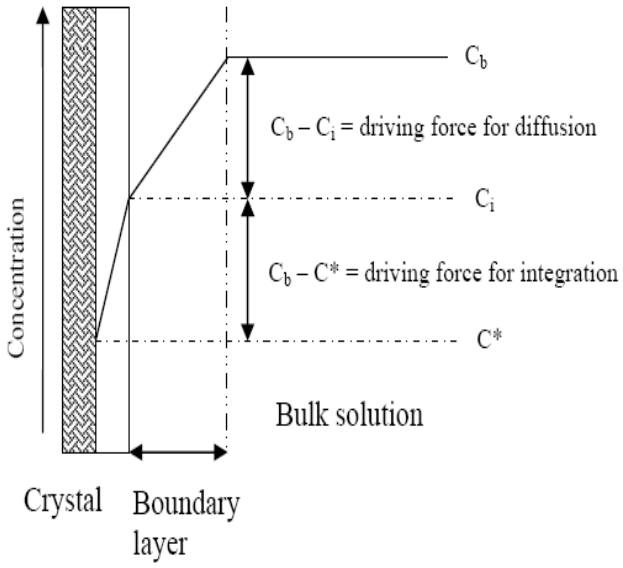

Figure 2.4: Concentration profile during crystal growth (source: Mullin, 2001).

For crystal growth that is limited by diffusion, $C_b - C_i >> C_i - C^*$ and the overall growth rate is expressed according to Equation 2.30 as shown below (Mullin, 2001);

$$G = k_d (C_b - C_i) \quad 2.30$$

where k_d is the diffusion mass transfer coefficient (m s^{-1}). If $C_i - C^* >> C_b - C_i$, the crystal growth process is dominated by surface integration and the overall growth rate is given by Equation 2.31 (Mullin, 2001).

$$G = k_r (C_i - C^*) \quad 2.31$$

where, k_r is the reaction rate constant for surface integration (m^3 mol^{-1} s^{-1}).

Mullin (2001) identified three possible mechanisms for surface integration controlled growth, i.e. spiral growth, growth by two dimensional nucleation, and rough growth. All three integration mechanisms depend on the supersaturation. At high supersaturation, the growth rate is controlled by surface integration and the growth units attach themselves anywhere on the crystal surface and the surface becomes rough, i.e. rough growth.

University of Cape Town

2.3.2.3. Aggregation

Aggregation is a process by which particles collide and adhere and are eventually cemented together to form stable particles or flocculates (Söhnel and Garside, 1992). Particle aggregation plays an important role in the formation of larger particles in precipitation and crystallization processes.

During precipitation, a dispersed solid-liquid system is formed. The stability of this dispersed system is determined by the extent to which the original degree of dispersion is maintained over a period of time (Söhnel and Garside, 1992). The initial dispersion may change as a result of formation of larger entities by particle aggregation (this process is called coagulation for small particles and agglomeration for larger particles). Aggregate formation depends on the transport of the primary particles due to Brownian motion, fluid motion or sedimentation, frequency of collision between moving particles and the nature of interactions that take place when these particles collide (Söhnel and Garside, 1992). The nature of the interactions that

take place when particles collide may be attractive or repulsive depending on the surface characteristics of the particles and the chemistry of the solution. The total number of particles is thus decreased during aggregation and the specific surface area of the solid phase is reduced.

The first aggregation frequency expression describing the time-dependent decrease in particle concentration due to aggregation by Brownian motion (i.e. perikinetic aggregation) was developed by Smoluchowski (1917) and is presented in Equation 2.32:

$$-\frac{dN}{dt} = \overline{\alpha}_p k_p N^2 \qquad 2.32$$

where N is the number of single particles per unit volume of suspension (# m^{-3}), $\overline{\alpha}_p$ is the probability that the collisions leads to formation of an aggregate and k_p is the rate constant (m^3 s^{-1}) which can be expressed as;

$$k_p = 4D\pi d \qquad 2.33$$

D is the diffusion coefficient (m^2 s^{-1}) and d is the particle diameter (m). The Stokes-Einstein expression for the diffusion coefficient of a spherical particle is given by Equation 2.34 below;

$$D = \frac{kT}{6\pi\eta d} \qquad 2.34$$

where η is the absolute viscosity. Thus, Equation 2.32 becomes,

$$-\frac{dN}{dt} = \overline{\alpha}_p \frac{4kT}{3\eta} N^2 \qquad 2.35$$

University of Cape Town

Equation 2.35 describes aggregation due to Brownian motion and it is usually for particles with d < 1 μm. The value of the parameter $\bar{\alpha}_p$ determines whether aggregation will be rapid ($\bar{\alpha}_p \approx 1$) or slow ($\bar{\alpha}_p << 1$) (Sönhel and Garside, 1992).

In an unstable suspension, where aggregation of larger particles is enhanced by mechanical stirring, orthokinetic aggregation occurs because the particles follow the fluid motion. The rate of decrease in particle number in such a system can be described by Equation 2.36 (Smoluchowski, 1917);

$$-\frac{dN}{dt} = \frac{2}{3}\bar{\alpha}_o G_{SR} d^3 N^2 \qquad 2.36$$

G_{SR} in the equation represents the shear rate (s^{-1}) and $\bar{\alpha}_o$ is the probability of a collision being effective. If the initial number of individual particles and the solid volume are constant during aggregation, the volume of solids present in suspension is given by Equation 2.37 below:

$$V = k_v {d_0}^3 N_0 \qquad 2.37$$

where N_0 and d_0 are the initial number of particles and initial particle diameter respectively. k_v is the volume factor and for a spherical particle it is given as;

$$k_v = \frac{\pi}{6} \qquad 2.38$$

Thus, Equation 2.36 can be re-written as:

$$-\frac{dN}{dt} = \frac{4}{\pi}\bar{\alpha}_o VGN \qquad 2.39$$

University of Cape Town

If both perikinetic and orthokinetic aggregation are active during the precipitation process, the overall rate of decrease in particle concentration is given by Equation 2.40.

$$-\frac{dN}{dt} = \bar{\alpha}_p \frac{4kT}{3\eta} N^2 + \frac{4}{\pi} \bar{\alpha}_o VGN \qquad 2.40$$

Orthokinetic agglomeration is important for larger particles and begins to dominate over perikinetic agglomeration if the size of one of the particles exceeds about 0.2 μm (Söhnel and Garside, 1992). Thus, the first term in Equation 2.40 is negligible if $d > 1$ μm and the second term is less important if $d < 1$ μm.

The mathematical theory of Smoluchowski is based on the assumption that the particle collision diameter does not change with time. However, this is only valid at the beginning of the aggregation process since the size of the aggregating particles increases with time. Therefore, the theory is only valid in the initial stages of the aggregation process (Söhnel and Garside, 1992).

In recent years, aggregation processes have been more commonly described in terms of the aggregation kernel, β, which is a measure of the rate with which a particle of size L aggregates with another particle of size λ (Hounslow et al, 2005). The aggregation kernel is viewed as a combination of two factors. The first factor is the product of the size independent portion of the rate constant, β_0 (m^3 s^{-1}), which is dependent on the operating conditions. The second factor is a function of particle size, $f(L, \lambda)$, which often reflects the mechanisms by which aggregation takes place (Sastry, 1975). Equation 2.41 gives the expression for the aggregation kernel.

$$\beta(L,\lambda) = \beta_0 \times f(L,\lambda) \qquad 2.41$$

Hounslow et al (1999) found that β_0 depends on the solution supersaturation by following the same dependency as the growth rate. They describe the aggregation rate, r_A, as the product of the collision rate and aggregation efficiency, φ, as shown in

University of Cape Town

Equation 2.42; where ε is the energy dissipation (W kg^{-1}), L and λ represent the particles of two different size classes and σ is the yield strength.

$$r_A = \beta_0(\varepsilon, L, \lambda)\varphi(\varepsilon, \sigma) \qquad 2.42$$

Aggregation processes are responsible for rapid enlargement of the particle size in most precipitation processes and occur parallel to crystal growth. Due to the rapid nucleation of primary particles at high levels of supersaturation, however, aggregation is favoured over crystal growth in most precipitation systems (Söhnel and Garside, 1992).

2.3.3. Population Balance

The population balance describes the way in which the size distribution of a particle population develops in time as a result of various kinetic processes. The population balance equation (PBE) can be used to predict the resulting particle size distribution and provide information on the active particle rate processes inside the reactor (Randolph and Larson, 1962; Hulbert and Katz, 1964). A general form of the population balance equation is given by Equation 2.43 (Randolph and Larson, 1988);

$$\frac{\partial n}{\partial t} + \frac{\partial (G_r n)}{\partial L} + n\frac{d(\log V)}{dt} + \frac{nQ}{V} = B - D \qquad 2.43$$

where $n(L,t)$ is the population density per suspension volume (V), Q is the total volumetric flow rate, and B and D represent the net birth and death density functions respectively. For a crystalliser operating at steady state and assuming constant suspension volume, no flow of particles into the reactor, size independent crystal growth and no particle birth or death, the population balance is given by Equation 2.44,

$$\frac{\partial n}{\partial t} + G_r \frac{\partial n}{\partial L} + \frac{n}{\tau} = 0 \qquad 2.44$$

University of Cape Town

where $\tau = V/Q$ is the mean residence time in the reactor. Integration of Equation 2.44 results in the well known logarithmic relation for the steady state particle size distribution (Söhnel and Garside, 1992):

$$n(L) = n^0 \exp\left(-\frac{L}{G_r \tau}\right) \qquad 2.45$$

where *n(L)* is the population density distribution function (# m^{-3}), n^0 is the population density of nuclei (# m^{-3}), G_r is the linear growth rate (m s^{-1}), L is the crystal size (m) and τ the residence time (s). The growth and nucleation rates can be determined directly from the gradient ($-1/G_r\tau$) and the intercept (ln n^0) of the straight line in a logarithmic-linear plot of Equation 2.45. Peters et al (1984) used this analysis to determine the nucleation and growth rates of the zinc sulphide system. The results showed that the plot was concave, with the concavity increasing with an increase in the residence time. The concavity in the logarithmic-linear plot usually indicates that nucleation and growth are not the only particulate processes. In another study, Veeken et al (2003a) investigated the effect of sulphide concentration on particle size for zinc sulphide formation using the same analysis. Large deviations in the model data fit were obtained and even though aggregation rates were not calculated, it was concluded that aggregation played an important role in zinc sulphide formation. Particle birth and death due to aggregation are common during the precipitation of sparingly soluble compounds and therefore, it is important to take this into account when determining the particle size distribution of the system. Equation 2.46 gives the population balance equation for a well mixed crystallizer, assuming size independent growth and aggregation.

$$\frac{\partial n}{\partial t} + G_r \frac{\partial n}{\partial L} + \frac{n}{\tau} = B - D \qquad 2.46$$

The birth and death terms included in Equation 2.46 are given by

$$B = \frac{L^2}{2} \int_0^L \frac{\beta[(L^3 - \lambda^3)^{1/3}, \lambda] n[(L^3 - \lambda^3)^{1/3}] n(\lambda)}{(L^3 - \lambda^3)^{2/3}} d\lambda \qquad 2.47$$

University of Cape Town

$$D = n(L)\int_0^\infty \beta(L,\lambda)n(\lambda)d\lambda \qquad 2.48$$

In cases where both aggregation and growth are active, a complete analytical solution to the population balance is not possible and thus a moment form of the population balance can be used (Bramley et al, 1996). For an ideally mixed vessel with constant volume and unclassified product removal, the population balance can be transformed into the moment equation and presented as shown in Equation 2.49 (Randolph and Larson, 1988);

$$\frac{dm_j}{dt} = \frac{m_j^{in} - m_j}{\tau} + 0^j B_0 + jG_r m_{j-1} + \overline{B_{agg,j}} - \overline{D_{agg,j}} \qquad 2.49$$

where B_0 is the boundary condition for the birth rate (# m^{-3}) at size L = 0. The jth moment of the number density function, $n(L)$, with respect to its internal coordinate, L, is defined according to Equation 2.50.

$$m_j = \int_0^\infty L^j n(L)dL \quad \text{j} = 0, 1, 2, 3\ldots \qquad 2.50$$

The zeroth moment is equal to the total number of particles, and the first, second and third moments are proportional, respectively, to the total length, area and volume of the particulate matter (Randolph and Larson, 1988). The birth and death functions in Equation 2.49 are defined as follows:

$$\overline{B_j} = \int_0^\infty L^j B(L)dL \qquad 2.51$$

$$\overline{D_j} = \int_0^\infty L^j D(L)dL \qquad 2.52$$

According to Hounslow et al (1988) the differential moment technique can be used together with the discretized population balance equation to calculate the rates. For size independent aggregation in a continuous system, using length as the internal

University of Cape Town

coordinate, the rate of change in the zeroth moment and the third moment are given by Equations 2.53 and 2.54, respectively.

$$\frac{dm_0}{dt} = -B_0 + \frac{m_0}{\tau} = -\frac{1}{2}\beta_0 m_0^{\ 2} \qquad 2.53$$

$$\frac{dm_3}{dt} = \frac{m_3}{\tau} = 3G_r m_2 \qquad 2.54$$

Thus, if the rates of change of the zeroth and the third moment are known, values of β_0 and G may be calculated directly from the experimental data. The particular forms of the birth and death functions obtained after the moment transformation depend on the specific models chosen to model the active particle rate processes. Al-Tarazi et al (2004) used the mixed-suspension mixed-product removal (MSMPR) method to measure the precipitation kinetics of zinc sulphide. Although the rate constants for nucleation, growth and aggregation were derived, it was shown that the MSMPR method was not suitable for studying and modelling the fast precipitation kinetics of metal sulphides.

University of Cape Town

2.4. Surface chemical properties of colloidal particles

Due to the high levels of supersaturation associated with the precipitation processes, a lot of tiny particles (> 10^{11} particles per m^3) are produced during the process (Söhnel and Garside, 1992). These particles remain in the submicron range and therefore are subjected to colloidal interactions (Kind, 2002). The colloidal particle interactions are determined by the charge on the surface of the particles (Stumm, 1992). Thus, the aqueous suspension stability of the colloidal particle dispersion depends on the surface charge of the particles. The charge on the surface of the particles is, in turn, determined by the chemistry and the composition of the solution (Stumm and Morgan, 1996).

Derjaguin and Landau (1941) and Verwey and Overbeek (1948) developed a quantitative theory (DLVO theory) to describe the stability of aqueous colloidal particle suspensions. The theory describes the interaction between charged surfaces in

a liquid medium according to the London-van der Waals forces of attraction and the electrostatic forces of repulsion, due to the overlap of the double layer of the counter-ions. The central concept of the DLVO theory is that the total interaction energy of the two surfaces or particles is given by the summation of the attractive and repulsive contributions (Hunter, 2001). This can be written as shown in Equation 2.55:

$$V_T = V_A + V_R \qquad 2.55$$

where V_T is the total interaction energy, V_A is the potential energy due to the London-van der Waals forces of attraction and V_R is the repulsive double layer interaction energy. The DLVO theory suggests that an energy barrier resulting from the repulsive interaction forces prevents the particles from adhering. However, if the particles collide with enough energy to overcome that barrier, the attractive interaction forces will pull them together where they will adhere strongly. Furthermore, the theory suggests an increase in suspension stability with increasing surface charge and decreasing ionic strength (Stumm and Morgan, 1996).

The London-van der Waals forces of attraction arise from the spontaneous electrical and magnetic polarizations which give a fluctuating magnetic field within the medium and the gap between the particles (Elimelech et al, 1995). For two spheres of equal radii, *a*, at an inter-particle distance, *D*, along the centre to centre axis, the interaction energy due London-van der Waals forces of attraction can be calculated according to Equation 2.56 (Liang et al, 2007);

$$V_A(D) = -\frac{A_H}{6}\left[\frac{2a^2}{D^2+4aD} + \frac{2a^2}{(D+2a)^2} + \ln\left(1-\frac{4a^2}{(D+2a)^2}\right)\right] \qquad 2.56$$

where A_H is the Hamaker constant and D is the inter-particle distance. Equation 2.56 only applies when the particles are close together and becomes very inaccurate when inter-particle distance is greater than 10% of the particle radius. The Hamaker constant includes the inverse dependence of the interaction energy on the inter-particle distance, and the direct dependence on the particle size (Elimelech et al, 1995). At extremely small inter-particle distances, the London-van der Waals forces

University of Cape Town

are always greater than the double layer repulsion forces since the interaction energy satisfies a power law (i.e. $V \propto -D^{-n}$), whereas the double layer interaction energy remains finite or increases far more slowly within the same separation range (Liang et al, 2007).

The repulsive forces arise from the electromagnetic interactions of the charged layer (i.e. the electrical double layer) surrounding the particles (Sönhel and Garside, 1992). A charged layer on the surface of the particle may arise due to selective adsorption of the ions, chemical reactions at the surface and/or lattice imperfections. The inner part of the electrical double layer is immobile and consists of tightly adsorbed ions. The outside part (diffuse layer) penetrates the solution adjacent to the particles and it is disturbed by random molecular motion in the liquid. The ions in this part of the double layer are, therefore, more diffusely distributed. When two charged particles approach each other in an electrolyte solution, their double layers overlap. The way in which the double layers respond to each other depends on the potential at the Stern plane, i.e. the boundary between the immobile and the diffuse part of the double layer (Hunter, 2001). If the potential at the Stern plane of the two approaching particles is the same, repulsion is experienced. For two spheres of radii, a_1 and a_2, the repulsive potential is given by Equation 2.57 (Elimelech et al, 1995),

$$V_R = 64\pi \frac{a_1 a_2}{a_1 + a_2}\left(\frac{kT}{ze}\right)\gamma_1\gamma_2 \exp(-\kappa D) \qquad 2.57$$

where k is the Boltzmann constant, T is the absolute temperature, z is the valence of the ions, e is the elementary electronic charge, D is the inter-particle distance and κ is the Debye-Hückel reciprocal length. The terms γ_1 and γ_2 are the dimensionless functions of surface potential. The pre-exponential term in Equation 2.57 depends on the zeta potential of the particles and it is always positive (repulsion) if the potentials are the same sign and negative (attraction) if they are of opposite sign.

In colloid chemistry, surface potential is often expressed in terms of zeta potential (Hunter, 2001). Zeta potential is the electrical potential that arises at the plane of shear due to the movement of the electrically charged phase (Hunter, 2001). The

University of Cape Town

relationship between the measured zeta potential and the double layer structure is still a subject of debate, since the shear plane cannot be located with any certainty. However, there is a clear correlation between zeta potential and colloid stability. It is usually assumed that the shear plane lies outside, but fairly close to the Stern plane and therefore the measured zeta potential is less than the true surface potential (Elimelech et al, 1995). The electrostatic double layer interactions are dependent on the ionic strength and the ions present in solution. Thus, the magnitude of the zeta potential is a function of the ionic strength and the ions present in solution (Hunter, 2001).

Baalousha (2009) investigated the aggregation behaviour of unpurified iron oxide nanoparticles at variable pH in the absence and presence of natural organic matter and showed that the DLVO theory can be successfully used to model the aggregation behaviour of these particles. Kobayashi et al (2005), on the other hand, studied the aggregation behaviour of amorphous and well characterised silica particles by potentiometric titrations, electrophoretic mobility and time resolved light scattering. The charging behaviour of the particles was found to be consistent with the basic Stern model. However, the aggregation behaviour was found to be very complex and deviated from the predictions of the DLVO theory. It was concluded that additional non-DLVO repulsive forces influenced the aggregation behaviour of the particles. In other studies, the existence of other non-DLVO forces, such as solvation (Doerr et al, 1998; Yu et al, 2000), hydration (Leikin et al, 1993) and hydrophobic forces (Israelachvili and Pashley, 1984; Claesson and Christenson, 1988; Rabinovich and Derjaguin, 1988) have been suggested. According to Liang et al (2007), the DLVO theory successfully explains the long range interaction forces for many systems but it does not account for interaction between surfaces or particles that are less than a few nanometers apart in other systems. This is because the theories of London-van der Waals and the double layer forces are continuum theories described on the basis of the bulk properties of intervening solvents. The DLVO theory does not take into account the nature of the molecules involved (i.e. the discrete size, shape and chemistry) in colloidal interactions (Liang et al, 2007).

The effect of surface characteristics on the solid-liquid separation characteristics of metal sulphides has been extensively studied in the flotation of sulphide minerals

University of Cape Town

(Fairthorne et al, 1997; Clarke et al, 1995; Fornasiero et al, 1992; Newell et al, 2007). According to Healy and Moignard (1976) and Moignard et al (1977), the charge on the surface of sulphide minerals is strongly influenced by pH, surface oxidation and surface adsorbing ions. Kolthoff and Moltzau (1935) studied precipitation of metal sulphides and showed that metal sulphide particles have strong adsorbent properties towards H_2S, HS^- and S^{2-}. Newell et al (2007) studied sulphidation of oxidised sulphide minerals and showed that the charge on the surface of the minerals and the floatability of oxidised sulphide minerals were improved by sulphide addition. In another study, Stén and Forsling (2000) studied lead sulphide precipitation and showed that the surface chemical properties of the particles produced were affected by the rate at which the sulphide was added to the lead solution.

2.5. Metal sulphide precipitation

Metal sulphide precipitation is an important industrial process. In hydrometallurgical processes, metal sulphide precipitation is most commonly used to remove impurities from concentrates containing valuable components. The Sherrit-Gordon ammonia leach process for the treatment of nickel-rich concentrates uses hydrogen sulphide (H_2S) to remove copper from the leach solution (Jackson, 1986). In nanotechnology, metal sulphide precipitation is used to produce nanocrystals with special properties, such as semiconductors, catalysts and cell components (Mathew et al, 2008; Jovanović et al, 2007; Deng et al, 2006).

Metal sulphide precipitation is an efficient process characterised by formation of highly insoluble metal salts, selective metal precipitation over a broad pH range and production of stable metal precipitates with potential for re-use (Bhattacharyya et al, 1981). However, the application of sulphide precipitation in wastewater treatment has previously been limited due to the use of expensive chemicals and the accompanying production of toxic H_2S gas when treating highly acidic effluents. Traditionally, metal sulphide precipitation was conducted using expensive chemical reagents, such as Na_2S, NaHS, CaS, FeS and H_2S. The introduction of biological processes for the safe and cost effective production of sulphide has widened the scope for using sulphide precipitation as a practical solution for large scale treatment of acidic effluents such as AMD.

University of Cape Town

The general reactions involved in metal sulphide precipitation involve pH-dependent aqueous sulphide speciation (Equations 2.58 and 2.59) (Jackson, 1986; Migdisov et al, 2001) and the reaction of the dominant sulphide species with the metal ions to form an insoluble metal sulphide precipitate (Equation 2.60).

$$H_2S_{(aq)} \leftrightarrow HS^-_{(aq)} + H^+_{(aq)} \qquad pK_1 = 6.99 \qquad 2.58$$

$$HS^-_{(aq)} + H^+_{(aq)} + \leftrightarrow S^{2-}_{(aq)} + 2H^+_{(aq)} \qquad pK_2 = 17.4 \qquad 2.59$$

$$Me^{2+}_{(aq)} + HS^-_{(aq)} \leftrightarrow MeS_{(s)} + H^+_{(aq)} \qquad 2.60$$

Several studies have been conducted on the precipitation of metal ions from solution as sulphides (Bryson and Bijsterveld, 1991; Mishra and Das, 1992; Harmandas and Koutsoukos, 1996). However, the chemical or molecular processes involved in the transformation of simple dissolved species to solid products are very complex and thus, the chemistry of metal sulphide formation is still not well understood (Luther et al, 1999). Djedidi and co-workers (2009) studied precipitation and dewatering characteristics of different metal precipitates (i.e. hydroxides, phosphates, carbonates and sulphides) and showed that the metal removal yields obtained in most cases were similar to the thermodynamically predicted yields. For metal sulphide precipitation, however, it was found that the kinetics of the process played an important role and the dewatering characteristics of the precipitates produced were poor compared to other metal precipitates. Peters et al (1984) investigated the residual metal concentration during zinc sulphide precipitation in the presence of EDTA and found that the residual concentration of the zinc ions was always higher than that predicted by the literature values for the zinc sulphide solubility.

Luther et al (1996) studied molecular processes involved in metal sulphide formation and presented experimental evidence showing that metal sulphide formation was preceded by formation of aqueous metal sulphide complexes. These complexes were later found to be higher order clusters which had high stability constants and were resistant to oxidation and dissociation (Rozan et al, 2000). In another study, Sukola et

University of Cape Town

al (2005) provided experimental evidence suggesting that the clusters produced during metal sulphide precipitation were a mixture of truly dissolved metal sulphide complexes and dynamic metal sulphide colloids. Ciglenečki et al (2005), on the other hand, provided evidence showing that these clusters were electrochemically active nanoparticles. Luther and Rickard (2005) focused on these clusters and described them as quantum sized particles which contained a discrete number of atoms in a molecule that was small enough to behave as dissolved specie. The researchers also found that the size of these clusters was dependent on the concentration of the reactants. When the concentration of the reactants was below 2 µM, the size of the clusters could be controlled but significant aggregation occurred when the concentration of the reactants was above 10 µM.

The formation of aqueous metal sulphide complexes plays an important role in different environmental and biological settings since they can complex up to 90 – 100% of the dissolved metal ions (Rozan et al, 2000; Luther and Rickard, 2005).

2.5.1. The mechanism of metal sulphide formation

The mechanism involved in metal sulphide formation was first discussed and proposed by Kolthoff and Moltzau (1935). According to the proposed mechanism, sulphide precipitation involves the reaction of sulphide ions to give first a metal bisulphide complex which, by secondary loss of protons, results in the formation of the metal sulphide as shown in Equations 2.61 and 2.62.

$$Me^{2+}_{(aq)} + H_2S_{(aq)} \rightarrow Me(HS^-)_{(aq)} \qquad 2.61$$

$$Me(HS^-)_{(aq)} \rightarrow MeS_{(s)} + H^+_{(aq)} \qquad 2.62$$

Although the existence of such intermediate complexes was generally accepted in metal sulphide precipitation, no experimental evidence was provided to prove their existence until much later. The first experimental evidence indicating the possible existence of intermediate metal sulphide complexes was provided by Rickard (1969) and Berner (1970). These researchers investigated pyrite formation and presented

University of Cape Town

experimental data that suggested an iron (II) monosulphide complex as a precursor to pyrite formation. Subsequently, Luther et al (1996) presented experimental evidence for intermediate metal sulphides complexes of Mn, Fe, Co, Ni, Cu and Zn. The actual involvement of these complexes in the reaction pathway, however, could not be determined due to the fast reaction kinetics of the process. Rickard (1989a) devised a flow-through T-tube system to study the fast precipitation reaction involved in iron (II) sulphide formation and presented the first detailed reaction pathway involved in the transformation of the dissolved aqueous ferric ions to insoluble iron (II) sulphide precipitate. The results of the study showed that the process of iron (II) sulphide formation was a two-stage reaction which involved iron bisulphide formation in the first stage and a condensation reaction in the second stage which resulted in the release of sulphide species into the solution (Rickard, 1989b).

Thereafter, Luther and co-workers (1999) investigated the formation of zinc sulphide (ZnS) using voltammetric methods and proposed a stepwise process for the formation of a stable ZnS phase. According to the proposed stepwise process, zinc sulphide formation starts with the zinc ions in aqueous solution as the hexaqua $Zn(H_2O)_6^{2+}$ ion. When sulphide is added to the solution, a ligand substitution reaction takes place and the sulphide species replaces the water in the first coordination sphere through a *dissociative* mechanism to form an aqueous metal sulphide complex. The resulting metal sulphide complexes then aggregate into soluble rings and molecular clusters (i.e. $Zn_3S_3(H_2O)_6$). Higher order clusters, which lead to precipitate formation, are formed when the zinc atoms on the one $Zn_3S_3(H_2O)_6$ combine with the sulphur atoms of another ring, with an associated loss of water. When additional sulphide is present in solution, condensation of $Zn_3S_3(H_2O)_6$ can also lead to formation of anionic complexes (i.e. $Zn_4S_6(H_2O)_4^{4-}$).

A similar investigation was conducted for copper sulphide (CuS) precipitation (Luther et al, 2002). The results show that trinuclear $Cu_3S_3(H_2O)_6$ clusters are also involved as the basic building blocks for higher order CuS molecular cluster formation and subsequent precipitation. However, the actual mechanism involved in the CuS formation is still not well defined since aqueous copper ions exist in two different forms (i.e. $Cu(H_2O)_6^{2+}$ and $Cu(H_2O)_5^{2+}$) and the molecular cluster condensation is accompanied by the reduction of Cu (II) to Cu (I).

University of Cape Town

Based on the identified aqueous metal sulphide complexes and clusters and the investigations into the rate of water exchange of different divalent aqueous metal ions, Luther and Rickard (2005) proposed a general mechanism involved in metal sulphide formation and summarised it as shown in Figure 2.5.

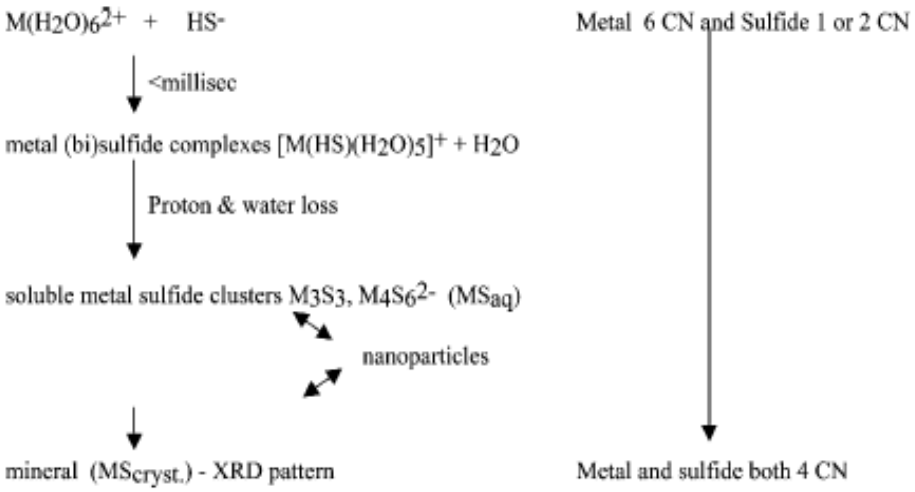

Figure 2.5: Summary of the process involved in the transformation of dissolved aqueous metal ions to sulphide minerals via sulphide precipitation (source: Luther and Rickard, 2005).

During the transformation process, major intra- and inter-molecular rearrangements occur and this leads to the change in the coordination number of both the metal and the sulphur (Rickard and Luther 2006).

2.5.2. The kinetics of metal sulphide formation

The kinetics of metal sulphide formation have been widely investigated. Bryson and Bijsterveld (1991) investigated the selective precipitation of cobalt from concentrated manganese sulphate solution and showed that the precipitation of manganese sulphide could be modelled using first order kinetics. The reaction for cobalt precipitation was found to have three kinetic stages with an induction period in the first stage, followed by rapid precipitation and a slow approach to equilibrium in the final stage. Similar results for cobalt sulphide precipitation were obtained by Mishra and Das (1992) in their investigation of zinc and cobalt precipitation from an ammoniacal solution

containing sulphate by controlled addition of sodium sulphide. The reaction for zinc sulphide formation was shown to follow first order kinetics. Lewis and Swaartbooi (2006), on the contrary, found that there was no induction time for cobalt sulphide formation when cobalt was precipitated from a mixed system containing nickel and cobalt. The reaction kinetics for both nickel and cobalt sulphide precipitation were found to be first order. The lack of an induction time for cobalt, in this case, was attributed to the presence of the nickel sulphide precipitate which acted as heterogeneous nuclei. Koumanakos et al (1990) investigated the spontaneous precipitation of cadmium sulphide in aqueous supersaturated solution at 25°C and showed that an induction time, inversely proportional to the solution supersaturation, preceded the onset of precipitation. A fourth order dependence on supersaturation for the rate of cadmium sulphide precipitation was obtained. Harmandas and Koutsoukos (1996) studied the spontaneous formation of iron sulphides in low ionic strength de-aerated aqueous solutions at 25°C and 80°C in neutral and slightly acidic pH. In neutral pH, mackinawite (FeS) precipitated directly from solution and under slightly acidic pH conditions amorphous iron sulphide was formed. The rate of precipitation of the amorphous iron sulphide was found to be second and first order dependent on the relative solution supersaturation at 25°C and 80°C, respectively.

Rickard (1995) investigated the kinetics of a fast precipitation reaction between aqueous iron (II) and dissolved sulphide at 25°C and showed that the process can be interpreted in terms of two competing reaction mechanisms, as shown in Equations 2.63 and 2.64.

$$Fe^{2+}_{(aq)} + H_2S_{(aq)} \rightarrow FeS_{(s)} + 2H^{+}_{(aq)} \qquad 2.63$$

$$Fe^{2+}_{(aq)} + 2HS^{-}_{(aq)} \rightarrow Fe(SH)_{2(s)} \qquad 2.64$$

The second stage for the reaction that proceeds according to Equation 2.64 involves condensation of the $Fe(SH)_2$ to FeS with the release of the sulphide back into the solution (Equation 2.65).

University of Cape Town

$$Fe(HS)_{2(s)} \rightarrow FeS_{(s)} + H_2S_{(aq)} \quad 2.65$$

The rates of the reactions in Equations 2.63 and 2.64 were described by the rate laws shown in Equations 2.66 and 2.67, respectively;

$$\frac{d[FeS]}{dt} = k_1[aFe^{2+}][aH_2S] \quad 2.66$$

$$\frac{d[Fe(SH)_2]}{dt} = k_2[aFe^{2+}][aHS^-] \quad 2.67$$

where aFe^{2+}, aH_2S and aHS^- are the activities of dissolved iron (II), hydrogen sulphide and bisulphide, respectively. The logarithm of k_1 and k_2 are the theoretical Eigen-Wilkins reaction rate constants. According to the Eigen-Wilkins mechanism, the rate of the reaction is determined by the rate of water exchange ($k_{H_2O_{ex}}$) in the inner sphere (Eigen and Wilkins, 1965). Thus, the rate of ligand substitution is mostly independent of the ligand and dependent on the characteristics of the metal. The rate constant for the formation of the inner sphere complexes during the formation of FeS with millimolar solutions of the reactants was found to be $>10^7$ M^{-1} s^{-1} (Rickard, 1995). Since the water exchange constant for most divalent aqueous metal ions are easily found in literature (Richens et al, 1997), these can be used as a first order estimation of the relative rates of formation of the metal sulphide complexes from solution. Luther and Rickard (2005) calculated the rate of formation for Cu, Zn, Ag and Pb sulphide complexes and found that the rate constant for the formation of sulphide complexes of these metals was faster (i.e. > 10^8 M^{-1} s^{-1}) than that obtained for Fe (II). This was the case because the rate of water exchange for Fe (II) is lower than that of the other metals by one order of magnitude or more.

University of Cape Town

2.5.3. Factors affecting metal sulphide precipitation

2.5.3.1. pH

The pH of the solution plays an important role in metal sulphide precipitation. As shown in Equations 2.58 and 2.59, aqueous sulphide speciation and thus the aqueous concentration of the reactive sulphide specie (i.e. HS^- or S^{2-}) is dependent on the pH of the solution. Figure 2.6 shows a diagrammatic representation of the pH-dependent aqueous sulphide speciation (Migdisov et al, 2001).

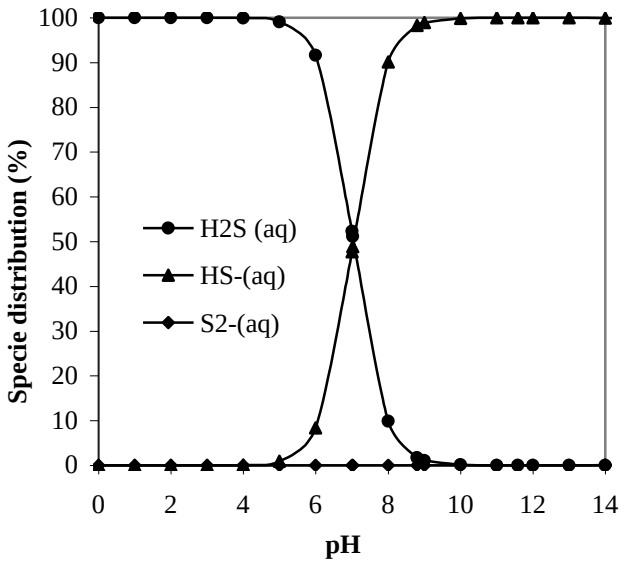

Figure 2.6: Aqueous hydrogen sulphide speciation (Migdisov et al, 2001).

Jackson (1986) describes the pH of the solution as the most important factor in metal sulphide precipitation. The relation between the sulphide ion (S^{2-}) concentration and the pH of the solution, for a saturation concentration of gaseous H_2S (i.e. ~ 0.09 mol L^{-1}) in water under a partial pressure of one atmosphere at 25°C, can be described according to Equation 2.68.

$$\log[S^{2-}] = \log 8.4 \times 10^{-26} + 2\text{pH} \qquad 2.68$$

For an increase of one pH unit, the sulphide ion concentration increases by two orders of magnitude. Rickard (1995) showed that the dominant reaction pathway during

iron(II) sulphide formation was dependent on the pH and total dissolved sulphide concentration. In neutral to alkaline pH, the bisulphide pathway resulting in the formation of $Fe(SH)_2$ was found to be dominant and the H_2S pathway dominated in acidic environments. Hammack et al (1994) investigated the effect of pH on copper sulphide precipitation using biologically produced gaseous hydrogen sulphide. The rate of gaseous H_2S dissolution was found to be low under acidic conditions and this led to a decrease in the total dissolved sulphide concentration required for metal precipitation.

The pH of the solution also determines the solubility of different metal sulphides. Metal ions such as copper react to form insoluble metal sulphides under very low pH conditions while other metal ions, such as manganese, only form insoluble metal sulphide at high pH. Figure 2.7 shows the relationship between pH and the solubility of different metal sulphides. The results in Figure 2.7 were calculated using OLI StreamAnalyzer Ver.3 at sulphide concentration of 10^{-3} M. It should be noted that the OLI StreamAnalyzer software does not have some of the latest metal sulphide solubility data and therefore the results presented in Figure 2.7 may not be the most accurate prediction of the given metal sulphide.

University of Cape Town

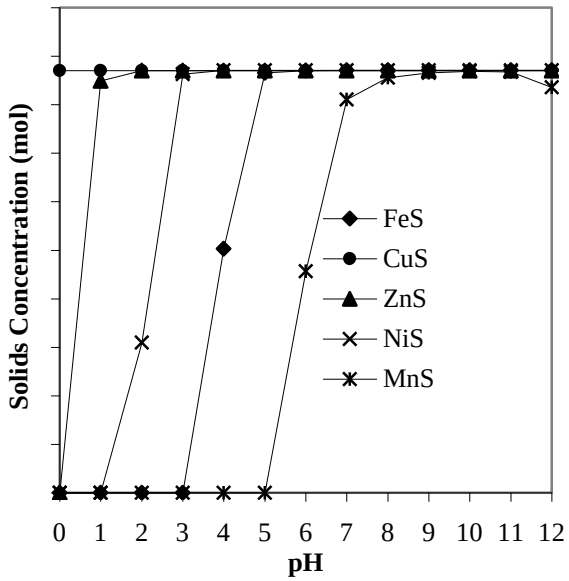

Figure 2.7: pH-dependent solubility of different metal sulphides (OLI Systems Inc, 2010).

The pH-dependent solubility of different metal sulphides has been successfully used to selectively recover metals ions from complex and simple mixed metal systems. Tokuda et al (2008) studied the reaction kinetics and selective precipitation of Cu, Zn, Ni and Sn with gaseous hydrogen sulphide in a single-metal and a multi-metal (Cu-Zn-Ni or Sn-Zn) model wastewater systems. The pH value was controlled at 1.5 for CuS and SnS precipitation, 4.5 for ZnS precipitation and between 6.4 and 7.0 for NiS precipitation. In all cases, the amount of metal ions precipitated from solution was almost complete and this was achieved using stoichiometric amounts of hydrogen sulphide. The selectivity of the process was found to be higher in the Cu-Zn-Ni system and more than 91% in the Sn-Zn system. The reaction rates obtained were found to be similar in both systems, indicating that precipitation of a specific metal was not affected by the presence of other metal ions. Tabak et al (2003) studied selective and sequential precipitation of metal ions from AMD using biologically produced hydrogen sulphide. The average precipitation efficiencies obtained were CdS (99.7%), CoS (99.1%), CuS (99.8%), FeS (97.1%), MnS (87.4%), NiS (47.8%) and ZnS (100%). The purity of the precipitates was more than 70% in all cases. Sampaio et al (2009) also investigated selective precipitation of copper from water containing both Cu and Zn in a continuously stirred tank reactor (CSTR) using controlled Na_2S addition at pH 3. The precipitation efficiency of the process and the purity of the precipitate produced were found to be almost 100%.

2.5.3.2. Reagent ratio

van Hille et al (2005) studied the effect of reagent ratio on copper sulphide precipitation in a seeded fluidised bed reactor using precipitation efficiency, precipitate recovery and morphology to quantify the process. The results of the study showed that the reagent molar ratio had a significant effect on the precipitation efficiency, recovery as well as the morphology of the copper sulphide precipitate. At low copper to sulphide molar ratio (i.e. excess sulphide concentration), the amount of metal ions precipitated from the solution was high but a very fine amorphous copper sulphide precipitate was formed. This led to difficulty in the recovery of the precipitate. Similar results were reported by Veeken et al (2003a) for an investigation into the effect of controlled sulphide addition on the precipitation efficiency and the size of the particles produced during zinc sulphide precipitation in a continuously

University of Cape Town

stirred tank reactor (CSTR). Shea and Helz (1988) suggested that the efficiency of the process was affected by the possible formation of soluble metal polysulphide complexes when an excess amount of sulphide was present in solution during the precipitation process. Consequently, Veeken et al (2003b) developed a new technique to control the amount of free sulphide present in solution during the precipitation process. In this technique, the sulphide sensitive (pS) electrode is used in combination with the pH electrode to control the amount of sulphide added to the reactor, by first measuring the amount of free sulphide present in solution.

2.5.3.3. Chelating agents and/or additives

Metal sulphide precipitation processes are affected by the presence of chelating agents or admixtures in solution. The presence of these substances influence the particle rate processes, the precipitate characteristics and the chemical composition of the precipitate (Söhnel and Garside, 1992). Bhattacharyya and Ku (1984) studied the precipitation behaviour of different metal sulphides in the presence of different chelating agents. The presence of strong chelating agents such as EDTA in solution was found to significantly reduce the precipitation efficiency for metal sulphides of higher solubility (e.g. ZnS and NiS) but had little effect on the more sparingly soluble metal sulphides (e.g. CuS and CdS). Additionally, the study showed that the presence of high concentrations of citrate caused partial dissolution of copper sulphide and the removal of cadmium was affected by the presence of nickel. Kim et al (2002) also showed that the removal of Ni, Zn and Pb by sulphide precipitation was affected by the presence of EDTA even though it had no effect on Cu removal.

Esposito and co-workers (2006) studied the effect of various substances (i.e. phosphate, EDTA, acetate, micro-nutrients and bicarbonate ions) on the particle characteristics of the precipitate produced during zinc sulphide precipitation using biologically produced sulphide. According to their findings, the presence of these substances in solution during the precipitation process has some effect on the size of the particles produced. The presence of bicarbonate ions in solution, however, was reported to have no effect on the characteristics of the resulting metal precipitate.

University of Cape Town

van Hille et al (2004) investigated the effect of adding different amounts of bicarbonate ions to the sulphide solution during metal sulphide precipitation. The bicarbonate ions were shown to be indirectly involved in the precipitation process. The morphology of the precipitates obtained, however, was found to be altered by the change in the concentrations of bicarbonate ions added. This was attributed to the effect of bicarbonate ions on the aqueous sulphide speciation.

2.5.3.4. Mixing

Due to the sparingly soluble nature of most precipitating systems, precipitation process are often characterised by reaction kinetics which are faster than the mixing time. In such processes, the product quality is strongly influenced by the manner in which the reactants are mixed and precipitates with varying particle size and morphology can be produced (Gösele and Kind, 1991). Therefore, mixing plays a very important role during precipitation of sparingly soluble compounds.

Precipitation reactions are traditionally conducted in stirred tank reactors. The hydrodynamics of a stirred tank reactor, however, vary spatially both in terms of meso-, micro- and macro-mixing (Torbacke and Rasmuson, 2001). Consequently, the spatial distribution of the supersaturation produced and thus, the characteristics of the particles produced vary from location to location inside the reactor. In recent years, several other reactor technologies, such as the fluidised bed reactor (Seckler et al, 1996; Zhou et al, 1999; Lee et al, 2001; Guillard et al, 2001; van Hille et al, 2005; Taty Costodes and Lewis, 2006) and the bubble column reactor (Wachi and Jones, 1991; Rigopoulos and Jones, 2001; Al-Tarazi, 2004) have been proposed as alternatives for precipitation of sparingly soluble compounds. However, the hydrodynamics of such systems are very complex. Kind (2002) proposed the use of the Y and the T-mixer during precipitation of sparingly soluble compounds. These types of mixing device render mixing as a non-limiting step during precipitation of sparingly soluble compounds and make the study of the precipitation kinetics of sparingly soluble compounds possible. Chiang et al (2007) investigated the use of the Y and the T-mixer for particle size control during manganese sulphide precipitation. The results of the investigation showed that the particle size distribution of the particles obtained using these devices was narrower than that obtained when the

University of Cape Town

reagents were added directly into the reactor. Al-Tarazi et al (2005) used the laminar jet reactor to eliminate the effects of mixing in order to study the fast precipitation kinetics of copper sulphide using gaseous H_2S as a precipitating reagent. The data produced showed that such a reactor could be successfully used to study the fast nucleation kinetics of metal sulphides.

2.6. Research motivation

The use of biosulphidogenic processes for the production of sulphide and bicarbonate alkalinity has the potential to position metal sulphide precipitation as a viable option for large scale treatment of acidic effluents. A substantial amount of research has been conducted to develop a fundamental understanding of the biological sulphate reduction process (Dvorak et al, 1992; Chang et al, 2000; Hao et al, 2007; Kaksonen et al, 2003; Oyekola et al, 2009) and numerous novel treatment technologies, based on sulphate reduction, have been successfully developed and implemented at industrial scale (Rowley et al, 1997; Dvorak et al, 1992; Rose et al, 2000; Hulshoff Pol et al, 2001; van Houten et al, 2006; Huismann et al, 2006). However, a number of challenges still exist around the precipitation step, particularly where the recovery of valuable metals is desired.

Due to the low solubility of metal sulphides and the high affinity between the reactants, metal sulphide precipitation reactions are inherently driven by very high levels of supersaturation. As a result, metal sulphide precipitation reactions are difficult to control and a large number of small particles are formed during the process. This leads to significant technical challenges with respect to solid-liquid separation and subsequent recovery of the precipitate. According to Luther and Rickard (2005), the particles produced during metal sulphide precipitation processes can be small enough to behave as dissolved species and complex up to 90 – 100% of the dissolved metal ions.

In order to obtain metal sulphide precipitates with good solid-liquid separation characteristics, effective control of the precipitation process is necessary. For optimal control and proper design of the precipitation process, the influence of operational and material parameters on the precipitation process must be known (Söhnel and Garside,

University of Cape Town

1992). The effect of process parameters on the practical aspects of metal sulphide precipitation and the mechanisms involved in particle formation are documented in literature (Veeken at al, 2003a; Veeken et al, 2003b; Al-Tarazi, 2004; Peters et al, 1984). However, much of the reported literature is empirical or illustrates feasibility and thus, the mechanistic relationship between operating conditions, process efficiency and the characteristics of the resulting particles is still not well understood. Franke and Mersmann (1995) studied the correlation between operating conditions and kinetic parameters as well as the product characteristics for precipitation of sparingly soluble substances (i.e. $CaSO_4.2H_2O$ and $CaCO_3$). The study showed that the dependence of the particle rate processes on the operational parameters determines the final product characteristics and in cases where mixing is rate limiting, the product characteristics are highly dependent on the design of the crystallizer, the specific power input and the reactant concentration. In recent years, considerable effort has been expended on the development of precipitation processes that produce precipitates with controlled properties (Bénet et al, 2002). The seeded fluidised bed reactor is one option that has been used for the precipitation of sparingly soluble metal salts (Seckler, 1994; Zhou et al, 1999; Guillard et al, 2001; van Hille et al, 2005; Aldaco et al, 2005). The reactor provides an ideal environment for controlled metal precipitation in a stable and easily controlled system. The large surface area provided by the seeds favours heterogeneous nucleation and facilitates operation with a slightly supersaturated solution to avoid spontaneous nucleation of small particles with poor solid-liquid separation characteristics. Seckler et al (1996) studied phosphate removal in a seeded fluidised bed reactor and showed that aggregation of the small particles produced during the process was important for optimum phosphate removal. The study suggested that the aggregation process could be improved by spreading the supersaturation more evenly throughout the reactor. Taty Costodes and Lewis (2006) adopted this approach and studied the use of multiple reagent feed points up the height of the reactor for nickel hydroxy-carbonate precipitation. The study showed that the amount of small particles or fines produced during the process could be effectively reduced by the use of multiple reagent feed points.

The fundamental studies into the mechanistic aspects of metal sulphide precipitation, on the other hand, are far more advanced (Shea and Helz, 1988; Rickard, 1995; Pattrick et al, 1997; Luther et al, 1999; Rozan et al, 2000; Luther et al, 2002;

University of Cape Town

Rickard and Luther, 2005; Sukola et al, 2005; Ciglenečki et al, 2005). However, the fundamental studies have not been effectively integrated with the applied studies that focus on metal removal and process efficiency. The fundamental work is typically restricted to very low concentrations and highly controlled environments, which are of limited value in most process based hydrometallurgical and wastewater treatment applications (Lewis, 2010).

The main objective of this study was to bridge the gap between the fundamental and practical aspects of metal sulphide precipitation by developing a clearer understanding into the relationship between operating conditions, process efficiency and particle characteristics. An original intention was to extend the approach of using a seeded fluidised bed reactor to manage the high levels of supersaturation and the resulting small particles produced during metal sulphide precipitation.

2.7. Research hypotheses

- The production of very small particles, with poor solid-liquid separation characteristics, during metal sulphide precipitation is caused by the high affinity between the reacting species and spontaneous formation of primary particles by homogeneous nucleation. Thus, by effectively controlling the inherently high levels of supersaturation associated with metal sulphide precipitation processes the particle characteristics can be improved.

- The surface properties of colloidal particles produced during metal sulphide precipitation processes are influenced by the conditions under which the particles are produced. Integration of sulphide precipitation fundamentals with an understanding of process conditions will provide predictive information on particle surface properties, allowing strategies for process improvement to be rationally developed.

University of Cape Town

2.8. Research objectives

Based on the previous research reviewed in the preceding sections and the hypotheses described above, the following objectives were developed for the current work.

1. To extend the approach used in other systems to manage the high levels of supersaturation produced during metal sulphide precipitation.

2. To investigate the effect of processing conditions on the characteristics of the precipitate produced during metal sulphide precipitation.

3. To study the effect of post-precipitation conditions on the surface properties of colloidal particles produced by sulphide precipitation for the downstream processing options.

University of Cape Town

CHAPTER 3
MATERIALS AND METHODS

3. Background

This chapter provides a detailed description of the materials and methods used in this study. The theoretical aspects of the methods used to analyse the data are also discussed.

3.1. Experimental set-up

3.1.1. Fluidised bed reactor

The reactor consisted of a Perspex column with an internal diameter of 2.6 cm and a total height of 175 cm. Reagent inlet (feed) ports and sampling ports were located at various points along the height of the reactor. The reagent inlet points were placed 10 cm apart, except for the first two inlet points which were placed 30 cm apart, starting 5 cm from the base of the reactor. Each inlet point was sealed with a rubber septum and a stainless steel tube (0.4 cm) protruding through the septum was used to inject the reagents into the bed. At the top of the column, there were two outlets which were used for recirculation and overflow of the treated water (i.e. effluent). A spherical glass bead, with a diameter of 1.5 cm, was used at the bottom of the reactor to support the seeds and allow for uniform distribution of the upward liquid flow. Figure 3.1 shows a schematic representation of the fluidised bed reactor set-up.

University of Cape Town

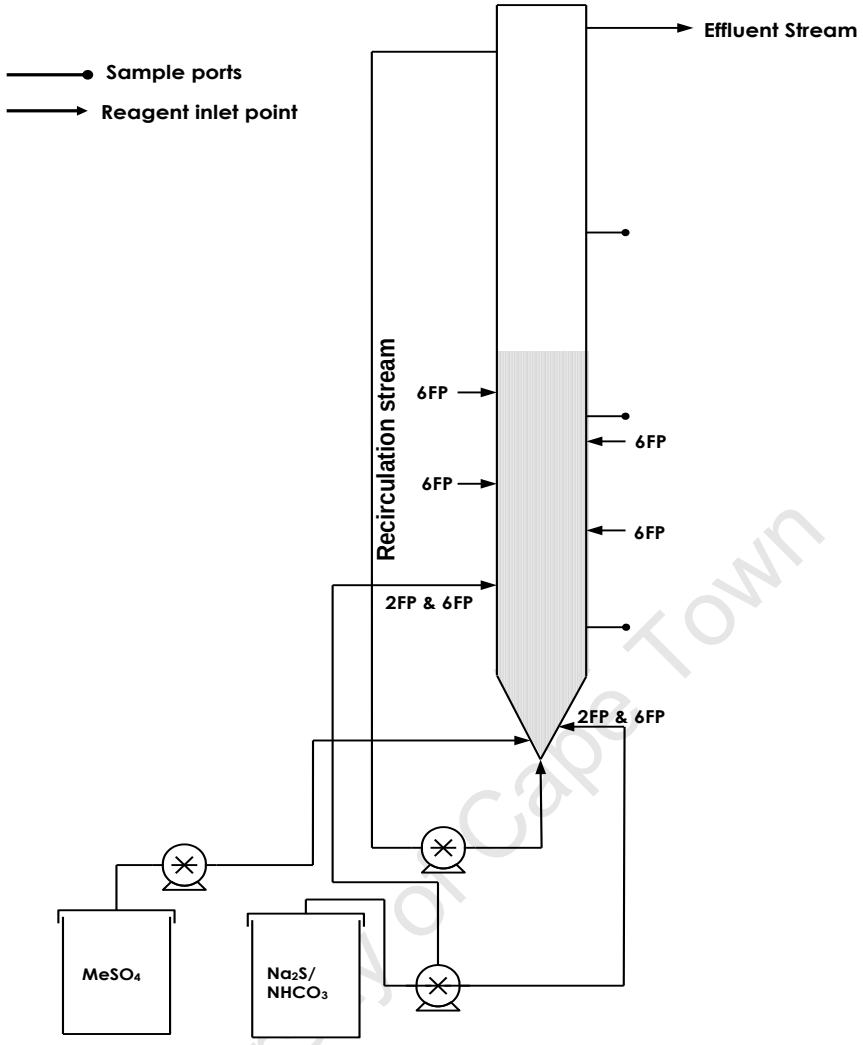

Figure 3.1: Schematic representation of the fluidised bed reactor set-up.

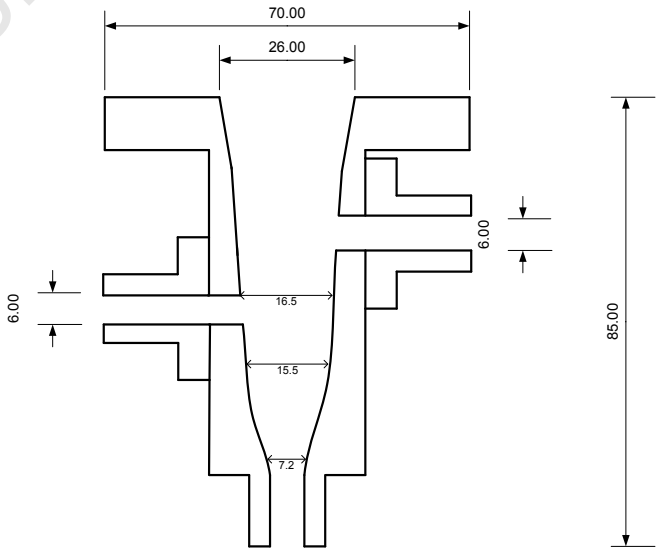

University of Cape Town

Figure 3.2: Details of the lower part of the fluidised bed reactor (measurements in mm).

The metal solution was pumped into the reactor using an inlet point located 3 cm from the base of the reactor. The re-circulation stream was pumped into the reactor from the bottom of the column and it was used to help fluidise the bed. Air was excluded from the system, as air bubbles ascending through the column could result in the loss of seed material to the re-circulation or effluent streams. Samples were collected in the recirculation flow outlet (i.e. 160 cm) and from three sampling points placed 40 cm apart up the height of the column, starting 30 cm from the base of the reactor. Each sampling port was sealed with a rubber septum and liquid samples were withdrawn from the centre of the column using a hypodermic syringe and a needle.

3.1.2. Continuously stirred tank reactor (CSTR)

The continuously stirred tank reactor experiments were performed in a 1.0 L glass vessel with a working volume of 900 mL. The reactor was equipped with four baffles and an outlet for the effluent. Mixing was achieved using an overhead stirrer fitted with a Rushton turbine. The impeller had four blades with a 5.6 cm diameter. The top of the reactor was covered with a lid that had ports for a pH electrode, reagent inlet, impeller shaft and nitrogen gas inlet. A schematic representation of the reactor set-up is shown in Figure 3.3.

University of Cape Town

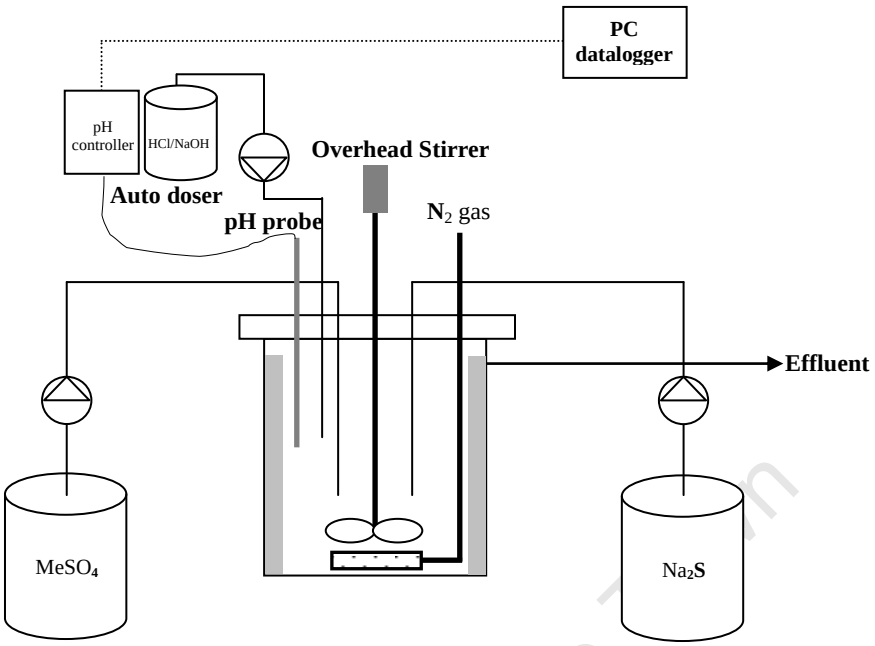

Figure 3.3: Schematic representation of the continuously stirred tank reactor set-up.

The metal and the sulphide solutions were pumped into the reactor using pre-calibrated Watson Marlow 520S (Falmouth, UK) pumps. A pH stat device (Metrohm 800 Dosino, Switzerland), in combination with a sulphide resistant pH electrode (Metrohm AG, Switzerland) was used for measuring and controlling the pH at a desired value by automatically dosing with 0.5 M HCl/1.0 M NaOH. The dosing device was connected to a computer unit equipped with control software (tiamo^{TM} version 1.2, Metrohm AG, Switzerland) for data logging and data was logged every 2 seconds.

3.1.3. Semi-batch reactor

Semi-batch experiments were conducted in a 2.0 L glass vessel. The reactor was equipped with four equally spaced baffles. Mixing was achieved using an overhead stirrer fitted with a Rushton turbine. The impeller had four blades with a 5.6 cm diameter The top of the reactor was covered with a lid that had ports for pH electrode, reagent inlet, impeller shaft and nitrogen gas inlet. Figure 3.4 shows a schematic representation of the reactor set-up.

University of Cape Town

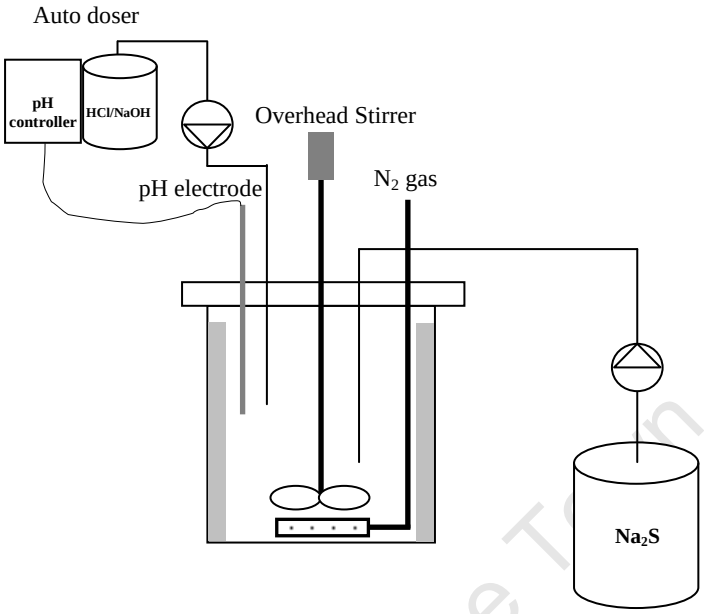

Figure 3.4: Schematic representation of the semi-batch reactor set-up.

For precipitation experiments requiring pH control, a pH stat device (Metrohm 800 Dosino, Switzerland), in combination with a sulphide resistant pH electrode (Metrohm AG, Switzerland), was used for measuring and controlling the pH at a desired value by automatically dosing with 0.5 M HCl/1.0 M NaOH. The dosing device was connected to a computer unit equipped with a control software (tiamo^{TM} version 1.2, Metrohm AG, Switzerland) for data logging and data was logged every 2 seconds.

3.2. Reagents

All the reagents ($CuSO_4.5H_2O$, $ZnSO_4.7H_2O$, $Na_2S.9H_2O$, $Ca(NO_3)_2.14H_2O$, $Al_2(SO_4)_3.18H_2O$, KCl, NaOH and HCl) used in this study were analytical grade chemicals obtained from Merck and Sigma-Aldrich. The solutions were made up to required concentrations using Millipore de-ionised water.

University of Cape Town

3.3. Analytical methods

3.3.1. Analysis of dissolved metal concentration

The concentration of dissolved metal ions was measured using atomic absorption spectroscopy (Varian SpectrAA 110) in an air-acetylene flame. The unfiltered samples collected from the fluidised bed reactor experiments were acid digested before analysis to dissolve all the fine particles that were present in the sample. The method used for acid digestion is described in detail in Appendix F.

3.3.2. pH measurements

The pH was measured using a Microprocessor pH Meter (pH 212) from Hanna Instruments. The pH electrodes were calibrated at pH 4 and 10 using pH buffer solutions (Merck) before every experiment.

3.3.3. Sulphide analysis

Total dissolved sulphide concentration was measured spectrophotometrically at 670 nm, following the colour development of methylene blue resulting from the reaction between the sulphide and the colorimetric reagent (*N*,*N*-dimethyl-*p*-phenylenediamine sulphate) in acid medium. Ferric chloride was used as a catalyst for this reaction (Cline, 1969). An appropriate volume of the sample was added to 200 µL of 1% zinc acetate immediately after the sample was collected from the reactor. This was diluted up to 5 mL using de-oxygenated water. A volume of 500 µL *N*,*N*-dimethyl-*p*-phenylendiamine hydrochloride solution and 500 µL of ferric chloride were added to the diluted sample. The sample was then thoroughly mixed and allowed to react for 15 minutes before the sulphide concentration was measured using a Merck Spectroquant® NOVA 60.

3.3.4. Alkalinity test

University of Cape Town

Bicarbonate alkalinity was analysed by titrating 5 mL samples with 0.1 N H_2SO_4 to pH 4.5 according to the standard method by APHA (1975) (APHA method number 2320). H_2SO_4 was continuously added using a burette while the pH was concurrently monitored. The volume of acid added was recorded at the pH end points, 8 ± 0.2 and 4.5 respectively. Values of the volume of H_2SO_4 utilised in titration were used to calculate the concentration of bicarbonate alkalinity. See Appendix F for calculation details.

3.3.5. Precipitate characterisation

Chemical and micro-structural analyses of the precipitates were conducted using X-ray diffraction (XRD) and scanning electron microscopy (SEM). Energy-dispersive X-ray spectrometry (EDX, employing an EDAX® analytical EDX system with SEM-EDS internal standard) was used for semi-quantitative elemental analysis of the precipitate. A PANalytical X'Pert Pro powder diffractometer with X'Celerator detector and variable divergence- and fixed receiving slits with Fe filtered Co-Kα radiation was used for XRD analysis. The XRD phases were indentified using X'Pert high score plus software and the relative amounts (weight %) were estimated using the Rietveld method (Autoquan Program). The precipitates were stored in an oxygen-free dessicator, before and after analysis, to minimise oxidation.

3.3.6. Particle size distribution measurement and analysis

The particle size distribution of the precipitates and suspended fine particles were measured using laser diffraction techniques (Malvern Mastersizer, MS S LB model and Malvern Zetasizer, Nano ZS model). All the PSD measurements were done within 5 minutes of collecting the samples.

The Malvern Mastersizer and Zetasizer gave the particle size distribution results as a volume distribution. This was converted to the number distribution according to the method described in Appendix C. A technique based on the moment transformation of the number density function n(L), described by Randolph and Larson (1988), was used to derive and describe the particle size distribution related information. This

University of Cape Town

technique has been successfully used by Bramley et al (1996), Ntuli and Lewis (2007) and Hove et al (2008).

3.3.7. Zeta potential measurements

The zeta potential of the particles was measured using the dynamic back light scattering technique (Malevern Zeta sizer, Nano ZS model). In all cases, the zeta potential of the particles which remained in suspension after the settled particles were removed from suspension was measured. Five measurements were carried out on all samples to ensure the reliability of the obtained results. An example showing the reproducibility of the zeta potential measurements is shown in Appendix D.

3.3.8. Settling measurements

The settling rate of the precipitate was measured by transferring the contents of the reactor into an Imhoff settling cone and measuring the change in the height of the suspension over time for two hours. The results were analysed in terms of the ratio between the initial suspension height (h0) and the final settled volume (h).

3.4. Techniques for process efficiency analysis

The process efficiency in the fluidised bed reactor was defined in terms of the total amount of metal ions precipitated from solution (i.e. conversion) and the amount of the precipitated metal sulphide recovered from suspension (i.e. removal efficiency) according to Equation 3.1 and 3.2, respectively;

$$\text{Conversion}(\%) = \frac{\text{Me}^{2+}_{\text{in}} - \text{Me}^{2+}_{\text{out,dissolved}}}{\text{Me}^{2+}_{\text{in}}} \text{x} \frac{100}{1} \qquad 3.1$$

$$\text{Removal Efficiency}(\%) = \frac{\text{Me}^{2+}_{\text{in}} - \text{Me}^{2+}_{\text{out,total}}}{\text{Me}^{2+}_{\text{in}}} \text{x} \frac{100}{1} \qquad 3.2$$

where Me^{2+}_{in} is the actual amount of metal ions reacting inside the reactor in mg L^{-1} (calculated as shown in Appendix A), $Me^{2+}_{out,dissolved}$ is the concentration (mg L^{-1}) of

University of Cape Town

the metal ions remaining in the filtrate after filtration using a 0.2 µm nylon membrane filter. Note that particles smaller than 0.2 µm would be considered here. $Me^{2+}_{out,total}$ represents the total metal concentration from the sample containing both dissolved metal ions and fine particles which could not be recovered from suspension (mg L^{-1}). The difference between the two terms is the amount of metal sulphide particles which remain in suspension as fines:

$$\text{Fines}(\%) = \text{Conversion}(\%) - \text{Removal Efficiency}(\%) \quad 3.3$$

For all the other reactor configurations, process efficiency was determined based on the amount of metal ions precipitated from solution according to Equation 3.4

$$\text{Process efficiency}(\%) = \frac{Me^{2+}_{feed} - Me^{2+}_{out,dissolved}}{Me^{2+}_{feed}} \text{x} \frac{100}{1} \quad 3.4$$

where Me^{2+}_{feed} is the initial metal concentration fed into the reactor (mg L^{-1}) and $Me^{2+}_{out,\ dissolved}$ is the concentration of the metal ions in the outlet stream or the concentration of metal ions which remained in solution after the precipitation reaction (mg L^{-1}).

The solution supersaturation was expressed in terms of the solubility product according to Equation 3.5;

$$S = \left(\frac{IAP}{K_{sp}} \right)^{\frac{1}{\nu}} \quad 3.5$$

where IAP is the ion activity product of the lattice ions in solution, K_{sp} is the solubility product of the salt and ν is the number of ions in a formula unit of the salt and it is equals to 2 in this case.

3.5. Experimental procedures

3.5.1. Effect of sulphide source on copper and zinc precipitation

University of Cape Town

All the experiments were conducted at room temperature (25 ± 2°C) using acid washed borosilicate glassware. Metal stock solutions were made up to a concentration of 1.574 mM. Sulphide and bicarbonate stock solutions were made up to 50 mM and 100 mM, respectively. Bacterial sulphate reduction reactor effluent was obtained from Dr Oluwaseun Oyekola (Centre for Bioprocess Engineering Research, UCT). The reactor was fed modified Postgate medium, with lactate as the sole carbon source, containing 2.5 g L^{-1} sulphate. The digester overflow had a pH of 7.80, an aqueous sulphide concentration of 33 mM and a bicarbonate concentration of 133.6 mM. A portion of the overflow was centrifuged at 7 000 rpm for 10 minutes to remove the bacterial cells and particulate organic matter. The centrifugation had no effect on the pH or sulphide concentration, but the bicarbonate concentration was reduced to 126.3 mM.

The experiments were performed in triplicates with a minimum of six metal to sulphide molar ratios, ranging from 0.5 to 2 and a bicarbonate to sulphide molar ratio of 4:1. A stoichiometric amount of sulphide bicarbonate mix (synthetic or biogenic in nature) was added to a 100 mL metal solution. The flasks were stoppered and placed on an orbital shaker for 120 minutes. The pH was measured after 1, 30, 60 and 120 minutes. After 60 and 120 minutes, a 10 mL sample was removed for metal analysis. A portion of the sample was filtered through a 0.2 µm nylon membrane filter, a portion centrifuged at 5 000 rpm for 5 minutes and another portion allowed to settle for 10 minutes. The metal concentration was determined in the filtrate and supernatants, respectively.

University of Cape Town

3.5.2. Effect of supersaturation control on process efficiency and particle characteristics

All the experiments were conducted at room temperature (25 ± 2°C) using the laboratory scale seeded fluidised bed reactor. At the start of each experiment, the reactor was filled to a resting height of 30 cm with silica sand (250 – 500 µm) as the seed material. Synthetic solutions containing a mixture of sulphide and bicarbonate ions were introduced via reagent feed points along the side of the reactor. The use of two (2FP) and six (6FP) reagent inlet points, and varying recirculation flow rates to

manage the high levels of supersaturation produced near the reagent inlet points was studied. Table 3.1 shows the operational conditions used for the experiments.

Table 3.1: Experimental conditions for the seeded fluidised bed reactor experiments.

Parameter	**Value**
Inlet Me^{2+} concentration	150 mg L^{-1}
Bed height at zero flow	30 cm
Inlet Me^{2+}/S^{2-} molar ratio	1:1
Inlet S^{2-}/HCO_3^- molar ratio	1:4
Inlet S^{2-}/HCO_3^- flow rate	120 mL min^{-1}
Inlet Me^{2+} flow rate	60 mL min^{-1}
Re-circulation flow rates	300 and 120 mL min^{-1}
Number of reagent feed points	2FP and 6FP

All the experiments were conducted for 360 minutes and samples were collected from each sampling port at varying time intervals. The sample bottles used for collecting the samples were acid washed, rinsed several times with Millipore water and dried in an oven before use. Two portions of the sample (20 mL each) were collected from each sampling port during each time interval. The one portion was filtered through a 0.2 μm nylon membrane filter and analysed to determine the dissolved metal concentration. This allowed supersaturation to be followed as a function of reactor height and time. The other portion was used to determine the pH at each axial position, the total metal concentration and the particle size distribution of the suspended solids. At the end of each experiment, the settling rate of the precipitate which could not be recovered from suspension was also measured.

The precipitate used for morphological and micro-structural analysis was obtained by removing the precipitate-rich liquor from the bottom of the reactor at the end of each experiment followed by freeze-drying for 48 hrs. The precipitate coated seed material (i.e. silica sand) was also removed from the reactor at the end of each experiment to determine the extent of coating using scanning electron microscopy (SEM).

University of Cape Town

3.5.3. Effect of reaction conditions on particle characteristics

The experiments were conducted at room temperature using a 1 L glass vessel operated as a continuously stirred tank reactor. The reactor was first filled with 900 mL of Millipore water and the water was de-oxygenated by bubbling with nitrogen gas for 20 minutes. Mixing was achieved using a Rushton turbine connected to an overhead stirrer at 620 rpm. After 20 minutes, the nitrogen gas flow rate was adjusted to maintain a slight positive pressure in the headspace. The reagents were then pumped into the reactor at the same flow rate (50 mL min^{-1}). The total flow rate of the reagents was kept constant at 100 mL min^{-1} in all the experiments while the initial metal ion (i.e. copper and zinc) concentration was kept constant at 500 mg L^{-1}. The operating pH was controlled at a desired level by adding required amounts of 0.5 M HCl or 1.0 M NaOH using the auto dosing device (Metrohm 800 Dosino, Switzerland).

A 25 mL sample was collected from the effluent stream every 10 minutes over a period of 90 minutes. The sample bottles used for collecting the samples were acid washed, rinsed several times with Millipore water and dried in an oven before use. A portion of the collected sample was used for particle size distribution (PSD) measurements. Another portion of the sample was used to measure the zeta potential of the particles which remained in suspension after the settled particles were removed. The effect of ionic strength and suspension pH on the zeta potential of the particles was established in a separate study (Chapter 6). The remaining portion of the sample was filtered through a 0.2 μm nylon membrane filter and used to determine the amount of metal ions remaining in solution. The settling rate of the precipitate was measured by transferring the contents of the reactor into an Imhoff settling cone and measuring the change in the height of the suspension over time for two hours.

University of Cape Town

3.5.4. Effect of post-precipitation conditions on surface properties of colloidal metal sulphide precipitates

3.5.4.1. Metal precipitation

Metal precipitation experiments were conducted in a 2.0 L glass vessel operated as a semi-batch reactor. Mixing was achieved using a Rushton turbine connected to an overhead stirrer at 620 rpm. The reactor was first filled with 1.5 L of the standard metal sulphate solution containing 2000 mg L^{-1} of the metal ions (i.e. copper or zinc ions). The metal solution was de-oxygenated by bubbling with nitrogen gas for 20 minutes. After 20 minutes, the nitrogen gas flow rate was reduced to maintain a slight positive pressure in the headspace. The metal ions were precipitated from solution by titrating with a standard sodium sulphide (3500 mg L^{-1}) solution. The sulphide solution was added to the reactor at a flow-rate of 11.5 mL min^{-1} using a pre-calibrated Watson Marlow 520S pump (Falmouth, UK). A pH stat device (Metrohm 800 Dosino, Switzerland), in combination with a sulphide resistant pH electrode (Metrohm AG, Switzerland), was used for measuring and controlling the pH at a desired value by automatically dosing with 0.5 M HCl/1.0 M NaOH. The copper sulphide precipitation reaction was conducted at pH 4.5 and the reaction for precipitation of the zinc ions was carried out at pH 6.

The sulphide solution was titrated into the reactor until the stoichiometrically equivalent amount of sulphide ions had been added. After sulphide addition, the reaction mixture was stirred for an additional 10 minutes before a 20 mL sample was collected from the reactor and filtered through a 0.2 μm nylon membrane filter. The filtrate was used to determine the concentration of the metal ions remaining in solution. The remaining reaction mixture was freeze dried for 48 hours. The freeze dried solids were washed several times with de-oxygenated water to remove any water soluble (non-sulphide) precipitates and the suspension from the final wash solution was freeze dried for another 48 hours. Subsequently, chemical and micro-structural analyses were performed on the precipitate.

University of Cape Town

3.5.4.2. Surface studies

The experiments for the surface studies were conducted using the experimental set-up shown in Figure 3.4. The reactor was first filled with 650 mL of the background electrolyte solution (1 – 100 mM KCl). The solution was de-oxygenated by bubbling with nitrogen gas for 20 minutes. After 20 minutes, the nitrogen gas flow rate was reduced to maintain a slight positive pressure in the headspace. The precipitate (0.25 g) was transferred to the reactor as a 100 mL suspension. After the suspension was added to the reactor, the reactor was allowed to equilibrate for 20 minutes before a required amount of the appropriate reagent was added to the reactor. For pH adjustments, standard solutions of 0.1 M HCl and 0.1 M NaOH solutions were used and a standard sodium sulphide solution (3500 mg L^{-1}) was used for the sulphide addition experiments. The cation addition experiments were conducted using standard solutions containing 0.5 M calcium and aluminium ions. Each time before and after the reagent was added to the reactor, the suspension was allowed to equilibrate for 20 minutes before sample collection. Thermodynamic modelling (OLI Stream Analyser ver.2) was used to determine the change in the ionic strength of the suspension when different reagents were added. The results showed that the major changes happened when the suspension pH was below pH 2 and above pH 11. As a result, all the experiments were conducted within this pH range, except for the experiments were the pH was naturally changed by the added reagent.

The bottles used for sample collection were acid washed, rinsed several times with Millipore water and dried in an oven before use. A 25 mL sample was collected from the reactor and a portion of the collected sample was used for particle size distribution measurements. Another portion of the sample was used to measure the zeta potential of the particles which did not readily settle.

University of Cape Town

CHAPTER 4
EFFECT OF SUPERSATURATION CONTROL ON PROCESS EFFICIENCY AND PARTICLE CHARACTERISTICS

4. Background

Metal sulphides are sparingly soluble in nature and very high levels of supersaturation are generally encountered during metal sulphide precipitation processes. According to Söhnel and Garside (1992), when the level of supersaturation produced during the precipitation process is very high, primary homogenous nucleation becomes the dominant mechanism by which primary particles are formed and this leads to production of very small particles. To produce precipitates with desirable particle characteristics (e.g. good solid-liquid separation characteristics), the level of supersaturation created during the precipitation process should be controlled such that primary particles are mainly formed through heterogeneous and/or secondary nucleation (Mersmann, 2001).

The level of supersaturation produced during crystallization of readily soluble compounds is usually controlled by the use of low reagent concentrations (Mullin, 2001). However, during precipitation of sparingly soluble compounds the supersaturation is high (i.e. $> 1 \times 10^3$) even at low reagent concentrations (Söhnel and Garside, 1992; Kind, 2002). For optimal control of precipitation processes, new innovative technologies are required (Bénet et al, 2002). The use of gaseous precipitating reagents in a bubble column has been proposed to control the high levels of supersaturation produced during precipitation of sparingly soluble compounds (Mishra and Kapoor, 1978; Wachi and Jones, 1991). In this technique, the rate at which supersaturation is generated is controlled by the mass transfer resistance of the gas dissolution. In addition, sulphide enters the reactor in a diffuse manner, from the bubbles, rather than from a point source as is typically the case with aqueous sulphide addition. The technique has been applied to different systems (Oktabyaş et al, 1994; Hammack et al, 1994; Wachi and Jones, 1990) and the kinetics of gas dissolution (Hostomsky and Jones, 1995; Higbie, 1935) and the hydrodynamics of such systems have been extensively studied and reviewed (Jones et al, 1992; Wachi and Jones,

University of Cape Town

1995; Rigopoulos and Jones, 2001). Al-Tarazi et al (2004) developed a mathematical model that describes precipitation of metal sulphides from aqueous solutions containing two different metals. The model predicts the rate of H_2S absorption, the size distribution of metal sulphide crystals and the selectivity of precipitation.

The seeded fluidised bed reactor has been demonstrated as a viable alternative for controlled precipitation of sparingly soluble metal salts (Seckler, 1994). The process is based on precipitation of metal salts onto the pre-classified seed material in a fluidised bed. Precipitation is induced by the addition of a precipitating reagent into the reactor. The seeds inside the reactor help promote heterogeneous primary nucleation and/or secondary nucleation. The reactor is also operated with a recirculation stream, which helps to reduce the level of supersaturation by diluting the concentration of the reagents fed into the reactor (Seckler et al, 1996; Zhou et al, 1999). Although it is difficult to achieve perfect mixing with an even distribution of supersaturation, in such a system, a flow pattern intermediate between the perfectly mixed and plug-flow configuration is possible (Taty Costodes and Lewis, 2006).

The seeded fluidised bed reactor technology was first developed for softening of drinking water (Graveland et al, 1983) as well as for the removal of phosphates from wastewater (Seckler, 1994; Battistoni et al, 2001). The technology was later extended to the removal of heavy metals from wastewater (Wilms and van Dijk, 1988; Zhou et al, 1999; Guillard and Lewis, 2001; Lee et al, 2004; van Hille et al, 2005; Aldaco et al, 2005). van Hille and co-workers (2005) studied the feasibility of copper sulphide precipitation in a seeded fluidised bed reactor and showed that the amount of copper ions removed from solution was very high, but most of the resulting copper sulphide precipitate left the reactor in the effluent streams as fine particles, rather than depositing onto the seeds. Lewis and van Hille (2006) studied copper, nickel and cobalt sulphide precipitation in a seeded fluidised bed reactor using different initial metal concentrations. The study showed that the amount of metal ions removed from solution and the resulting metal precipitate recovered from suspension were influenced by the initial metal concentration for nickel and cobalt. At low initial metal concentrations metal removal from solution and precipitate recovery from suspension were high but this was reduced when the initial metal concentration was high.

University of Cape Town

Seckler et al (1996) studied the mechanisms involved in particle formation during calcium phosphate precipitation in a seeded fluidised bed reactor and showed that aggregation of the small particles produced during the process was important for optimum phosphate removal. The study suggested that the aggregation process could be improved by distributing the supersaturation more evenly through the reactor and increasing the hydraulic retention time. Taty Costodes and Lewis (2006) adopted this approach and studied the use of multiple reagent feed points up the height of the reactor for nickel hydroxy-carbonate precipitation. The amount of small particles (fines) produced inside the reactor was significantly reduced when multiple reagent feed points were used. This was attributed to effective control of the high levels of supersaturation produced near the reagent inlet point.

In this chapter, the aim was to investigate the effect of supersaturation control on process efficiency and particle characteristics for metal sulphide precipitation in a seeded fluidised bed reactor using multiple reagent feed points and different recirculation flow rates. The investigation was carried out by first assessing the effect of biological and synthetic sulphide sources on copper and zinc precipitation. Synthetic solutions containing a mixture of sulphide and bicarbonate ions were, subsequently, used for metal precipitation in the fluidised bed reactor. The use of two (2FP) and six (6FP) reagent feed points and two different recirculation flow rates (i.e. 300 and 120 ml min^{-1}) was studied for copper and zinc sulphide precipitation reactions.

University of Cape Town

4.1. Materials and methods

4.1.1. Experimental design

The experimental program was divided into two parts. The first part was designed to assess the effect of sulphide source on copper and zinc precipitation. Batch experiments were conducted using synthetic solutions (sulphide and bicarbonate) and overflow from a bacterial sulphate reduction reactor. For the latter, experiments were conducted with either raw effluent or effluent that had been centrifuged at 7000 rpm for 10 minutes to remove cells and particulate organic matter. The effect of metal to

sulphide molar ratio on precipitation efficiency was investigated and the results for the three different reagents were compared.

In the second part of the study, copper and zinc sulphide precipitation experiments were conducted in a laboratory scale seeded fluidised bed reactor using synthetic solutions containing a mixture of sulphide and bicarbonate ions. The use of multiple reagent feed points and decreased recirculation flow rate to manage the high level of supersaturation near the reagent inlet points were studied. The multiple reagent feed points investigation was carried out using two (2FP) and six (6FP) inlet points at a recirculation flow rate of 300 mL min^{-1}. The recirculation flow rate study was conducted using the 2FP reactor configuration for zinc sulphide precipitation at two different flow rates (i.e. 300 and 120 mL min^{-1}). The process was characterised by measuring the amount of the metal ions precipitated from solution (i.e. conversion), the amount of metal precipitate recovered from suspension (i.e. removal efficiency) and the particle size distribution and zeta potential of the small particles which could not be recovered from suspension (i.e. fines) as a function of reactor height and time. All the experiments in this investigation were carried out in triplicates to verify the repeatability and reproducibility of the results.

University of Cape Town

4.1.2. Experimental procedure

The reactor set-up, analytical techniques and experimental procedures used in this investigation are described in detail in Sections 3.1.1, 3.3, 3.5.1 and 3.5.2.

4.2. Results and discussion

4.2.1. Effect of sulphide source on copper and zinc precipitation

The results obtained for copper and zinc sulphide precipitation using synthetic sulphide and digester overflow after 120 minutes are shown in Figure 4.1. The results in Figure 4.1(B) show that the amount of zinc ions precipitated from solution was not affected by the sulphide source for all metal to sulphide molar ratios tested. However, the pH was slightly lower in the biological system. This was attributed to the presence of residual organic acids, mainly acetate, which originated from the growth medium.

For metal to sulphide molar ratios below 1, an excess amount of sulphide was present in solution and the pH was significantly higher in the synthetic system, given the absence of organic acids.

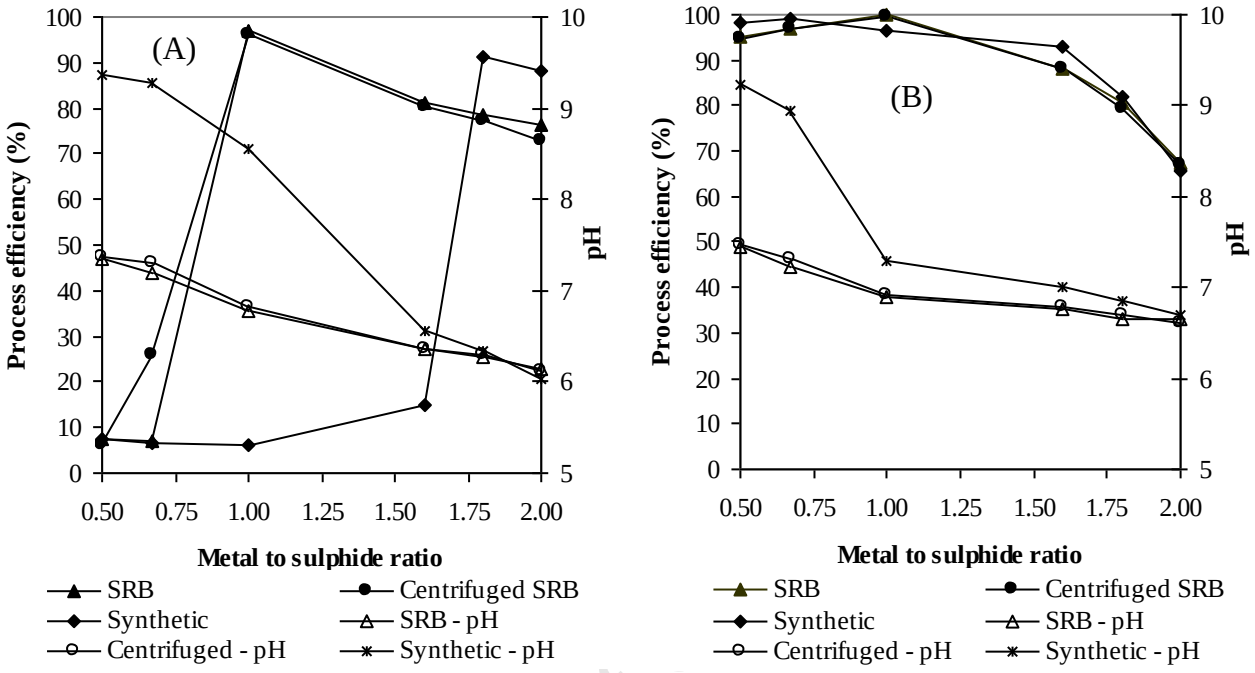

Figure 4.1: Change in process efficiency and pH as a function of metal to sulphide molar ratio after 120 minutes for (A) copper and (B) zinc sulphide precipitation reactions carried out batch-wise using different sulphide sources at an initial metal concentration of 1.574 mM.

The trends for copper sulphide precipitation (Figure 4.1(A)) were found to be significantly different from those obtained for zinc despite the fact that the reagent conditions (i.e. metal to sulphide molar ratio, sulphide to bicarbonate ratio and the amount of dissolved organic acids) were similar for both systems. The difference in pH and process efficiency when metal to sulphide molar ratio was above 1 was attributed to the difference in the amount of copper and zinc ions that were precipitated from solution as hydroxides. Excess metal ions were present in solution when metal to sulphide molar ratio was above 1 and some of these were precipitated as copper hydroxide or hydroxy-sulphate. Thermodynamic modelling (Visual MinteQ ver. 3.0) confirmed that these precipitates are less soluble than the corresponding zinc forms at the pH values observed, accounting for the difference in the two systems. An example of the Visual MinteQ calculation is shown in Appendix I and the results

University of

predicted 100% copper sulphide precipitation when the metal to sulphide molar ratio was stoichiometric or excess sulphide was present in solution.

When the metal to sulphide molar ratio was below 1.6, for the synthetic sulphide system, a significant decrease in the amount of copper removed from solution was observed. A decrease in the amount of copper removed from solution, however, was only obtained when the metal to sulphide molar ratio was below 1 in the biological systems. The observed difference in the amount of copper removed from solution, on the one hand, can be explained according the formation of very small copper sulphide particles, which passed through a 0.2 µm filter and could not be sedimented by centrifuging at 5 000 rpm, as a result of very high supersaturation. The presence of dissolved organic acids in the digester overflow led to this phenomenon only being observed at a lower metal to sulphide molar ratio. The organic acids buffered the system at a lower pH value, effectively pushing the sulphide speciation equilibrium to produce lower amount of reactive sulphide specie (i.e. HS^-). In the presence of excess sulphide, the organic acids were no longer able to buffer the pH as effectively and this led to an increase in the amount of reactive sulphide species and high levels of supersaturation. Consequently, the amount of copper removed from solution was only decreased at a lower metal to sulphide molar ratio due to formation of very small copper sulphide particles when excess sulphide was present in solution.

Another possible explanation for the observed difference in the results for copper removal is the sulphide induced reduction of Cu(II) to Cu(I). Pattrick et al (1997) showed that 1 mole of Cu(II) is reduced by 0.5 moles of sulphide during copper sulphide precipitation and the precipitate that is predominantly formed during copper sulphide precipitation is covellite (CuS) which is a Cu(I) compound. Thus, a rapid drop in process efficiency for copper when the metal to sulphide molar ratio was below 1.6, in the case of synthetic sulphide, suggests reduction was possibly the dominant process. In the case of the biological sulphide, the reduction process might have been suppressed by the chelating effect of the organic acids that were present in the sulphide solution. Strong Cu(II) chelators shift the Cu(II)/Cu(I) redox potential downwards, making the reductants less effective (Bhattacharyya and Ku, 1984).

University of Cape Town

4.2.2. Process efficiency in the fluidised bed reactor

Data showing the establishment of pseudo-steady state and reproducibility of the results from the seeded fluidised bed reactor experiments are shown in Appendix A. All data presented as a function of reactor height, in this chapter, were obtained after operating the reactor for 270 minutes.

If the fluidised bed reactor is considered to be a plug-flow, the concentration of the reactants and products change progressively as the material passes through the reactor. Figure 4.2 shows the results for the change in process efficiency as a function of reactor height for copper and zinc sulphide precipitation conducted using two (2FP) and six (6FP) feed point reactor configurations. The results show that the concentration of dissolved metal ions was reduced up the height of the reactor in all cases. According to Figure 4.2(A), the amount of copper ions consumed at the bottom of the reactor was low at ± 35% when the 2FP configuration was used, but an increase of ± 10% was obtained as the material progressed up the height of the reactor.

When 6FP was used, the amount of copper precipitated at the bottom of the reactor was high (± 75%), but appeared to decrease up the height of the reactor and stabilise at ± 45%. Neither of these observations were consistent with predicted copper sulphide precipitation. This phenomenon is discussed in greater detail, in relation to the particle size data, below.

In the case of zinc, the amount of dissolved metal ions precipitated from solution was very high at the bottom of the reactor when 2FP was used, reaching almost 100% within the first 30 cm. Only ± 50% of the dissolved material was precipitated at the bottom of the reactor for the 6FP but the amount of the precipitated zinc ions was gradually increased up the height of the reactor reaching almost 100%.

University of Cape Town

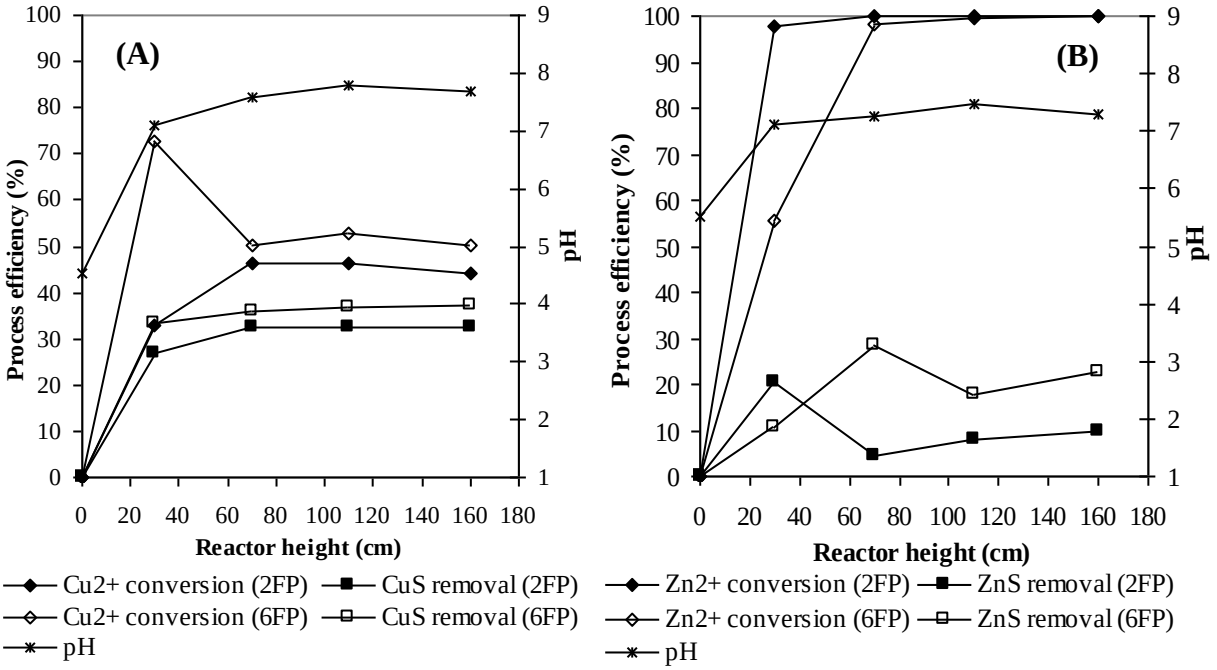

Figure 4.2: Process efficiency and pH as a function of reactor height for (A) copper and (B) zinc sulphide precipitation reactions carried out using two (2FP) and six (6FP) reagent feed points in a fluidised bed reactor using metals solutions containing 150 mg L^{-1} metal ions and metal to sulphide molar feed ratio of 1.

The results obtained for copper were unexpected since copper sulphide is highly insoluble and, if copper and sulphide ions are reacted in stoichiometric amounts, thermodynamic predictions indicate almost 100% of the dissolved copper should react to form an insoluble copper sulphide precipitate (Appendix I). The results for the particle size distribution of the fine copper sulphide particles (Figure 4.4(A)), which could not be recovered from suspension, showed that the particles had a mean particle size less than 0.1 μm. Since the amount of copper ions precipitated from solution was quantified in terms of the material that passed through a 0.2 μm filter, the very small copper sulphide particles were included in the filtrate. The actual amount of copper precipitated was likely substantially higher than this value. Evidence for this was provided by the dark brown colour of the filtrate. This result highlighted the challenges associated with the recovery of very fine copper sulphides.

The data for 6FP reactor configuration at the first sample point (30 cm) is also inconsistent with only copper sulphide precipitation. Based on stoichiometry, less than 20% of the copper should have been removed as copper

University of Cape Town

sulphide. The additional copper conversion at this point can be attributed to the formation of copper hydroxide ($Cu(OH)_2$) or brochantite ($Cu_4(OH)_6SO_4$), as a consequence of the pH. These precipitates are larger than the pore size of the filter and were therefore retained. The extent of copper recovery decreased after this point, to approximately 50%, due to the conversion of hydroxide precipitates to fine grained sulphides following further sulphide addition. Additional evidence for this is presented in the particles size discussion.

The difference observed in the amount of zinc precipitated at the bottom of the reactor when the 2FP and 6FP reactor configurations were used was attributed to the change in the amount of sulphide fed into that part of the reactor. The amount of sulphide added to the bottom part of the reactor was three times higher when the 2FP configuration was used and this resulted in an increased amount of metal removal. Zinc sulphide precipitation was characterised by a distinct induction time (Appendix B), which helped facilitate the formation of a smaller number of larger particles (Figure 4.4(B)). These larger particles did not pass through the 0.2 µm filter leading to the high conversions. Despite this the system remained dominated by primary nucleation and the amount of precipitated metal salt recovered from suspension was low. In the case of the 6FP, the amount of sulphide added to the reactor was split over a larger range across the height of the reactor. Hence, the amount of zinc ions removed from solution was gradually increased up the height of the reactor. The zinc removal recorded at the first sample point was greater than anticipated based on zinc sulphide stoichiometry, suggesting some hydroxide precipitation at this point. Thermodynamic modelling (Visual MinteQ ver. 3.0) confirmed this, but to a lesser extent than for copper.

The overall zinc conversion obtained in this study was found to be significantly higher than the conversion previously reported by Lewis and van Hille (2006) for copper (65%), nickel (90%) and cobalt (80%) sulphide precipitation in a seeded fluidised bed reactor using aqueous solutions containing only sulphide ions for the same initial metal concentration and metal to sulphide molar ratios. The high metal conversion obtained was attributed to the presence of bicarbonate ions in solution during the precipitation process. A study by Karbanee et al (2008) showed that nickel sulphide precipitation was dependent on the availability of reactive sulphide species (i.e. HS^-

University of Cape Town

and S^{2-}) in solution, which was in turn dependent on the pH of the solution. Due to the buffering effect of bicarbonate ions, the pH of the solution remained relatively unchanged between pH 7 and 8. Under these conditions, sulphide speciation equilibrium tends towards HS^- ions and therefore precipitation of metal ions was enhanced. The enhanced metal precipitation, however, was obtained at the expense of particle characteristics and the amount of metal precipitate recovered from suspension was found to be generally lower than previously reported (van Hille et al, 2005; Lewis and van Hille, 2006).

When the metal solution is continuously fed at the bottom of the reactor and the incoming precipitating reagent stream creates supersaturation, nucleation occurs immediately. If the level of supersaturation produced near the reagent inlet point is controlled below the level of primary nucleation, which results in the formation of tiny particles with poor solid-liquid separation characteristics, an increase in removal efficiency is obtained (Taty Costodes and Lewis, 2006). When molal based solubility data in Table 2.2 was used to calculate the supersaturation, the supersaturation obtained at the bottom of the reactor, near the reagent inlet point, when 2FP was used for zinc sulphide precipitation was 1.04×10^6 and this was reduced to 3.82×10^5 by the use of 6FP. In the case of copper, the level of supersaturation produced at the bottom of the reactor was 4.63×10^8 for the 2FP and 1.71×10^8 for the 6FP. Although the use of six feed points did reduce the supersaturation levels, these remained well within the primary nucleation region. This supports the data, which show no significant improvement in metal sulphide recovery, associated with increasing the number of reagent feed points.

Acccording to Seckler et al (1996), the amount of precipitated metal salt recovered from suspension during metal precipitation in a seeded fluidised bed reactor is a function of the quantity of the material precipitated onto the seeds due to fine-grain aggregation, settling due to fine-fine aggregation and/or a combination of these two mechanisms. Guillard and Lewis (2001) and Taty Costodes and Lewis (2006) studied nickel carbonate precipitation in a seeded fluidised bed reactor and showed that growth of the metal precipitate onto the seed surface was the main factor responsible for removal of the formed metal precipitate from suspension. van Hille and co-workers (2005) studied copper sulphide precipitation in a seeded fluidised bed reactor

University of Cape Town

and found that the coating efficiency of the copper sulphide precipitate onto the seed surface was very poor. In the current study, the extent of metal sulphide deposition onto the seed surface was investigated by SEM on sectioned particles. The results showed that the metal precipitate layer on the seed material was insignificant (Appendix B), relative to previous studies (Guillard and Lewis, 2001; Taty Costodes and Lewis, 2006), indicating very limited heterogeneous nucleation and/or fine-grain aggregation. Zhou et al (199) investigated the effect of residence time on process efficiency for metal carbonate precipitation in a seeded fluidised bed reactor and showed that the coating efficiency of the metal precipitated was not significantly affected by the change in residence time. Hence, the effect of residence time on coating efficiency was not investigated in this study.

4.2.3. Fine particle evolution

The recovery of precipitated metal from suspension in a seeded fluidised bed reactor is affected by the formation of small particles (i.e. fines), which are difficult to recover from suspension. To investigate the progress of precipitation up the height of the reactor, the amount and characteristics of the fine particles were evaluated as a function of the reactor height.

Figure 4.3 shows the results for the change in the proportion of the feed metal reporting as fines as a function of reactor height. The results for copper are somewhat misleading as particles below 0.2 μm passed through the filter and were not recorded as converted copper. These very fine particles were not accounted for in the total fines, resulting in low values on the graph (Figure 4.3(A)). The spike in the 6FP curve at 30 cm is a consequence of the reduced amount of sulphide added to that point and the presence of larger copper hydroxide particles. The copper conversion at this point (Figure 4.2) was higher than could be accounted for by sulphide precipitation and includes hydroxide precipitates formed as a result of pH. Copper sulphide is thermodynamically more stable and upon addition of further sulphide the hydroxides would convert to very fine copper sulphide, resulting in the observed decrease in fines up the height of the reactor.

University of Cape Town

In the case of zinc, the amount of fine particles produced was substantial when the 2FP configuration was used and slightly reduced by the use of 6FP, as seen in Figure 4.3(B). These results are consistent with the process efficiency results (Figure 4.2) and show that most of the zinc sulphide formed during the precipitation process remained in suspension as fine particles. The amount of fines was slightly reduced by the use of the 6FP, as a result of the reduced supersaturation at the reagent inlet points coupled with the induction time phenomenon.

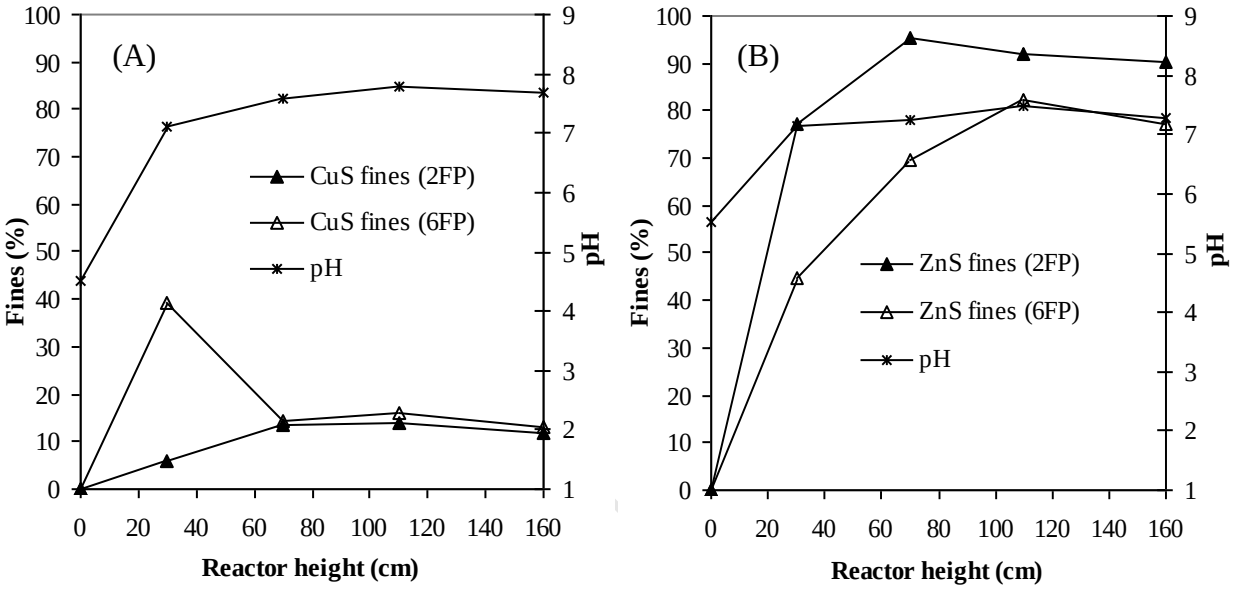

Figure 4.3: Fines concentrations and pH as a function of reactor height for (A) copper and (B) zinc sulphide precipitation reactions carried out using two (2FP) and six (6FP) reagent feed points.

The results in Figure 4.4 show the number based particle size distribution results for the evolution of fine particles up the height of the reactor. In particle technology, the particle size distribution width provides information regarding growth or condensation of the primary particles by aggregative mechanisms to form larger particles (Hove, 2008). The height of the distribution peak and the area under the graph, are directly related to the number of particles present in suspension and the shift in the location of the distribution indicates an increase (i.e. shift to the right) or a decrease (i.e. shift to the left) in the median particle size (Hove, 2008).

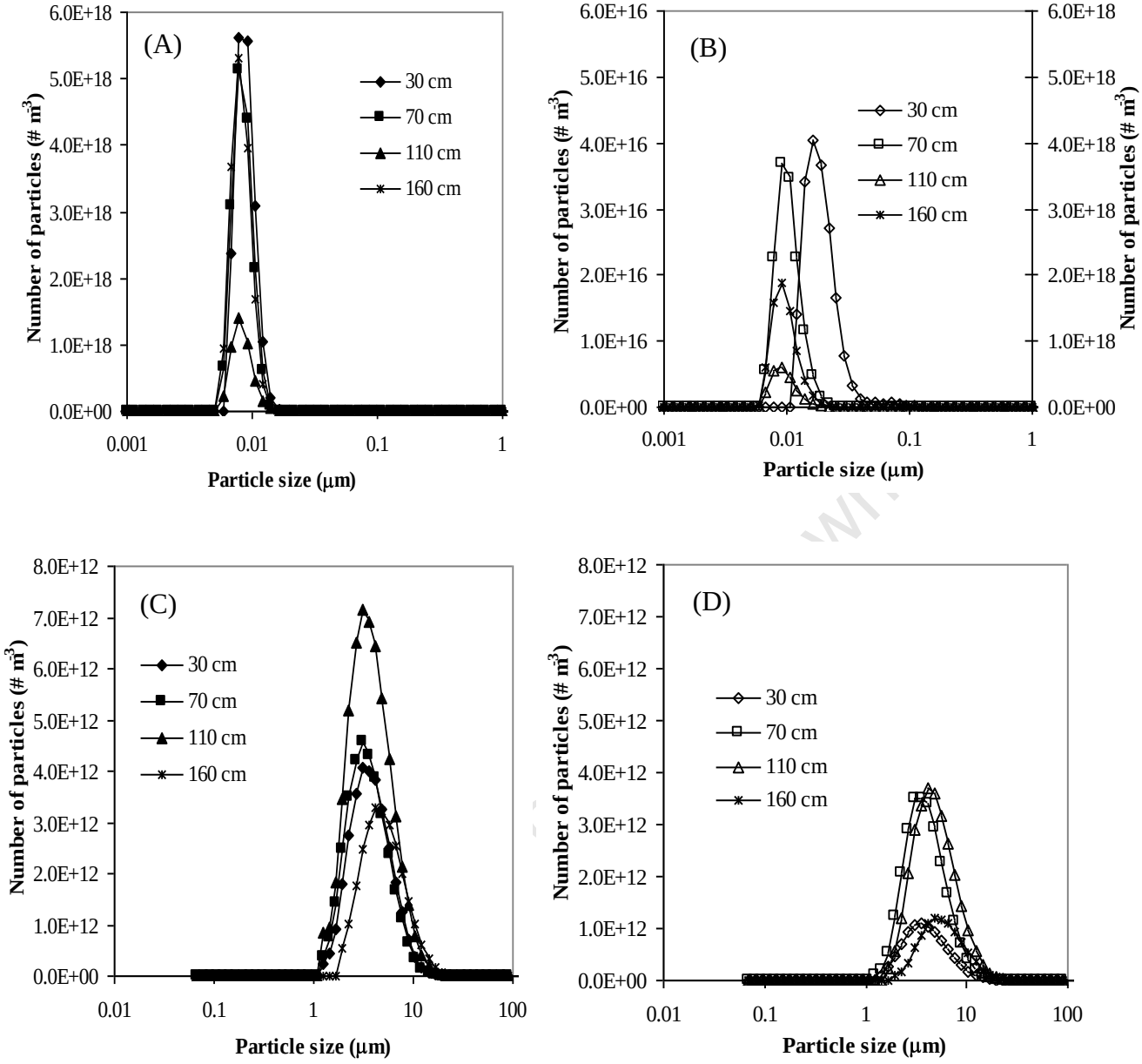

Figure 4.4: Particle size distribution of fine particles as a function of reactor height for copper 2FP (A), 6FP (B) and zinc sulphide 2FP (C), 6FP (D). Data for 70 – 160 cm in (B) represented on secondary *y*-axis.

The results for the particle size distribution of fine copper sulphide particles obtained using 2FP show that a very large number of small particles (i.e. < 0.1 μm) was already present at the bottom of the reactor (i.e. 30 cm) and this was not significantly changed up the height of the reactor. A minimum was observed at 110 cm, but the result was considered insignificant since the number of particles was very high (> 10^{18} # m^{-3}) and a decrease in particle number was less than one order of magnitude. When the 6FP was used, the particle size distribution width was relatively broad and the peak

height (particle number) at the bottom of the reactor was significantly lower (i.e. < 4.5 x 10^{16} # m^{-3}), which is consistent with the existence of both copper sulphide and copper hydroxide particles. The mean particle size shifted to the smaller size range, the distribution width became narrower and the peak height was significantly increased higher up the column as further sulphide addition led to the conversion of hydroxide precipitates to copper sulphide. For zinc sulphide precipitation, the particle number was initially low at the bottom of the reactor and increased gradually up the height of the reactor, until a decrease and a slight shift to the right was obtained at 160 cm when both 2FP and 6FP were used. However, the number of zinc sulphide fines obtained using 6FP was smaller than that obtained using 2FP in all cases.

For both the 2FP and 6FP experiments there was a significant difference between the copper and zinc data. In all cases the number of copper particles were up to four orders of magnitude higher than the corresponding case for zinc. In addition to this, the average particle size for zinc sulphide was up to 100 times larger than the copper sulphide particles. The greater width of the particle size distribution curves suggest that aggregation played a more prominent role in zinc precipitation. Despite this, coating onto the seed particles was poor.

The results in Figure 4.4 also correspond with the process efficiency data in Figure 4.2 and show that the mean particle size of the fine copper sulphide was less than 0.2 μm, the pore size of the filter used to differentiate between dissolved metal ions and fine particles. Thus, the unsual process efficiency (Figure 4.2(A)) obtained for copper can be explained taking into account the size of the fine copper sulphide particles.

To establish the solid-liquid separation characteristics of the fine particles under quiescent conditions, the settling rate of the fines was measured over a period of 2 hours. Figure 4.5 shows the results for the settling behaviour of the fine particles which could not be recovered from suspension. The results show that the zinc fines had relatively good solid-liquid separation characteristics under quiescent conditions. The copper sulphide particles, on other hand, showed very poor solid-liquid separation and remained stable in suspension.

University of Cape Town

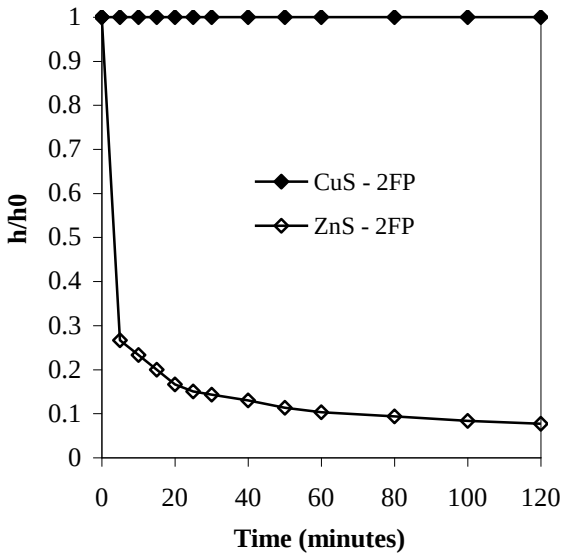

Figure 4.5: Settling characteristics of fine copper and zinc sulphide particles obtained from precipitation in a FBR using 2FP.

The effect of electrostatic forces on the kinetic stability of the fine particle suspensions was established by determining the charge on the surface of the particles using zeta potential measurements. The results for average zeta potential of the particles as a function of reactor height are shown in Figure 4.6. The magnitude of the negative zeta potential for the copper sulphide fines obtained from the bottom of the reactor was high (i.e. > – 50 mV) and the zeta potential decreased slightly up the height of the reactor when 2FP was used. When 6FP was used, the zeta potential of the fines obtained from the bottom of the reactor was around – 42 mV and remained relatively unchanged up the height of the reactor. In the case of zinc, the zeta potential of the particles remained relatively unchanged around – 10 mV when 2FP was used. The charge on the surface of the particles obtained from the bottom of the reactor was around 0 mV when 6FP was used but the magnitude of the negative zeta potential was increased up the height of the reactor reaching a maximum of ± – 10 mV at 160 cm. The magnitude of the negative zeta potential obtained for the copper sulphide particles was significantly higher than that obtained for the zinc sulphide.

University of Cape Town

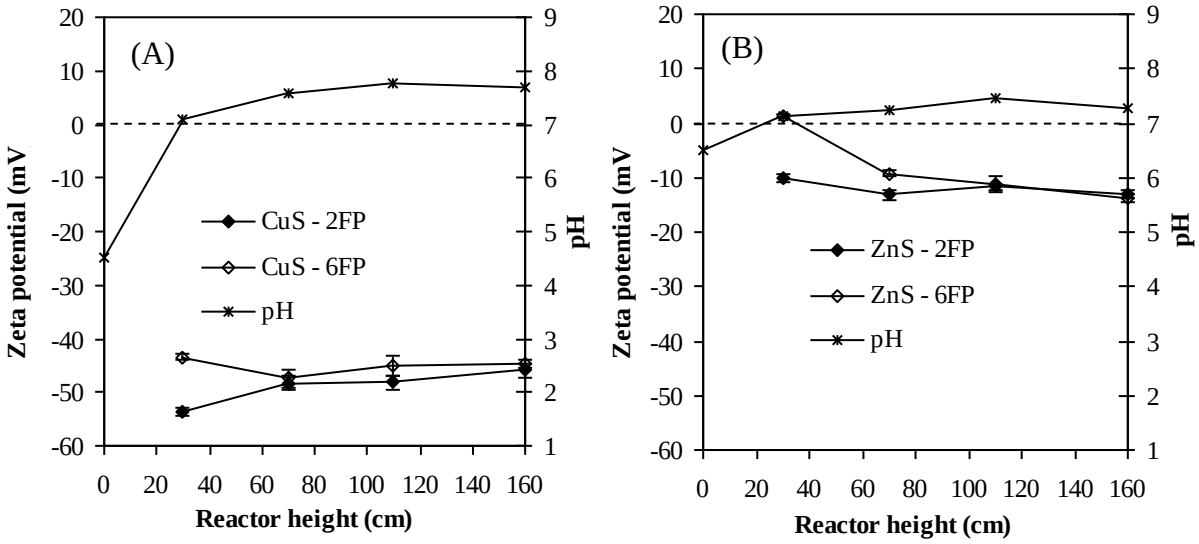

Figure 4.6: Change in zeta potential of fine particles up the height of the reactor during (A) copper and (B) zinc sulphide precipitation in FBR.

These results are consistent with the process efficiency and particle size distribution results shown in Figure 4.2 and Figure 4.4. The difference in the results obtained for copper and zinc can be explained in terms of the difference in the induction time of copper and zinc sulphide precipitation reactions and the variation in the amount of sulphide available near the reagent inlet points when 6FP and 2FP reactor configurations were used. Pattrick et al (1997) studied the reaction between copper and aqueous sulphide and showed that the reaction was almost instantaneous for concentrations below 318 mg L^{-1}, resulting in the formation of a brown Cu-S complex. Thus, when sulphide was added to the reactor the precipitation reaction was faster than the mixing time. This resulted in the formation of new copper sulphide particles before the reagents could be completely mixed (Gösele and Kind, 1991). Consequently, the copper sulphide particles were possibly exposed to unreacted sulphide which adsorbed onto the surface of the particles (Kolthoff and Moltzau, 1935). Based on the pH in the reactor, the sulphide would predominantly be in the HS^- form and its adsorption would impart a negative charge to the particle surface. Zinc sulphide precipitation, on the other hand, was characterised by an induction time in the region of 5 seconds (Appendix B) which allowed for more complete mixing of the reagents before new particles were formed. When 2FP was used, the amount of sulphide added to the bottom of the reactor was relatively high. This was reduced when the 6FP was used. As a result, the amount of free sulphide available for

University of Cape Town

adsorption onto the surface of the particles was lower, leading to the particles removed from the first sample point having less negative zeta potentials. As the fine particles travelled up the height of the reactor they were exposed to sulphide from the subsequent reagent feed points and this led to a slight increase in the magnitude of the negative zeta potential (Figure 4.6(B)). Thus, the poor settling behaviour of the copper sulphide fines can be attributed to the highly negative surface charge carried by the particles.

4.2.4. Effect of recirculation flow rate on process efficiency

The effect of recirculation flow rate on process efficiency and pH as a function of time for zinc sulphide precipitation in a seeded fluidised bed reactor is shown in Figure 4.7. This investigation was only conducted for zinc sulphide precipitation, since the particles formed during copper sulphide precipitation were too small and highly charged to undergo any significant changes due to the change in mixing efficiency and hydraulic retention time. The extent of precipitation was not affected by the change in recirculation flow rate. However, the amount of precipitate recovered from suspension and the solution pH were affected. More than 20% of the precipitated metal was recovered from suspension after 30 minutes when 300 mL min^{-1} was used. Thereafter, the amount of recovered precipitate was reduced to less than 10% and remained relatively unchanged until the experiment was terminated after 360 minutes. When 120 mL min^{-1} was used, a maximum removal efficiency of ± 20% was achieved and this remained relatively unchanged throughout the process. The pH of the solution, on the other hand, was slightly higher when low recirculation flow rate was employed.

University of Cape Town

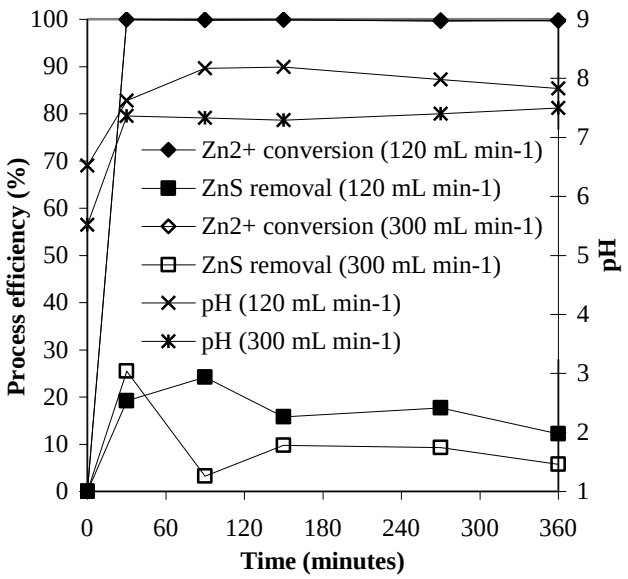

Figure 4.7: Change in process efficiency and pH as a function of time when 2FP configuration was used at two different recirculation flow rates for zinc sulphide precipitation in a FBR with an initial metal concentration of 150 mg L^{-1} and metal to sulphide molar feed ratio of 1.

The results for the amount of metal precipitated from solution showed that the extent to which the reagents were mixed had little effect on conversion and this was attributed to the reaction time being faster than the hydraulic retention time of the reactor. A decrease in removal efficiency after 30 minutes showed that the amount of precipitate retained by the reactor at high recirculation flow rate was limited. The observed change in the pH of the solution indicated a change in solution chemistry and this was attributed to a change in the extent to which the added sulphide reacted with the metal ions at the bottom of the reactor due to reduced mixing efficiency. The change in solution chemistry due to the change in mixing efficiency was also found to have an effect on the surface characteristics of the fine particles produced. Figure 4.8 shows the results for the change in zeta potential as a function of time for the fine particles produced using different recirculation flow rates.

University of Cape Town

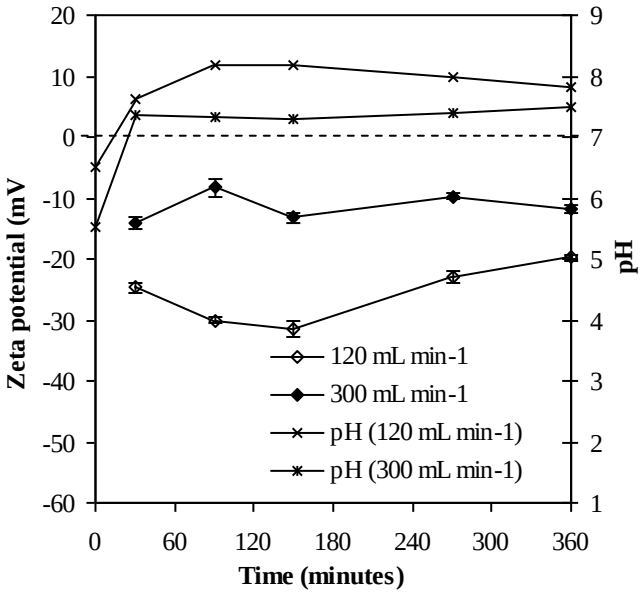

Figure 4.8: Change in zeta potential of suspended fine particles as a function of time for zinc sulphide precipitation in FBR using different recirculation flow rates.

When the recirculation flow rate was decreased the extent to which the reactants were mixed at the bottom of the reactor was also decreased. As a result, the probability of HS^- ions adsorbing to the already formed particles, rather than reacting with free metal and releasing the proton, was increased. This explains the observed increase in solution pH and the more negative zeta potential. These results show that the extent to which the reactants are mixed during metal sulphide precipitation and the time the particles spend inside the reactor has an effect on process efficiency and the characteristics of the particles produced.

University of Cape Town

4.3. Conclusions

Batch precipitation tests found that the origin of the sulphide (biogenic or chemical) did not affect the precipitation mechanism to a significant degree. In the case of zinc, similar metal removal efficiency was achieved for all metal to sulphide molar ratios tested irrespective of the sulphide source. For copper, the presence of residual organic acids in the anaerobic digester overflow helped to control the pH (pH < 7.5). This led to the formation of particles which could be recovered by filtration or centrifugation, until the metal to sulphide molar ratio dropped below 1. In the presence of a stoichiometric excess of sulphide very small particles, similar to those formed using the synthetic sulphide, dominated. However, for all molar ratios tested the recoveries

were not improved by the presence of cells and particulate organic matter, implying that primary nucleation remained the dominant mechanism. Therefore, subsequent experiments were performed with synthetic sulphide/bicarbonate solutions.

A decrease in the level of supersaturation, due to the use of multiple reagent feed points, during metal sulphide precipitation in a seeded fluidised bed reactor did not significantly affect process efficiency and the solid-liquid separation characteristics of the resulting metal precipitate. The extent of zinc precipitation was very high (almost 100%) when both 2FP and 6FP reactor configurations were used. However, most of the zinc sulphide precipitate exited the reactor in the effluent stream as fine particles. In the case of copper, the reported metal ion removal was low (i.e. ± 45%) for both the 6FP and 2FP reactor configurations due to the formation of fine particles that passed through the 0.2 μm filter. These particles were found to have a mean size of ± 0.01 μm and a very high surface charge (– 50 mV). The zinc sulphide particles, on the other hand, had a low surface charge (– 10 mV) and a mean particle size of ± 5 μm.

Under quiescent conditions, the zinc sulphide fines were effectively removed from suspension by settling while the copper sulphide fines formed a stable suspension. The difference in the characteristics of the copper and zinc sulphide particles was attributed to the difference in the induction time of these two systems and the greater adsorption of negatively charged sulphide specie (HS^-) onto the copper sulphide precipitate.

The change in recirculation flow rate was found to have a slight effect on process efficiency, pH and particle characteristics. When the recirculation flow rate was reduced from 300 mL min^{-1} to 120 mL min^{-1}, the amount of precipitate recovered from suspension was increased by almost 5%, the pH increased from pH 7.5 to pH 8 and the magnitude of the negative charge on the surface of the particles was increased from – 10 mV to – 25 mV. The change in pH and the charge on the surface of the particles was attributed to an increase in the amount of free sulphide available in nucleation volume due to a decrease in the extent to which the reagents were mixed at low recirculation flow rate.

University of Cape Town

CHAPTER 5
EFFECT OF REACTION CONDITIONS ON PARTICLE CHARACTERISTICS

5. Background

Most of the published literature on metal sulphide precipitation, related to practical applications, has focused on metal sulphide precipitation kinetics and/or the selective precipitation of metal ions from solution (Bryson and Bijsterveld, 1991; Rickard, 1995; Jandova et al, 2005, Sampaio et al, 2009) without investigating the effect of processing conditions on the nature of the resulting precipitates and their processing characteristics. Al-Tarazi (2004) studied the effect of operating conditions on the particle rate processes associated with metal sulphide precipitation under different regimes of pH, metal to sulphide molar ratio and residence time, using an MSMPR reactor. The study showed that all these factors had an effect on the particle rate processes. Veeken et al (2003a), on the other hand, studied zinc sulphide precipitation in a continuously stirred tank reactor using controlled sulphide addition at pH 6.5. The study showed that the amount of zinc precipitated from solution and the particle size of the resulting zinc sulphide precipitate were strongly affected by the concentration of sulphide present in solution. Although these studies provide important information regarding the effect of operating conditions on the particle characteristics, a fundamental understanding into the relationship between these is still lacking. The relationship between processing conditions and product characteristics during precipitation is determined and controlled by the solid-liquid equilibria, precipitation kinetics, colloid-surface chemistry and the reactor selection and design (Demopolous, 2009). The aim of this investigation was to develop a more fundamental understanding into the effect of reaction conditions on particle characteristics, taking into account the mechanism involved in particle formation and the surface chemical aspects of the particles produced.

The effect of metal to sulphide molar ratio and operating pH on the nature of the copper and zinc sulphide precipitates was investigated. Information related to the particle size distribution (PSD) and surface characteristics were used to relate the

University of Cape Town

effect of reaction conditions to the nature and the solid-liquid separation characteristics of the precipitates.

5.1. Materials and methods

5.1.1. Experimental design

The experimental programme for this investigation was divided into two phases. In the first phase, the effect of metal to sulphide molar ratio on the precipitation process at a constant pH was investigated. All the experiments were conducted at pH 6 and the effect of metal to sulphide molar ratios of 2.00, 1.00 and 0.67 on copper and zinc sulphide precipitation behaviour was investigated. In the second part of the work, an investigation into the effect of operating pH on the precipitation process was conducted. The investigation was carried out by operating the precipitation process at different pH values, while maintaining the metal to sulphide molar ratio at 0.67. For copper sulphide, pH 2, 4 and 6 and for zinc sulphide pH 3, 4, 6 and 8 were investigated. The process was characterised by studying the extent of precipitation, the particle size distribution, the surface charge carried by the particles and the settling rate of the precipitate.

5.1.2. Experimental procedure

The reactor set-up, analytical techniques and experimental procedure used in this investigation are described in detail in Sections 3.1.2, 3.3 and 3.5.3, respectively.

5.2. Results

All the results reported in this investigstion were obtained when the process was operating at steady state. The residence time in the reactor was 9 minutes and all experiments were conducted over a period of 90 minutes. Samples were collected every 10 minutes and results for the change in PSD, zeta potential and precipitated metal concentration over time showed that steady state was attained after 30 minutes for both copper and zinc sulphide precipitation (see Appendix D).

University of Cape Town

5.2.1. The effect of metal to sulphide molar ratio and operating pH on precipitation efficiency

The results for copper and zinc precipitation under conditions of different metal to sulphide molar ratio and operating pH values are shown in Table 5.1. The results show that the extent of copper and zinc precipitation increased as the amount of sulphide added, represented by a decrease in metal to sulphide molar ratio, increased. This data is consistent with results previously reported by van Hille and co-workers (2005) for copper sulphide precipitation in a fluidised bed reactor and Veeken et al (2003b) for zinc sulphide precipitation in a CSTR, using controlled sulphide addition. When more than the stoichiometric amount of sulphide was added and the operating pH was decreased, the extent of copper and zinc precipitation decreased. In all cases, the amount of copper ions precipitated from solution was higher than the amount of zinc ions precipitated. This can be attributed to the pH-dependent speciation of aqueous sulphide, as shown in Equations 5.1 and 5.2 (Migdisov et al, 2001).

$$H_2S_{(aq)} \leftrightarrow HS^-_{(aq)} + H^+_{(aq)} \qquad pK_1 = 6.99 \qquad 5.1$$

$$HS^-_{(aq)} + H^+_{(aq)} + \leftrightarrow S^{2-}_{(aq)} + 2H^+_{(aq)} \qquad pK_2 = 17.4 \qquad 5.2$$

As the operating pH of the system decreased the relative proportion of $H_2S_{(aq)}$ increased, resulting in a decrease in the amount of the species involved in the reaction (HS^- and S^{2-}) (Karbanee et al, 2008). A portion of the H_2S was lost from the system in the gaseous phase.

University of Cape Town

Table 5.1: Extent of Cu^{2+} and Zn^{2+} precipitated from solution under different conditions of metal to sulphide molar ratio and operating pH for experiments conducted in a CSTR using an initial metal concentration of 500 mg L^{-1}.

Metal to sulphide ratio	**Operating pH**	**% Cu^{2+} precipitated**	**% Zn^{2+} precipitated**
2	6	80.76 ± 1.70	57.48 ± 5.39
1	6	93.32 ± 1.61	71.54 ± 3.24
0.67	6	97.94 ± 0.29	93.54 ± 0.95
0.67	4	88.19 ± 1.17	83.27 ± 0.45
0.67	3	-	83.09 ± 1.53
0.67	2	87.54 ± 1.63	-*
0.67	8	-	99.95 ± 0.01

*ZnS was found to be soluble at pH 2.

At the highest metal to sulphide molar ratio (2), 80% of the copper was precipitated, even though stoichiometry suggests only 50% could be precipitated as copper sulphide. Modelling this situation using the thermodynamic modelling package Visual MinteQ ver. 3.0 yielded a predicted removal of over 99%, with 50% as covellite (CuS) and the remainder as brochantite ($Cu_4(OH)_6SO_4$). The presence of copper hydroxysulphate within the precipitate was confirmed by XRD analysis (results not shown). The discrepancy between predicted and measured removal was attributed to kinetic factors since model calculations are based on thermodynamic equilibria and do not take the reaction time into account. In the case of zinc, hydroxysulphate precipitates do not form under similar conditions and the model predicted 50% precipitation as zinc sulphide. In all cases where sufficient or excess sulphide was added Visual MinteQ predicted 100% metal sulphide precipitation, irrespective of pH.

5.2.2. The effect of metal to sulphide molar ratio on particle characteristics

The results for number based particle size distribution of the particles produced under different experimental conditions are shown in Figure 5.1. The secondary *y*-axis in Figure 5.1(A) represents the results obtained for metal to sulphide molar ratio of 0.67

University of Cape Town

(note scale change). The interpretation of the results for copper sulphide precipitation at a metal to sulphide molar ratio of 2 is complicated due to the formation of copper hydroxysulphate. The results in Figure 5.1(A), however, show an increased peak height and a narrower distribution in the smaller size range when copper was precipitated in the presence of excess sulphide (i.e. metal to sulphide molar ratio < 1). The peak height is directly related to the number of particles present in suspension (Hove, 2008). The data show that the total number of particles obtained was substantially higher when the metal to sulphide molar ratio was less than 1. The distribution width provides information regarding condensation of the primary particles, by aggregative mechanisms, to form larger particles (Hove, 2008). Thus, the narrow distribution in the smaller size range, obtained when the metal to sulphide molar ratio was less than 1 indicates limited condensation of the initially formed primary particles. In the case of zinc, the effect of changing the metal to sulphide molar ratio on particle number distribution was very small, having a negligible effect on both the peak height and the distribution width. The peak heights obtained for zinc were slightly smaller than those obtained for copper, in all cases, indicating that the total number of particles present in suspension was smaller. Moreover, the width of the distributions obtained for zinc, in all cases, was wider than that obtained for copper. This suggests that condensation of the primary particles, by aggregation, was more pronounced in the case of zinc than it was in the case copper.

University of Cape Town

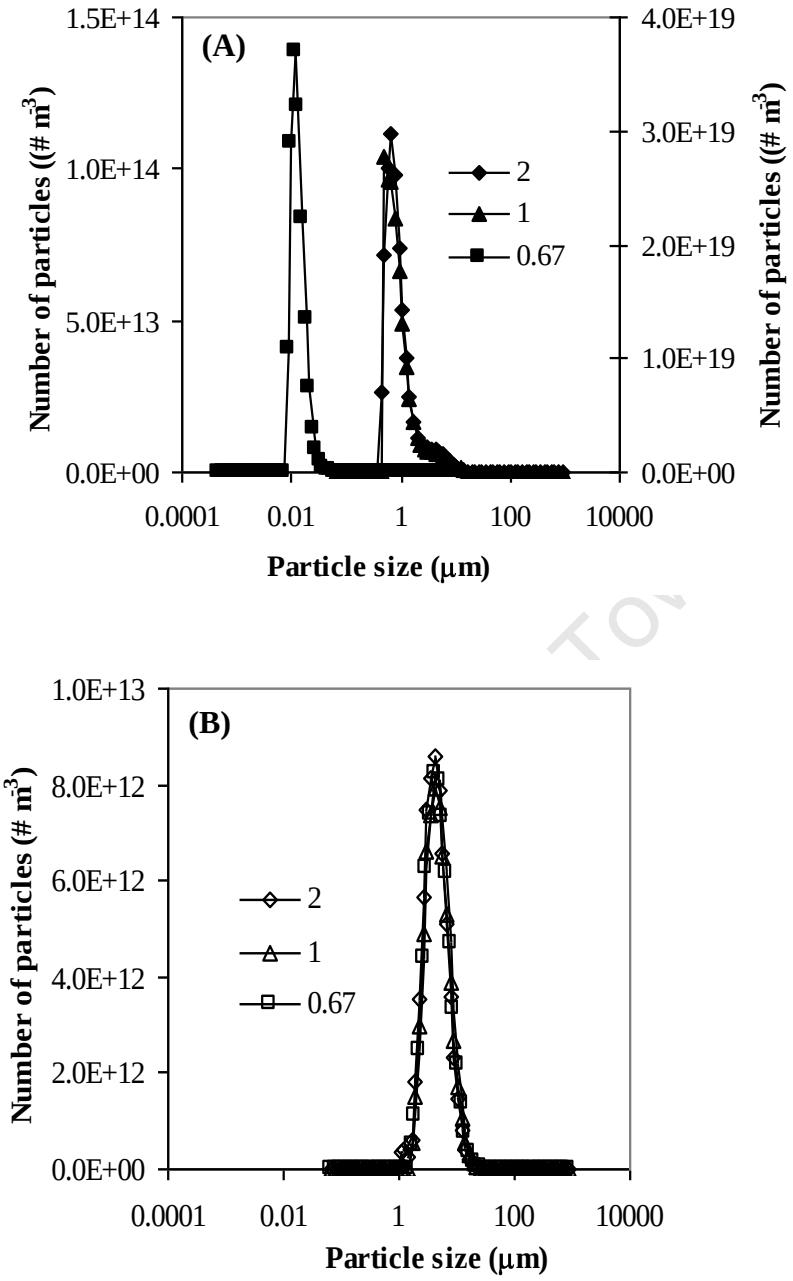

Figure 5.1: Change in PSD of (A) copper sulphide and (B) zinc sulphide precipitates as a function of metal to sulphide molar ratio at pH 6. Data for molar ratio of 0.67 in (A) represented on secondary y-axis.

Figure 5.2 shows the change in number based mean size ($\bar{L}_{1.0}$) and the second moment (*m2* – equivalent to surface area) as a function of metal to sulphide molar ratio. The $\bar{L}_{1.0}$ results, shown in Figure 5.2(A), are consistent with the number based particle size distribution data presented in Figure 5.1 and show that the number based

mean size of copper sulphide particles was always smaller than that of zinc sulphide particles produced under similar conditions. Furthermore, the number based mean size of the copper sulphide particles produced in the presence of excess sulphide was significantly smaller than that obtained in the absence of excess sulphide.

Figure 5.2(B) shows that *m2* and thus, the surface area of the copper sulphide particles increased substantially in the presence of excess sulphide (molar ratio reduced from 1 to 0.67). It decreased slightly when the ratio was changed from 2 to 1, probably due to the presence of brochantite. In the case of zinc sulphide, a decrease in metal to sulphide molar ratio resulted in a slight decrease in *m2*. The *m2* obtained for both copper and zinc sulphide was similar when the metal to sulphide molar ratios of 2 and 1 were used. This indicates that the surface area of the resulting precipitates was similar for the two metals when a stoichiometric, or less than stoichiometric, amount of sulphide was used to precipitate metal ions from solution.

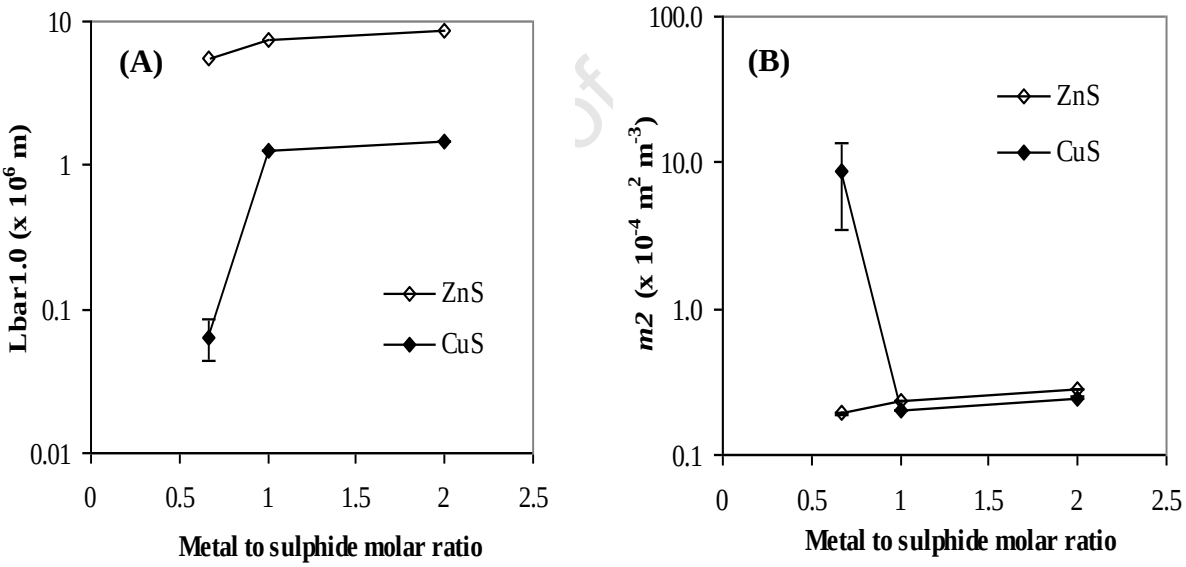

Figure 5.2: Change in (A) $\bar{L}_{1.0}$ and (B) *m2* for metal sulphide precipitates produced using different metal to sulphide molar ratios at pH 6.

Supersaturation is the thermodynamic driving force behind every precipitation process and the level of supersaturation in a precipitating system governs particle rate processes, such as nucleation, growth and aggregation (Söhnel and Garside, 1992). The level of supersaturation in a precipitating system is determined by the activity of

the reacting species and the solubility product of the precipitate. Due to the sparingly soluble nature of most metal sulphides ($K_{sp} < 10^{-15}$), metal sulphide precipitation processes are characterised by high levels of supersaturation, even at low reagent concentrations. As a result, primary nucleation is the dominant mechanism responsible for particle formation and very small particles are generally formed. The results in Figure 5.2 show that the change in sulphide availability had a relatively small effect on the size and surface area of the zinc sulphide particles, but strongly affected the size and surface area of the copper sulphide particles. The solubility product of copper sulphide is much lower than that of zinc sulphide (Table 2.2). Thus, the degree of supersaturation created during copper sulphide precipitation is naturally higher than that of a zinc sulphide system at similar reagent concentrations. While this would appear to account for the observed differences, results from previous studies by Lewis et al (2008) showed that a substantial change in supersaturation during metal sulphide precipitation had a negligible effect on the particle size of the final product produced during metal sulphide precipitation. This was due to the fact that even at reagent concentrations below 0.1 mM the supersaturation was still in the region dominated by primary nucleation. Similarly, the substantial differences in $\bar{L}_{1.0}$ and *m2* for copper sulphide at metal to sulphide molar ratios of 0.67 and 1 cannot be accounted for by changes in supersaturation.

In crystallisation, the overall surface area of the particles can increase as a result of breakage, nucleation or molecular growth and decrease as a result of aggregation (Ntuli et al, 2007). Nucleation and breakage result in the creation of more small particles which contribute to the increased surface area of the system. The magnitude of the increase in surface area is greater in the case of nucleation since a large number of smaller particles are created. Aggregation results in a decrease in the surface area as a result of cementation between the particles. Precipitation processes are inherently driven by very high levels of supersaturation which is rapidly reduced during nucleation. As a result growth is suppressed, leaving nucleation and aggregation as the two dominant mechanisms which determine the surface area of the resulting particles (Söhnel and Garside, 1992). The data presented in Figure 5.2 show that neither the mean particle size nor surface area change appreciably in the zinc system, suggesting the particle formation processes were not significantly affected by metal to

University of Cape Town

sulphide molar ratio. However, in the copper sulphide system the presence of excess sulphide (metal to sulphide molar ratio < 1) resulted in a large increase in particle number (Figure 5.1(A)) and overall surface area and a decrease in particle size. Reducing the metal to sulphide molar ratio from 1 to 0.67 resulted in a less than 5% increase in metal removal, therefore the observed difference cannot be attributed to enhanced nucleation, rather suggesting the suppression of aggregation in the presence of excess sulphide.

According to Kind (2002), the particles ultimately observed during precipitation processes are secondary particles, built by aggregation of primary particles. Furthermore, the stability and subsequent aggregation of the primary particles in aqueous suspension is determined by the balance between the van der Waals forces of attraction and the electrostatic forces of repulsion, due to the electrical charge on the surface of the particles (Derjaguin and Landau, 1941; Verwey and Overbeek, 1948). If the particles obtained in this study are regarded as secondary particles, as purported by Kind (2002), the charge on the surface of the particles plays an important role in aggregation of the primary particles.

Figure 5.3 shows the effect of the nature of metal sulphide particles, produced under the conditions of different metal to sulphide molar ratios, on the settling characteristics. The copper sulphide particles produced under the conditions of higher metal to sulphide molar ratio (Figure 5.3(A)) had relatively good settling characteristics, both in terms of settling rate and settled volume. However, the very small copper sulphide particles produced using metal to sulphide molar ratio less than 1 had very poor settling characteristics. On the contrary, the zinc sulphide precipitate showed relatively good settling characteristics, irrespective of the metal to sulphide molar ratio employed in the precipitation process (Figure 5.3(B)). This is consistent with the size and surface area properties (Figure 5.2). Nonetheless, the final settling volume for the zinc sulphide precipitates was, in all cases, higher than that of the copper sulphide precipitates obtained using similar metal to sulphide molar ratios. The relatively smaller settled volume of the copper sulphide can be accounted for by the smaller particle size (Figure 5.2(A)) which resulted in reduced void volume and a more compact structure.

University of Cape Town

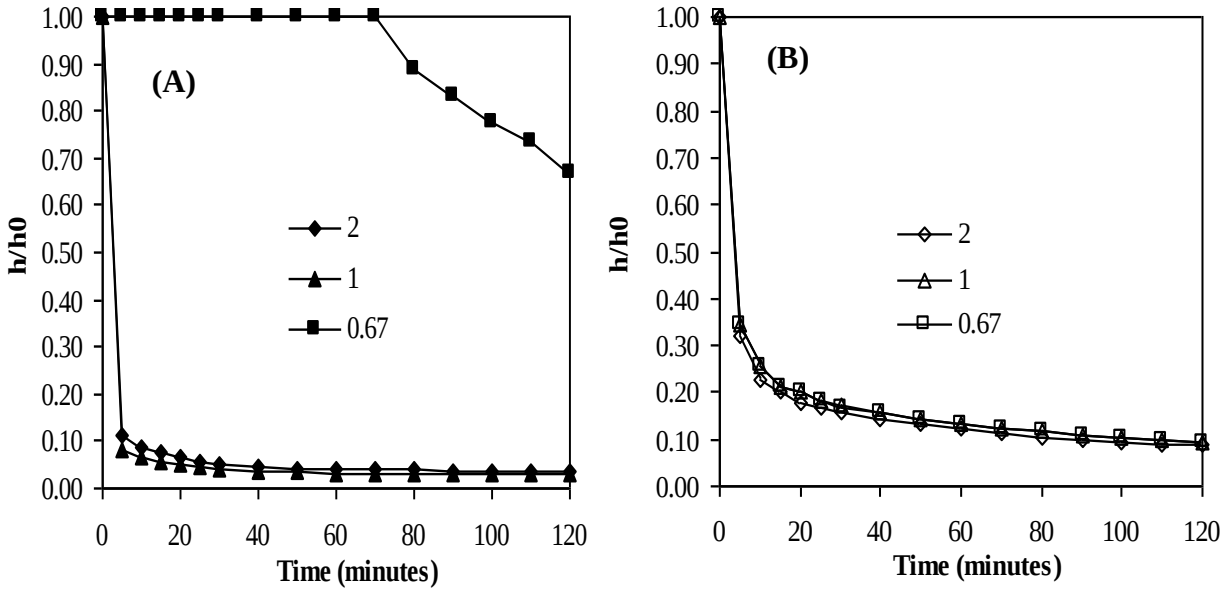

Figure 5.3: Settling rate of (A) copper sulphide and (B) zinc sulphide precipitates produced under different metal to sulphide molar ratios at pH 6.

According to DLVO theory (i.e. quantitave theory of colloid stability), the stability of the particles in aqueous suspensions is determined by the balance between the van der Waals forces of attraction and the electrical forces of repulsion due to the electrical charge on the surface of the particles (Derjaguin and Landau, 1941; Verwey and Overbeek, 1948). The electrical charge on the surface of the particles may be caused by chemical reactions at the surface, lattice imperfections and surface adsorption. Kolthoff and Moltzau (1935) observed that metal sulphides strongly adsorbed H_2S, HS^- and S^{2-}. Thus, the particles produced in the presence of excess sulphide were more likely to carry a significant surface charge and therefore become stabilised in suspension due to the electrical forces of repulsion. This phenomenon, in addition to the very small particle size, was identified as the possible reason for the poor settling characteristics of the copper sulphide precipitate produced in the presence of excess sulphide. To evaluate this, the surface characteristics of the particles which did not readily settle were investigated, using zeta potential measurements, to quantify the surface charge of the particles produced under different metal to sulphide molar ratios.

University of Cape Town

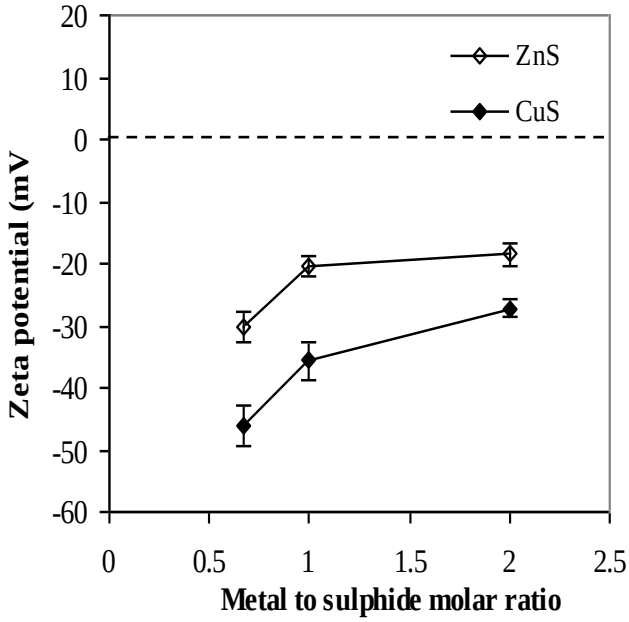

Figure 5.4: Change in zeta potential of the metal sulphide particles as a function of metal to sulphide molar ratio at pH 6.

The results depicting the surface charge of particles which did not readily settle are shown in Figure 5.4. The zeta potential became less negative with an increase in the metal to sulphide molar ratio for both copper and zinc sulphide particles. However, the magnitude of the zeta potential for the copper sulphide particles was larger than that of the zinc sulphide particles produced under similar conditions.

For the copper sulphide particles produced in the presence of excess sulphide, the zeta potential obtained was substantially more negative than that of the particles produced in the absence of excess sulphide (as seen in Figure 5.4). These results are consistent with particle number, size, surface area and settling characteristic data and suggest a situation where the high supersaturation resulted in the rapid nucleation of a large number of small particles, followed by the adsorption of excess sulphide onto the particle surface, imparting the negative charge. The surface charge suppressed aggregation of the primary particles, resulting in a substantially reduced mean particle size. The small, highly charged particles were stabilised in suspension, which resulted in the poor settling characteristics.

University of Cape Town

5.2.3. The effect of operating pH on particle characteristics

The results for the effect of operating pH on the number based particle size distribution for both copper and zinc sulphide precipitation processes are shown in Figure 5.5. The secondary *y*-axis in Figure 5.5(A) represents the results obtained when the precipitation process was conducted at pH 6. For copper sulphide precipitation, the peak height of the number based particle size distribution was significantly decreased when the operating pH was changed from 6 to 4 and the peak height increased slightly when the operating pH was further reduced from 4 to 2. The particle number distribution was also significantly shifted to the larger size range when the operating pH was decreased from 6 to 4 and slightly shifted to the smaller size range when the operating pH was further reduced from 4 to 2. The peak height is directly related to the total number of particles present in suspension and the observed decrease shows that the total number of particles present in suspension was substantially reduced when the process was operated at a lower pH. The observed increase in the distribution width when the operating pH less than pH 6 was employed, on the other hand, supports condensation of the initially formed primary particles by aggregative mechanisms and shows that copper sulphide precipitates with larger particle size were obtained when the process was operated using operational pH values less than 6. In the case of zinc, the peak height and the width of the particle number distribution were slightly increased when the operating pH less than pH 6 was employed and slightly increased again at pH 8.

University of Cape Town

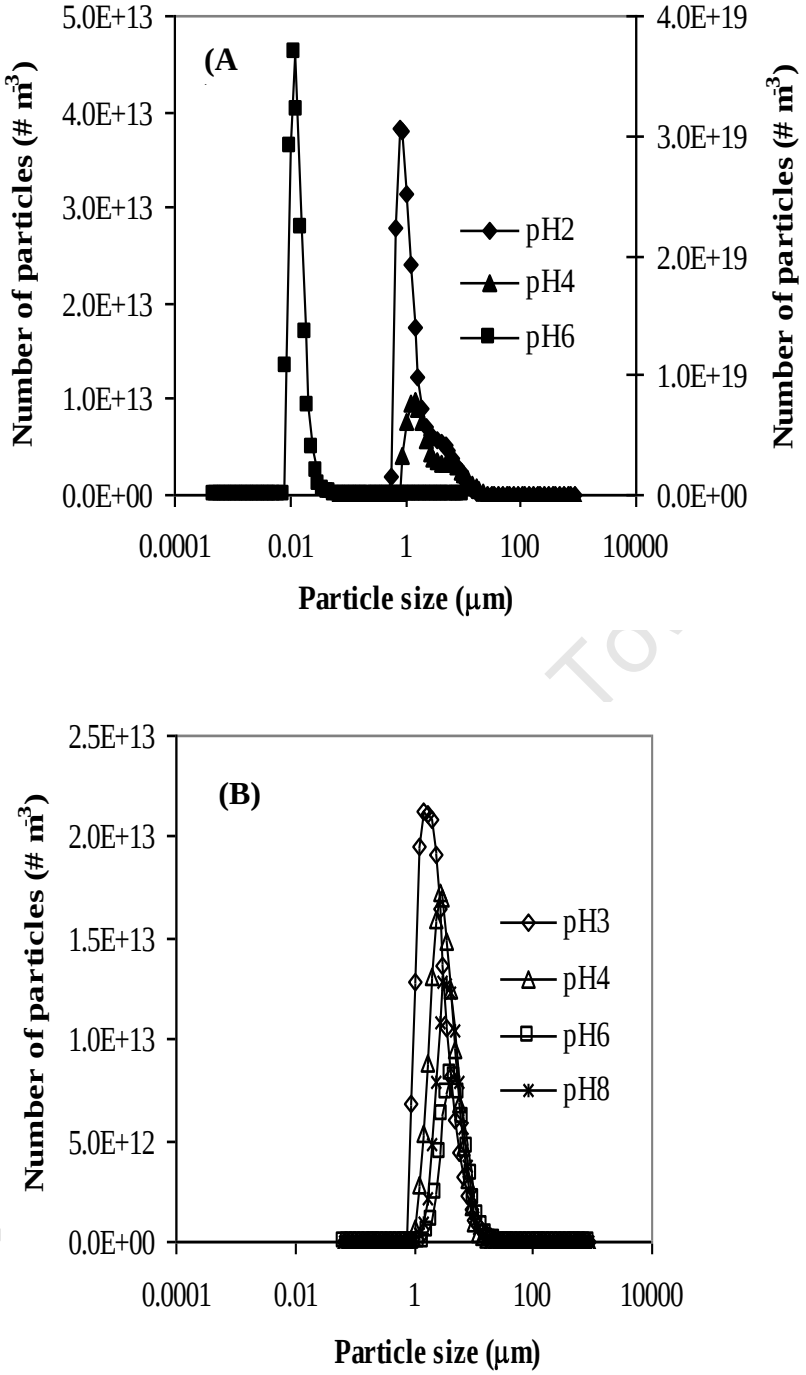

Figure 5.5: Change in PSD of (A) copper sulphide and (B) zinc sulphide precipitates as a function of operating pH at metal to sulphide molar ratio of 0.67. Data for pH 6 in (A) represented on secondary y-axis.

The results for the change in the number based mean size ($\bar{L}_{1.0}$) and the second moment (*m2*) for copper and zinc sulphide particles produced under different operational pH conditions are shown in Figure 5.6. The results in Figure 5.6(A) show

that $\overline{L}_{1.0}$ was significantly increased when the operating pH for copper sulphide precipitation was decreased from 6 to 4 and $\overline{L}_{1.0}$ at pH 2 was slightly smaller than that obtained at pH 4, but still significantly larger than $\overline{L}_{1.0}$ obtained at pH 6. For zinc sulphide precipitation, $\overline{L}_{1.0}$ was slightly decreased when the operating pH was decreased below 6 and $\overline{L}_{1.0}$ was also slightly decreased when the process was operated at pH 8. These trends are in agreement with the number based particle size distribution results shown in Figure 5.5 and indicate that there is an optimal pH at which larger copper and zinc sulphide precipitates can be obtained. The results also show that the difference in the mean size of the copper and zinc sulphide particles was not substantial when the operating pH was less than pH 6.

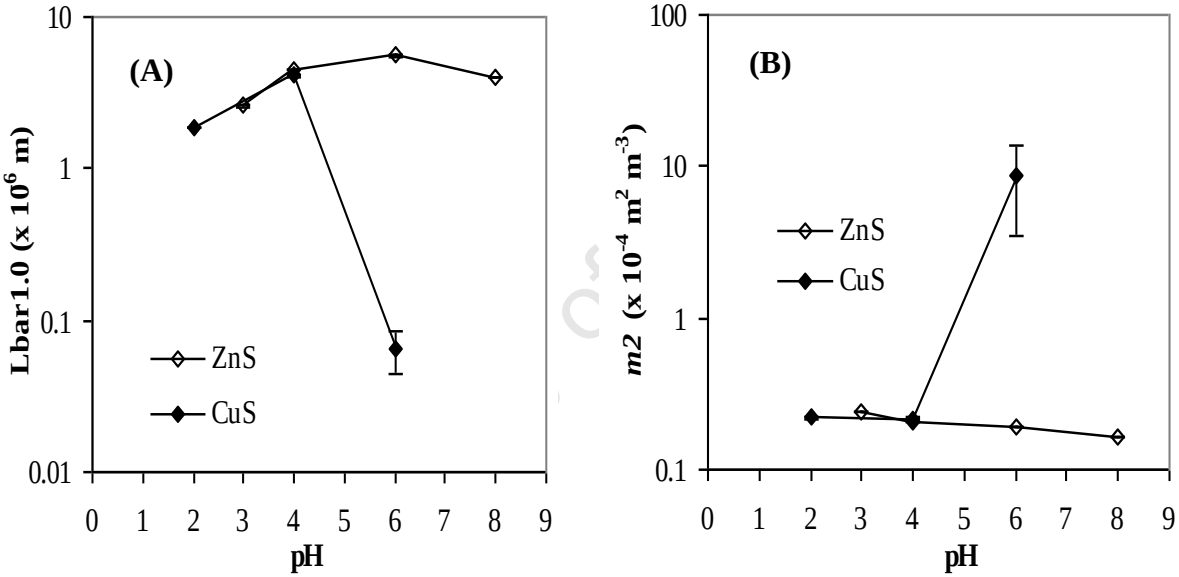

Figure 5.6: Change in (A) $\overline{L}_{1.0}$ and (B) *m2* for metal sulphide precipitates produced using metal to sulphide molar ratio of 0.67 under different operating pH conditions.

The results in Figure 5.6(B) show that *m2* (related to surface area) for zinc sulphide was slightly increased when the operating pH was decreased. In the case of copper, when the operating pH was decreased from 6 to 4, *m2* was significantly decreased and when the operating pH was changed from 4 to 2, *m2* was slightly increased. These results indicate that the overall surface area of copper sulphide particles produced using operating pH values less than 6 was substantially lower. The observed decrease in the surface area cannot be accounted for by the ± 10% decrease in the amount of metal ions precipitated (i.e. conversion) when the operating pH was changed from 6 to

4. A similar decrease in conversion was obtained in the case of zinc sulphide when the operating pH was decreased from 6 to 4, but the change in *m2* was very small. The data presented in Figure 5.6 suggest that at pH 6 a large number of small copper sulphide particles are produced and their aggregation is suppressed.

According to Kolthoff and Moltzau (1935), sulphide precipitation involves the reaction of bisulphide ions (HS^-) to initially form the metal hydroxysulphide, which by the secondary loss of hydrogen results in the formation of the metal sulphide. Lewis and van Hille (2006) and Karbanee et al (2008) have also suggested that the principal sulphide species participating in the sulphide precipitation reaction was the bisulphide ion. Thus, the results shown in Figure 5.5 and Figure 5.6 can be explained according to the pH-dependent speciation of aqueous hydrogen sulphide ($H_2S_{(aq)}$) as shown in Equations 5.1 and 5.2.

The pK_2 value used in this study, as shown in Equation 5.2, is the value most recently determined by surface sulphidation of crystalline sulphur (Migdisov et al, 2001) and it is in good agreement with other non-calorimetrically determined pK_2 values (Giggenbach, 1971; Meyer et al, 1983; Licht et al, 1990). There is good agreement of values for the pK_1 in literature but the values for pK_2 vary considerably between 12 and 18 (Giggenbach, 1971; Meyer et al, 1983; Licht et al, 1990; Garrels and Naeser, 1958; Wagmam et al, 1968; Stephens and Cobble, 1971).

As the operating pH of the precipitating system is decreased, the relative proportion of $H_2S(aq)$ increases and the concentration of the HS^- ions available is decreased. While this may reduce the supersaturation, the effect on precipitation is likely to be negligible due to the magnitude of the supersaturation. More significantly, a downward shift in the pH reduces the amount of HS^- ions available to adsorb to the particle surface. The $H_2S_{(aq)}$ ions may still adsorb, but their neutral charge will not affect the surface charge of the particles. This effect is illustrated in Figure 5.7. In all cases the zeta potential of the particles which do not settle readily became less negative as the operational pH decreased. When the zeta potential of the particles tends toward zero, aggregation of the initially formed primary particles becomes more favourable. At operational pH values below 6, a significantly smaller number of

University of Cape Town

copper sulphide particles with larger mean particle size and smaller surface area were obtained. Once again, the magnitude of the negative charge was greater for the copper sulphide relative to the zinc sulphide, which accounts for the observed differences in particle properties. The number of particles in suspension was increased when an operating pH below 6 was employed and the number of particles was also increased at pH 8. The observed increase in the number of particles at an operational pH of 8 can be attributed to the increase in the concentration of the negatively charged, surface adsorbing, sulphide species at high pH. As these experiments were performed at a stoichiometric excess of sulphide, sulphidation of any hydroxide precipitate that may have formed at pH 8 would occur. The surface charge on the zinc sulphide particles at pH 8 was similar to that of copper sulphide at pH 4, so a further increase in the pH of the zinc system may lead to more negatively charged particles and suppression of aggregation. There appears to be a threshold potential, in the region of -40 mV, below which particle aggregation is suppressed.

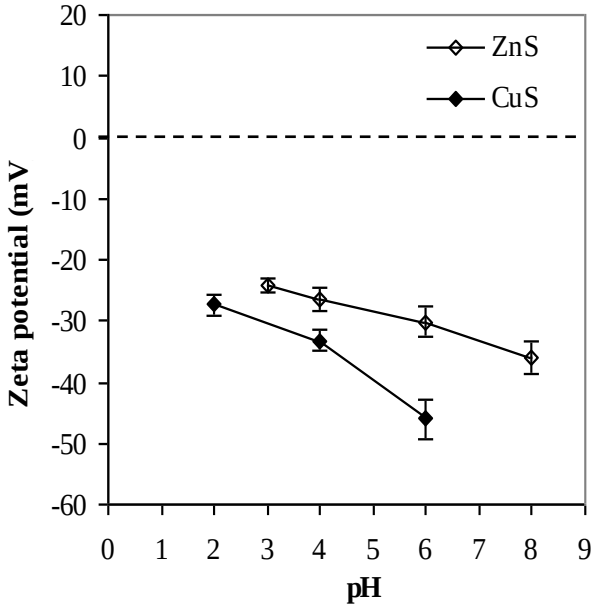

Figure 5.7: Effect of operating pH on the zeta potential of metal sulphide precipitates produced at a metal to sulphide molar ratio of 0.67.

The results for the change in the settling rate of the particles produced at different operational pH values are shown in Figure 5.8. In most cases, a decrease in the operating pH was shown to have a positive effect on the settling characteristics of the particles. The poor settling characteristics obtained for copper sulphide at pH 6 were

significantly improved when the process was operated at low pH and the precipitate with the best settling and dewatering characteristics was obtained at pH 2. Although the settling characteristics of zinc sulphide precipitates were relatively good for all the different operational pH values, the more compact precipitates with improved dewatering characteristics were obtained at pH 4 and 3.

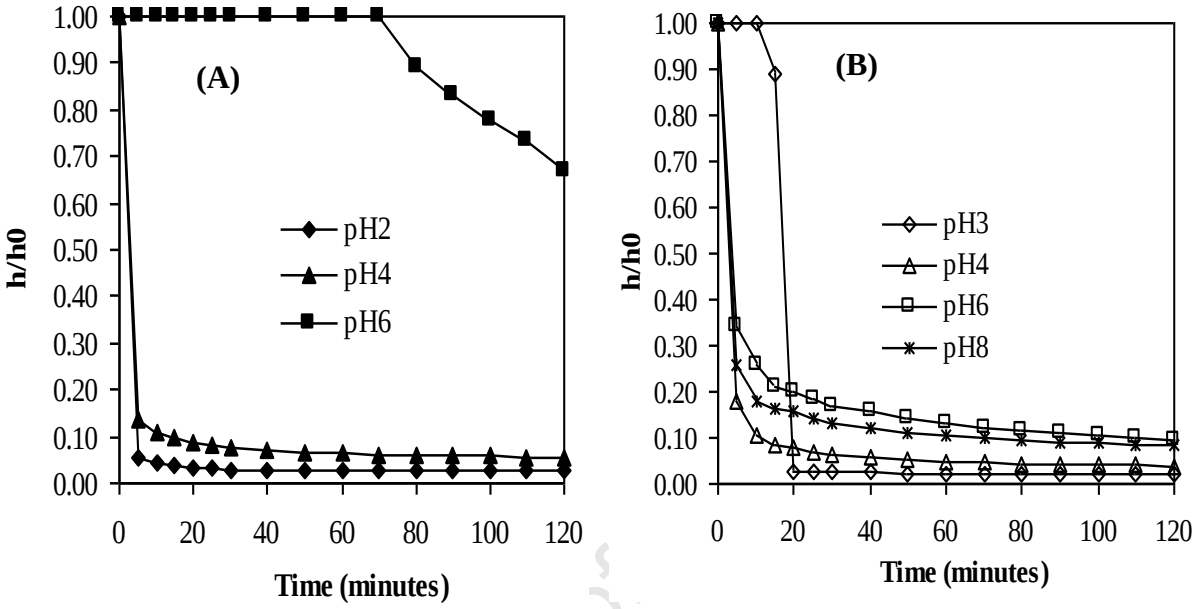

Figure 5.8: Settling rate of (A) copper sulphide and (B) zinc sulphide precipitates produced using metal to sulphide molar ratio of 0.67 at different operating pH.

Furthermore, the good settling characteristics observed for copper at low pH values can be directly linked to the mean particle size and the zeta potential results as shown in Figure 5.6 and Figure 5.7, respectively. At low pH, the zeta potential for the copper sulphide particles was less negative and the mean particle size was significantly increased. Thus, the electrical forces of repulsion amongst particles were reduced and particle settling due to gravitational force was improved as the mean particle size was increased.

5.3. Conclusions

Supersaturation, resulting from changes in metal to sulphide molar ratio and operating pH, has been shown to have a significant effect on the amount of copper and zinc ions precipitated from solution. An increase in the amount of sulphide present in solution

for sulphide precipitation was found to have a positive effect on the copper and zinc sulphide precipitation when the process was operated at pH 6. The nature, surface and settling characteristics of the copper and zinc sulphide precipitates were found to be strongly influenced by sulphide availability, speciation and operating pH. A large number of copper sulphide particles with small mean size, a highly negative surface charge and poor settling characteristics were obtained when the copper sulphide precipitation process was conducted in the presence of excess sulphide at pH 6. The surface charge of the particles and their subsequent behaviour was influenced by the adsorption of the negatively charged sulphide specie (i.e. HS^-) onto the surface. When the process was conducted at operating pH values less than 6, with excess sulphide present in solution, the zeta potential became less negative and suppression of aggregation was reduced. As a result the particle size increased more than twenty-fold, while the number of particles in suspension decreased and the settling characteristics of the resulting precipitates improved. For zinc sulphide precipitation, a small change in the number of particles in suspension and the mean particle size was obtained across the range of experimental conditions tested. However, an increase in the relative sulphide concentration resulted in an increase in the magnitude of the zeta potential of the particles when the process was operated at pH 6. When the precipitation process was conducted with excess sulphide at operational pH values less than pH 6, the zeta potential was reduced and the settling and dewatering characteristics of the precipitates were improved. Consequently, the pH-dependent aqueous sulphide speciation was found to be the most important factor influencing the nature and solid-liquid separation characteristics of the copper and zinc sulphide precipitates produced during sulphide precipitation processes.

University of Cape Town

CHAPTER 6
EFFECT OF POST-PRECIPITATION CONDITIONS ON SURFACE PROPERTIES OF COLLOIDAL METAL SULPHIDE PRECIPITATES

6. Background

Colloidal particles, which are produced during metal sulphide precipitation processes often cause problems with the recovery of the precipitate from suspension. In such cases, chemicals are often added to particle suspensions to bring about formation of large settleable particles through agglomeration of the smaller particles (Stumm, 1992; Hogg, 2000). In water and wastewater treatment, this process is referred to as coagulation and the mechanisms involved are charge neutralisation or "sweep coagulation" (Lettermann et al, 1999). Charge neutralisation occurs when surface adsorbing species, such as cations, are added to a highly charged particle suspension and adsorption onto the surface of the particle results in charge neutralisation. In "sweep coagulation", the highly charged particles are enmeshed in the growing hydroxide precipitate. According to Letterman et al (1999), the rate of charge neutralisation is usually much lower than the rate of enmeshment when a voluminous hydroxide precipitate is formed.

Many studies have been conducted on coagulation of colloidal particle suspensions (Duan and Gregory, 2007; Xiao et al, 2008; Amirtharajah and Mills, 1982). The most commonly used coagulants are aluminium and iron salts, such as aluminium sulphate and ferric chloride (Xiao et al, 2008). These metal salts produce numerous positive intermediate polymeric species in solution before precipitation of the hydroxide (Wang et al, 2009; Xiao et al, 2008). The intermediate species adsorb and destabilise the charged particles. In cases where an amorphous solid phase is formed, the hydroxide floc may also entrap the highly charged particles (Dentel, 1991). In recent years, a new generation of inorganic polymeric flocculants (e.g. polyaluminium chloride and polyiron chloride) have become more and more popular (Yan et al, 2008; Tang and Stumm, 1987; Wang et al, 2002). These compounds are partially neutralised salts with a significant polymeric fraction. Preformed polymeric species have the

University of Cape Town

advantage of being more effective under a variety of water quality conditions due to their chemical speciation (Yan et al, 2008).

Several studies have been conducted on the surface properties of metal sulphides (Fairthorne et al, 1997; Clarke et al, 1995; Fornasiero et al, 1992; Newell et al, 2007). However, most of the reported studies were carried out using highly crystalline sulphide minerals to characterise the effect of various operating conditions on their floatation behaviour. Knowledge of the effect of operating parameters on the surface properties of colloidal and amorphous precipitates produced by sulphide precipitation reactions, on the other hand, is still limited. According to Healy and Moignard (1976) and Moignard et al (1977), the charge on the surface of sulphide minerals is strongly influenced by pH, surface oxidation and surface adsorbing ions.

The objective of this investigation was to study the effect of various operating conditions on the surface properties of colloidal particles produced by metal sulphide precipitation for the option of downstream processing. The investigation was carried out using colloidal particles produced from copper and zinc sulphide precipitation reactions. The effect of suspension pH and the addition of sulphide, divalent (Ca^{2+}) and trivalent (Al^{3+}) cations on particle characteristics (i.e. surface charge, mean particle size and surface area) was studied.

This investigation can provide valuable information to inform rational decision making around downstream processing of metal sulphide suspensions produced under the conditions where the precipitation reaction cannot be adequately managed.

6.1. Materials and methods

6.1.1. Experimental design

The experimental programme was divided into two phases. In the first phase, copper and zinc ions were precipitated from solution by sulphide precipitation using synthetic sodium sulphide solutions in a semi-batch reactor. In the second phase, the effect of suspension pH, addition of sulphide, divalent (Ca^{2+}) and trivalent (Al^{3+}) cations on the characteristics of the precipitates suspended in background electrolyte solutions (KCl)

University of Cape Town

of concentrations ranging between 1 – 100 mM was studied. The change in the surface properties was characterised using zeta potential measurements and the mean size and surface area of the particles were analysed using particle size distribution (PSD) related information.

6.1.2. Experimental procedure

The suspension pH experiments were conducted using three different background electrolyte concentrations (i.e. 1 mM, 10 mM and 100 mM) and the pH of the suspension was varied between pH 2.5 and 11 using NaOH and/or HCl. Different background electrolyte concentrations were used to establish the effect of ionic strength on surface potential. For the sulphide addition experiments, the precipitates were suspended in 10 and 100 mM background electrolyte solutions, and the sulphide concentration added to the precipitate suspension was varied between 0 – 7 mM. The cation addition experiments were carried out by suspending the precipitates in 10 mM background electrolyte solution and cation concentration ranging between 0 – 5 mM was added to the precipitate suspension. Potassium chloride (KCl) solutions were used as a background electrolyte in all cases.

The reactor set-up, analytical techniques and experimental procedures used in this investigation are described in detail in Sections 3.1.3, 3.3 and 3.5.4.

6.2. Results and discussion

6.2.1. Precipitate characterisation

The XRD and EDAX results for the semi-quantitative chemical analysis of the precipitates obtained from the precipitation reactions are presented in Figure 6.1 and Table 6.1. The reference patterns for the XRD results shown in Figure 6.1 are presented in Appendix E. Figure 6.1(A) shows the XRD pattern for the precipitate obtained from the copper sulphide precipitation reaction. The crystalline phase analysis of the precipitate showed that the composition of the precipitate was ± 63% covellite (CuS) and ± 37% copper hydroxysulphate ($CuSO_4.(H_2O)_5$). The XRD peaks for the precipitate obtained from the zinc sulphide precipitation reaction were broad,

University of Cape Town

as seen in Figure 6.1(B). According to Jovanović et al (2007), broad XRD peaks are obtained when the particles have a poor crystalline structure and the size of the particles is in the submicron range. Hence, the precipitate obtained from the zinc sulphide precipitation reaction was classified as highly amorphous and the crystalline phases present in the precipitate could not be determined.

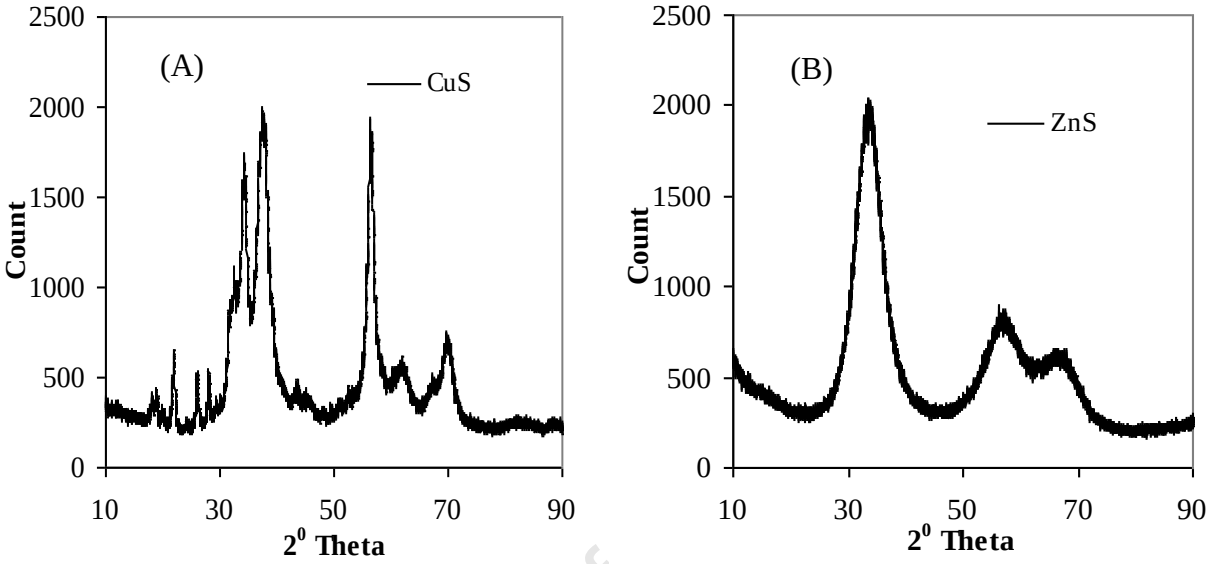

Figure 6.1: XRD results for the precipitates produced from (A) copper and (B) zinc sulphide precipitation reactions.

The EDAX results in Table 6.1 show that the precipitate produced from copper sulphide precipitation reaction had a very high content of copper and sulphur; and a small amount of oxygen. The small amount of oxygen obtained was attributed to the copper hydroxysulphate which was identified by the XRD (Appendix E). The zinc sulphide comprised only zinc and sulphur. The relative proportions were in close agreement with high purity commercial zinc sulphide and zinc sulphide produced using biogenic hydrogen sulphide as reported by Rhadika et al (2006). The chemical composition of the compounds, as shown in Table 6.1, was found to be non-stoichiometric and this was attributed to the semi-quantitative nature of the EDAX analysis.

University of

Table 6.1: EDAX results of the produced copper and zinc precipitates

Sample	Element	Mass (weight %)	Mass (atomic %)
Copper Sulphide	S	29.18	43.78
	O	1.16	3.49
	Cu	69.66	52.73
Zinc Sulphide	S	28.13	44.38
	O	-	-
	Zn	71.87	55.62
Zinc Sulphide*	S	30.60	47.40
	Zn	69.40	52.60
Zinc Sulphide[#]	S	30.30	47.00
	Zn	69.70	53.00

*Commercial zinc sulphide and [#]zinc sulphide produced using biogenic hydrogen sulphide (Rhadika et al, 2006).

To verify the chemical composition of the copper precipitate, the precipitate was re-suspended in de-ionised water and stirred at room temperature for 1 hour. When the concentration of the filtrate from the stirred suspension was analysed, it was found that 32% of the copper ions that were present in the original copper sulphate solution (i.e. the copper sulphate solution used at the beginning of the precipitation reaction) were still present within the precipitate. The analysis of the samples collected from the reactor at the end of the precipitation experiments showed that ± 60% of the dissolved copper ions and ± 87% of the dissolved zinc ions were precipitated from solution when the precipitation reactions were terminated. It was therefore clear that the unreacted zinc ions were properly removed from the zinc precipitate by washing the freeze dried precipitate. The unreacted copper ions, on the other hand, were not effectively removed from the copper precipitate. The lower than expected amount of copper and zinc ions precipitated from solution was attributed to the operational pH which was below pK_1, in both cases, and therefore resulting in the loss of some of the added sulphide as gaseous H_2S.

University of Cape Town

6.2.2. Effect of pH on surface properties

The results in Figure 6.2 show the change in zeta potential as a function of pH for the copper and zinc precipitates suspended in different concentrations of background electrolyte solutions. Both metal precipitates exhibited negative zeta potentials, indicating that the precipitates were un-oxidised or slightly oxidised metal sulphides with sulphur-rich surfaces (Healy and Moignard, 1976; Fairthorne et al, 1997). In the case of copper (Figure 6.2(A)), the magnitude of the negative zeta potential was increased when the pH was increased for the 1 and 10 mM suspensions. The zeta potential of the particles suspended in 100 mM background electrolyte solution, on the other hand, became less negative at pH 6. According to Clarke and co-workers (1995), the zeta potential versus pH curve of the sulphide minerals becomes less negative as the surface of the mineral becomes increasingly covered with the metal oxide/hydroxide species due to surface oxidation. Thermodynamic modelling (Visual MinteQ ver. 3.0) was conducted to determine if the formation of metal oxide/hydroxide was possible when the copper precipitate was suspended in different concentrations of potassium chloride under varying pH conditions. The results showed dissociation of copper ions and formation of different aqueous copper hydroxide (e.g. $Cu(OH)_3^-$, $Cu_2(OH)_2^{2+}$, Cu_2OH^{3+}, $Cu_3(OH)_4^{2+}$ and $CuOH^+$) and copper chloride (i.e. $CuCl^+$, $CuCl_3^-$, $CuCl_4^{2-}$) complexes. The results also showed that the concentration of these aqueous copper complexes was dependent on the pH of the solution and the concentration of the background electrolyte solution. The relative proportion of the Cu_2OH^{3+} complex was predicted to be very high, reaching a maximum at pH 6, when 100 mM background electrolyte solution was used. As a result, adsorption of this positively charged complex onto the surface of the particles was seen as the one possible reason for the observed increase in zeta potential.

Senanayake (2009) reviewed chloride assisted mineral sulphide oxidation and proposed a chloride concentration dependent surface reaction mechanism. According to the proposed mechanism, oxidation of sulphide minerals involves surface reaction mechanisms via the formation of a mixed-ligand complexes in the form of adsorbed or dissolved species (e.g. Cu(OH)Cl). Surface adsorbed chloride ions are involved in the surface reaction and the rate of the surface chemical reaction is dependent on the chloride ion concentration. Thus, formation of copper oxide/hydroxide due to chloride

University of Cape Town

induced surface oxidation of the particles was seen as another possible reason for the observed increase in the zeta potential at pH 6 when 100 mM background electrolyte solution was used. The trends observed for the 1 and 10 mM were similar to those observed for elemental sulphur (Healy and Moignard, 1976), and showed that surface adsorption of Cu_2OH^{3+} complex or chloride induced surface oxidation was limited under the conditions.

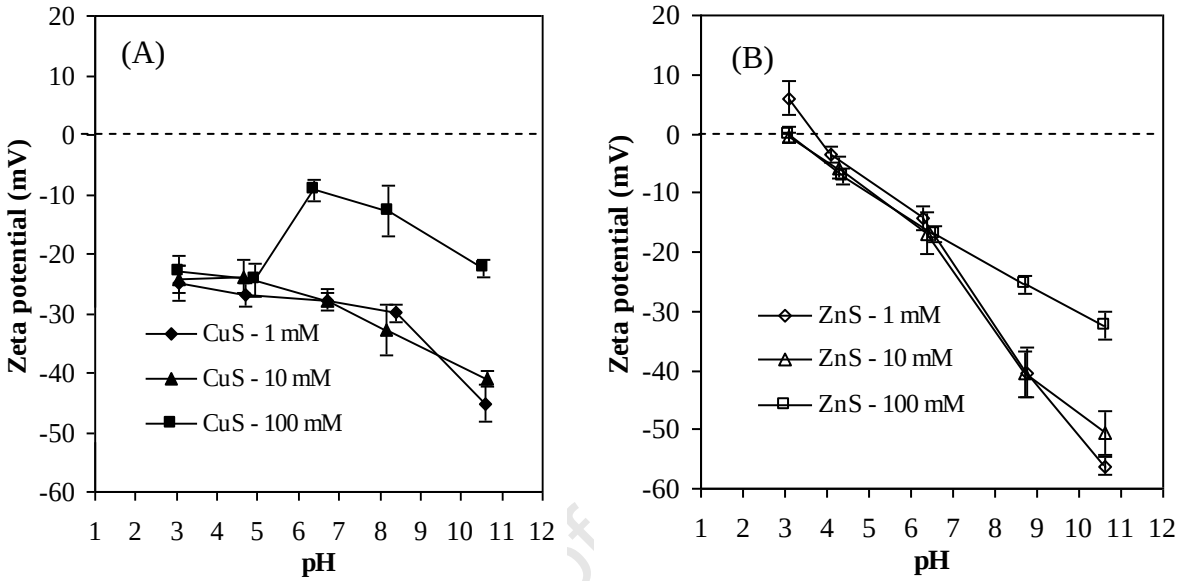

Figure 6.2: Change in zeta potential as a function of suspension pH for the (A) copper and (B) zinc precipitates suspended in KCl electrolyte solutions of different concentrations.

For the zinc precipitate (Figure 6.2(B)), the zeta potential of the particles was close to zero around pH 3.5 and when the pH of the suspension was increased the zeta potential became more negative. The change in the magnitude of the decrease in zeta potential was similar for the 1 and 10 mM suspensions, but reduced for the 100 mM suspension. The magnitude of the negative zeta potential increase obtained in the case of zinc was higher than that obtained for the copper precipitate in all cases.

The zeta potential which was close to zero around pH 3.5 indicated the point of zero charge or the iso-electric point of the particles. Similar pH values for the point of zero charge have previously been reported for synthetic zinc sulphide particles (Williams and Labib, 1985; Nicolau and Menard, 1992). The consistent decrease in the zeta potential when the pH was increased showed that the surface of the particles was not

oxidised or it was only slightly oxidised. The zeta potential of the un-oxidised sulphide minerals decreases with increasing pH due to surface adsorption of the negatively charged hydroxy ions (Fornasiero et al, 1992). The observed deviation when the pH was above 6 for the 100 mM suspension was attributed to the compression of the electrical double as the ionic strength of the suspension increased due to the concentration of the background electrolyte solution.

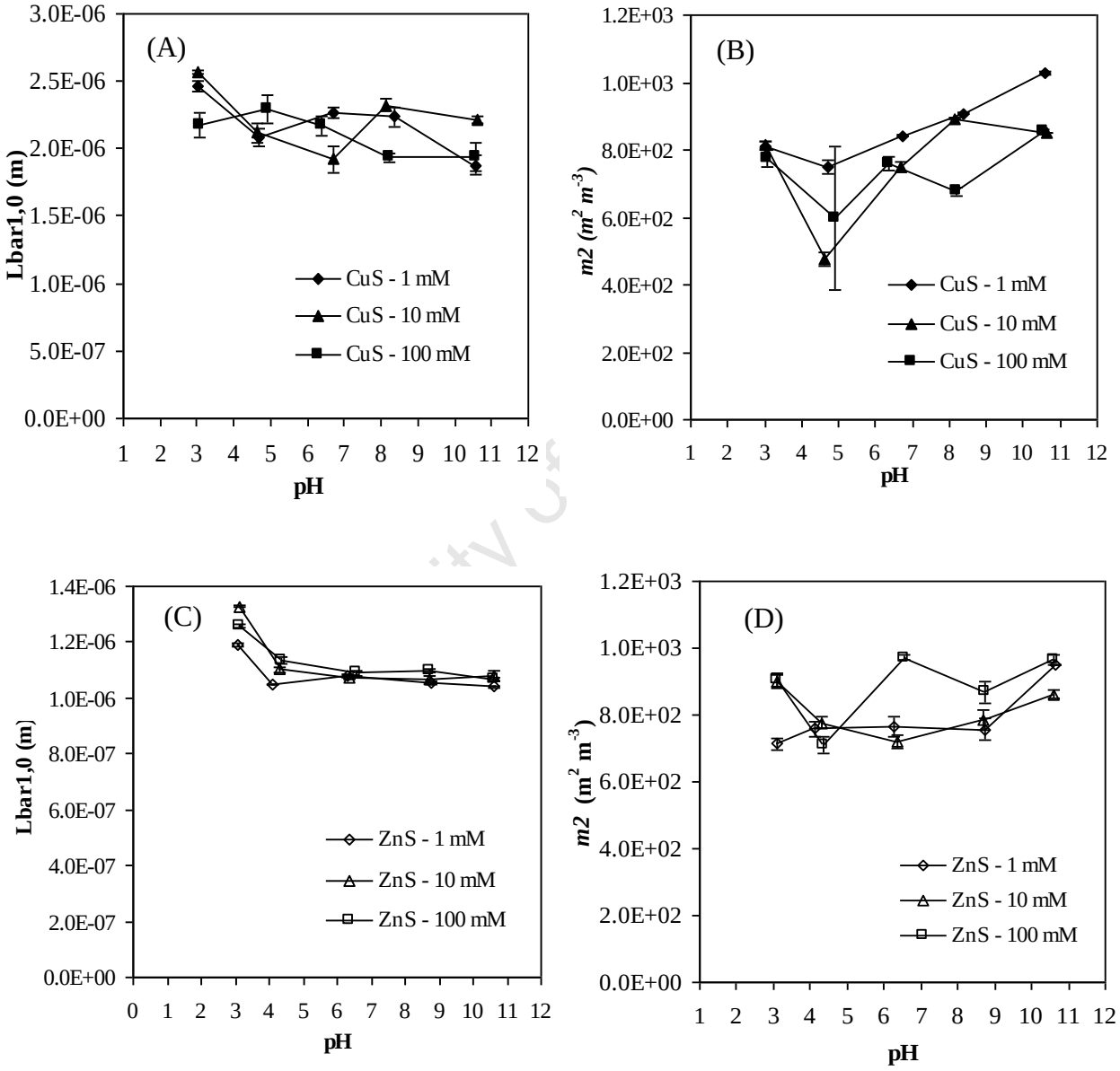

Figure 6.3: Change in $\bar{L}_{1.0}$ and *m2* as a function of pH for copper (A, B) and zinc (C, D) precipitates suspended in KCl electrolyte solutions of different concentrations.

According to the quantitative theory of colloid stability, particle aggregation is enhanced when the particles have a low surface charge (Derjaguin and Landau, 1941; Verwey and Overbeek, 1948). Aggregation increases the size of the particle and decreases the overall surface area of the particles. Thus, the change in the charge on the surface of the particles can directly influence the size and the specific surface area of the particles.

Figure 6.3 shows the change in the number based mean size ($\overline{L}_{1.0}$) and the second moment (*m2* - equivalent to surface area) as a function of pH for copper and zinc precipitates suspended in different concentrations of background electrolyte solutions. As can be seen from Figure 6.3(A) and (C), the change in the pH of the suspension and the background electrolyte concentration had a small effect on $\overline{L}_{1.0}$. A slight decrease in $\overline{L}_{1.0}$ was obtained when the pH was initially increased from 2.5 to 4 in the case of zinc. When the pH of the suspension was above 4, the change in $\overline{L}_{1.0}$ was negligible and similar for all the background electrolyte concentrations. The slight decrease in $\overline{L}_{1.0}$ obtained was found to be consistent with an increase in the zeta potential (Figure 6.2) and suggest that the mean size of the particles was slightly decreased when the charge on the surface of the particles was slightly increased. In the case of copper, a small decrease was initially obtained for the 1 and 10 mM suspensions when the pH was increased from 3 to 4.5. The change in $\overline{L}_{1.0}$ was highly erratic when the pH was above 4 and this was attributed to the possible formation of copper hydroxide due to the precipitation of the dissociated Cu^{2+} ions. Similar to the zinc, the slight decrease in $\overline{L}_{1.0}$ when the pH was changed from 3 to 4 in the case of the 1 and 10 mM copper suspensions was related to the change in zeta potential. The $\overline{L}_{1.0}$ obtained for the zinc precipitate was found to be generally smaller than that obtained for the copper precipitate. This was seen as the possible explanation for the results in Figure 6.2 which showed that the magnitude of the negative zeta potential increase was higher for the zinc precipitate.

Figure 6.3(B) and (D) show that the change in the pH of the suspension and the background electrolyte concentration had some effect on the second moment (*m2*) of both the copper and zinc particles. When the suspension pH was increased from 3 to

University of Cape Town

just above 4, in the case of copper, *m2* was decreased and the magnitude of the decrease was higher for the 10 mM suspension than it was for the 1 mM suspension. The change in *m2* at pH 4.5 for the 100 mM suspension was difficult to interpret due to the large error in the results. Above pH 4.5, *m2* was generally increased when the pH of the suspension was increased. The magnitude of the increase was found to be slightly affected by the background electrolyte concentration even though the results were erratic above pH 6 for the 10 and 100 mM suspensions. The results for the zinc precipitate show an initial decrease in *m2* when the pH of the suspension was initially changed from 2.5 to 4, in the case of 1 and 10 mM suspensions. Above pH 4, the results for *m2* were erratic in all cases but a slight increase in *m2* was generally observed. Since the observed general increase in *m2* after pH 4 was slightly higher for the copper precipitate, it was postulated that this was due to the formation of the additional surface area as a result of copper hydroxide formation. This was suggested because the change in the magnitude of the negative zeta potential was much higher for the zinc precipitate and therefore, an increase in *m2* for the zinc suspensions was expected to be much higher. Nonetheless, the observed changes in $\overline{L}_{1.0}$ and *m2* were small and it was concluded that the change in the charge on the surface of the copper and zinc particles due to the change in the pH of the suspension did not have a significant effect on the mean particle size and surface area of the particles.

6.2.3. Effect of sulphide addition on surface properties

Figure 6.4 shows the results for the change in zeta potential and suspension pH as a function of the sulphide concentration added to the 10 and 100 mM suspensions of the copper and zinc precipitates. The results in Figure 6.4(A), for the copper suspensions, show that the zeta potential was negative and the magnitude of the negative zeta potential was increased when the concentration of the sulphide added to the suspension was increased up to ± 3 mM. When the concentration of the sulphide added to the suspension was increased, thereafter, the zeta potential remained relatively unchanged. The pH of the suspension was unchanged when a small amount of sulphide was initially added to the suspension and a sharp increase followed by a gradual increase was obtained when the concentration of the added sulphide was increased. The results also showed that the change in the background electrolyte

University of Cape Town

concentration had no significant effect on the zeta potential and the pH of the suspension. In the case of zinc, as seen in Figure 6.4(B), addition of a small amount of sulphide resulted in a significant increase in the magnitude of the negative zeta potential and the pH of the suspension. An increase in the amount of sulphide added resulted in a small change in the zeta potential and a gradual increase in the pH of the suspension. The magnitude of the negative zeta potential increase was significantly reduced when the 100 mM background electrolyte solution was used.

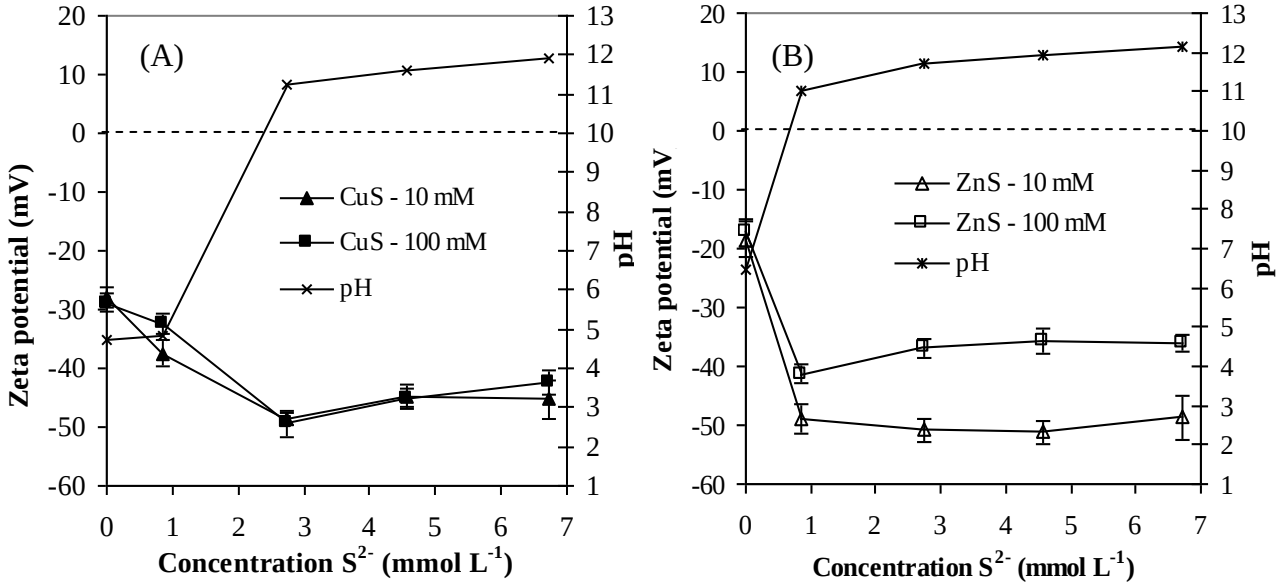

Figure 6.4: Change in zeta potential and the pH of the suspension as a function of the concentration of sulphide added to the (A) copper and (B) zinc precipitates suspended in 10 and 100 mM KCl electrolyte solutions.

According to Healy and Moignard (1976) and Fairthorne et al (1997), the negative zeta potential on both the copper and the zinc precipitate prior to sulphide addition indicated that the precipitates were un-oxidised or slightly oxidised metal sulphides with sulphur-rich surfaces. When sulphide was added to the suspension, the magnitude of the negative zeta potential was increased due to surface adsorption of the negatively charged sulphide specie (i.e. HS^-). Newell et al (2007) studied sulphidation of oxidised metal sulphides and showed that the process was associated with strong chemisorption of the negatively charged bisulphide ions followed by the formation of a sulphide-rich surface through anionic exchange. The formation of the sulphide-rich surfaces, in this investigation, was achieved by addition of a small amount of sulphide. Hence, a sharp increase in the magnitude of the negative zeta

potential when a small amount of sulphide was initially added to the precipitate suspensions. The zeta potential remained relatively unchanged when the concentration of the sulphide added to the precipitate suspensions was increased suggesting the saturation of the free sulphide adsorbing sites on the surface of the particles. The small change in the zeta potential obtained when a small amount of sulphide was initially added to the copper suspensions was attributed to the consumption of the added sulphide by the Cu^{2+} ions dissociated from the copper hydroxysulphate component of the precipitate to form copper sulphide. The pH data (Figure 6.4(A)) support this hypothesis as the sulphide addition did not significantly increase the pH, as was the case for the zinc experiment. Sulphide solutions are highly alkaline and the presence of free sulphide ions in an unbuffered solution results in a significant increase in pH.

University of Cape Town

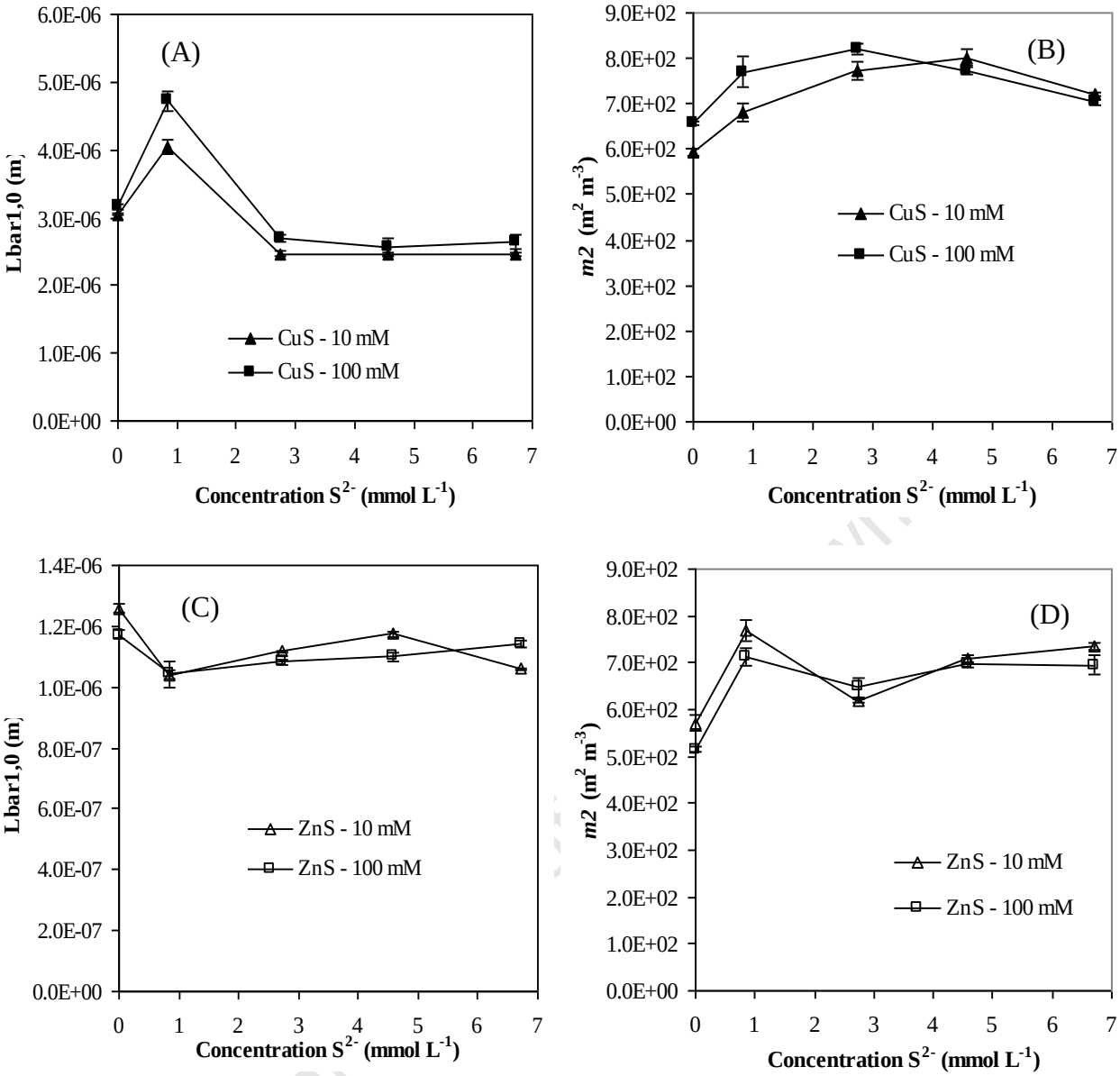

Figure 6.5: Change in $\bar{L}_{1.0}$ and *m2* as a function of the concentration of sulphide added to the copper (A, B) and zinc (C, D) precipitates suspended in 10 and 100 mM KCl electrolyte solutions.

The effect of added sulphide concentration on $\bar{L}_{1.0}$ and *m2* for the 10 and 100 mM copper and zinc suspensions are shown in Figure 6.5. The results in Figure 6.5(A) show a slight increase in $\bar{L}_{1.0}$ when a small amount of sulphide was initially added to the precipitate suspensions of copper. The initial increase in $\bar{L}_{1.0}$ was followed by a decrease until a minimum was reached when ± 3 mM of the sulphide was added. The results also show that $\bar{L}_{1.0}$ was always slightly higher for the 100 mM suspension. Figure 6.5(C) show that $\bar{L}_{1.0}$ was decreased when the same amount of sulphide was

initially added to the precipitate suspensions of zinc. The behaviour observed for the zinc precipitate suspension was found to be consistent with the zeta potential results shown in Figure 6.4(B) and show that the mean size of the particles was decreased when the surface charge was increased due to sulphide adsorption. The trends obtained for the copper suspensions were attributed to the copper sulphide precipitation reaction. When sulphide ions were initially added to the copper suspensions, the dissociated Cu^{2+} ions reacted with the added sulphide to form additional copper sulphide particles. The observed increase in $\overline{L}_{1.0}$ suggest that the supersaturation which was created when the dissociated ions reacted with the added sulphide ions brought about formation of new particles but some of the particles that were already present in the suspension were also aggregated and/or flocculated, hence an increase in $\overline{L}_{1.0}$.

The results in Figure 6.5(B) show that *m2* was increased when the concentration of the sulphide added to the precipitate suspension was increased until a maximum was reached for the copper suspension. The maximum was reached at a slightly higher sulphide concentration for the 10 mM suspension. The results also show that *m2* was always slightly higher for the 100 mM suspension and only after a maximum was reached the magnitude of *m2* was lower. In the case of zinc, *m2* was slightly increased when a small amount of sulphide was initially added to the precipitate suspension and the change in *m2* was very small when more sulphide was added to the suspension. These trends were found to be consistent with the zeta potential results shown in Figure 6.4 and showed that the change in the charge on the surface of the copper and zinc particles influenced the mean size and the specific surface area of the particles in suspension.

6.2.4. Effect of cation addition on surface properties

The results in Figure 6.6 show the change in zeta potential and the pH of the suspension when different concentration of Al^{3+} and Ca^{2+} ions were added to the 10 mM suspensions of copper and zinc precipitates. When a small amount of Al^{3+} ions was added to the precipitate suspensions, the zeta potential of the particles became significantly less negative and the pH of the suspensions was slightly decreased for

University of Cape Town

both precipitates (Figure 6.6(A)). An increase in the amount of Ca^{2+} ions added to the suspensions resulted in a slight increase in the zeta potential of the particles while the pH of the suspension remained relatively unchanged (Figure 6.6(B)).

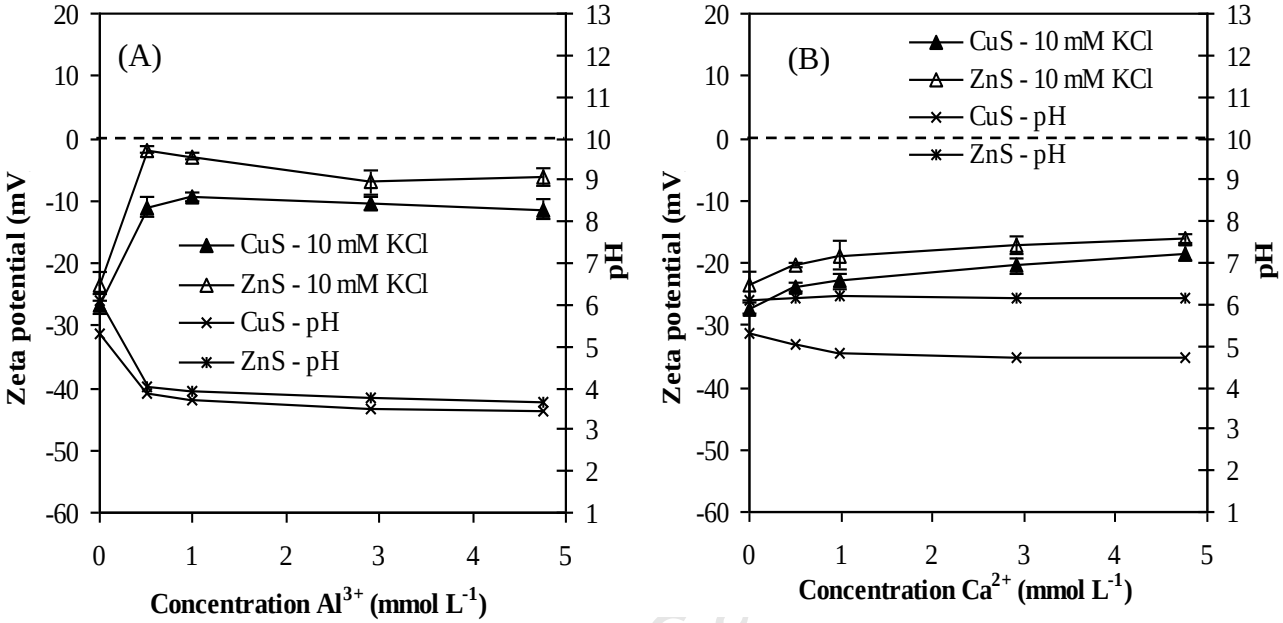

Figure 6.6: Change in zeta potential and the pH of the suspension as a function of different concentrations of (A) trivalent (Al^{3+}) and (B) divalent (Ca^{2+}) cations added to the copper and zinc precipitates suspended in 10 mM KCl electrolyte solution.

The use of aluminium salts for charge neutralization and coagulation of colloidal particle suspensions is well documented (Dentel, 1991; Stumm, 1992; Hogg, 2000; Lettermann et al, 1999) and several mechanisms have been proposed to this effect (Duan and Gregory, 1996; Dentel, 1991). When aluminium salt is added to aqueous solutions, hydrolysis of Al^{3+}ions takes place and different monomeric (i.e. $Al(OH)^{2+}$, $Al(OH)_2^{+}$, $Al(OH)_3$, $Al(OH)_4^{-}$) and polymeric (i.e. $Al_2(OH)_2^{4+}$, $Al_3(OH)_4^{5+}$, $Al_{13}O_4(OH)_{24}^{7+}$) aqueous complexes are formed (Dentel, 1991). A decrease in the magnitude of the negative charge on the surface of the particle occurs due to surface adsorption of these complexes. In cases where the charge on the surface of the particle was caused by surface adsorbing species, adsorption of Al^{3+} ions on particle surface can occur by formation of complexes between aluminium and surface hydroxy groups of the particle (i.e. surface complexation)(Duan and Gregory, 1996). If the pH of the suspension favors aluminium (III) hydroxide formation, the charged particle surface may be enmeshed into a growing aluminium hydroxide $Al(OH)_3$ particle (Dentel,

1991). Thus, the results for the change in zeta potential and pH of the suspension when Al^{3+} ions were added to the precipitate suspension (Figure 6.6(A)) can be explained according to surface adsorption of aqueous Al^{3+} ions onto the surface of the precipitates. Since the charge on the surface of the particles was caused by surface adsorption of the negatively charged sulphide species, adsorption of aqueous Al^{3+} ions onto the surface of the precipitate was achieved through surface complexation.

A slight increase in the zeta potential obtained when the concentration of Ca^{2+} ions added to the precipitate suspensions was increased can be attributed to the surface adsorption of these positively charges ions. Moignard et al (1977) studied the uptake of Ca^{2+} ions by zinc sulphide and found that the uptake was pH-dependent (i.e. Ca^{2+} ions uptake increases with an increase in pH). The study also found that the adsorption of Ca^{2+} ions on the ZnS/H_2O interface involved the diffusion of the Ca^{2+} ions into the Stern layer without the release of an equivalent number of protons. Hence, the pH remained relatively unchanged when the Ca^{2+} ions where added to the precipitate suspensions. If the Ca^{2+} ions were added to the precipitate suspension conditioned at a higher pH, the magnitude of the zeta potential increase would possibly be much higher than that obtained in this investigation. The observed difference in the results obtained for Ca^{2+} and Al^{3+} addition can also be explained according to the Schulza-Hardy rule. The rule states that the ion that causes a soluble to coagulate is opposite in sign to the electric charge of the colloidal particle and the coagulating power increases with valency of the ion (Stumm, 1992).

University of Cape Town

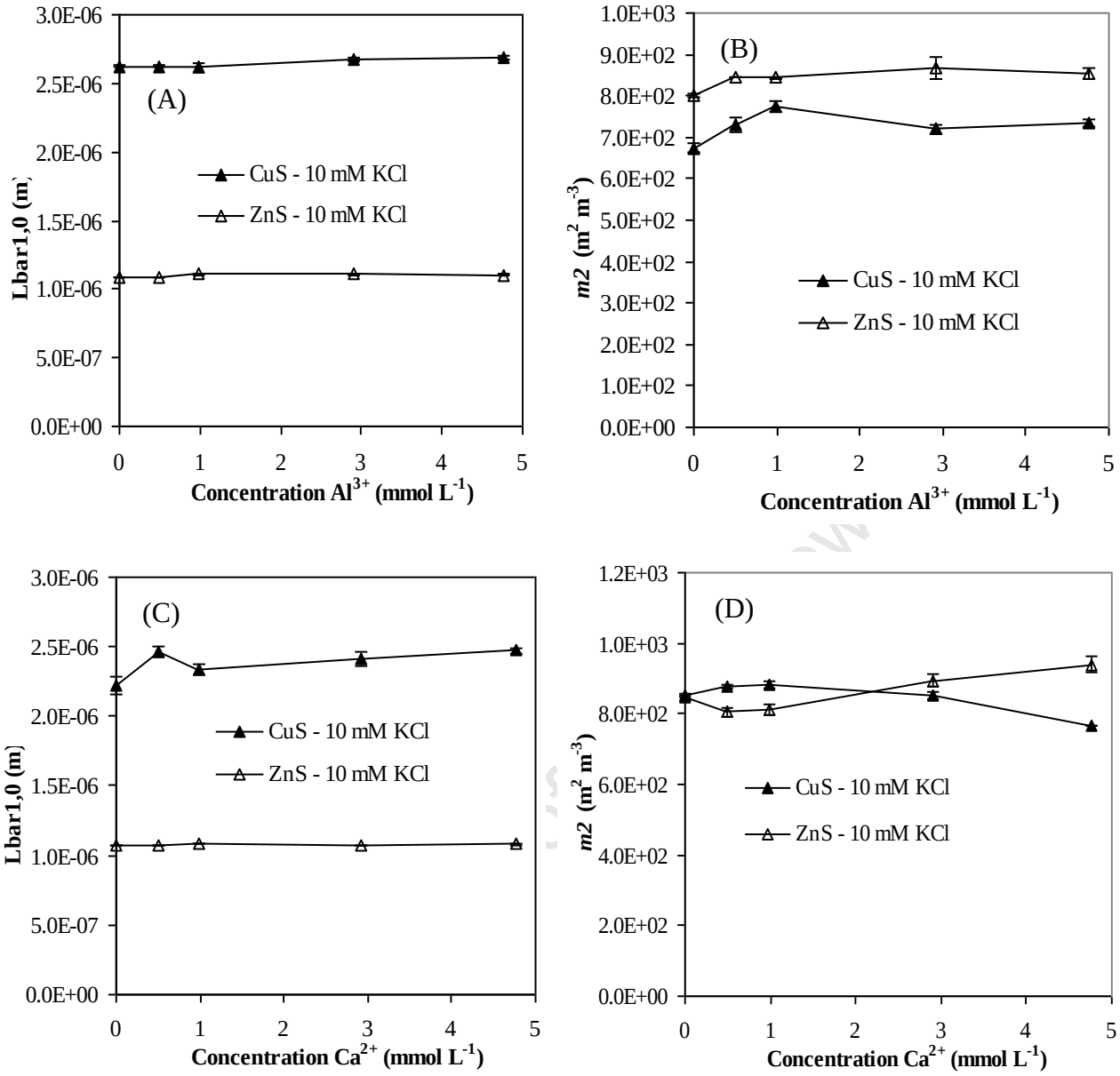

Figure 6.7: Change in $\bar{L}_{1.0}$ and *m2* as a function of the different concentrations of Al^{3+} (A, B) and Ca^{2+} (C, D) ions added to the copper and zinc precipitates suspended in 10 mM KCl electrolyte solution.

The results presented in Figure 6.7 show the change in $\bar{L}_{1.0}$ and *m2* when different concentrations of Al^{3+} and Ca^{2+} ions were added to the 10 mM suspensions of the copper and zinc precipitates. For the copper precipitate, as seen in Figure 6.7(A) and (B), $\bar{L}_{1.0}$ remained relatively unchanged and *m2* increased slightly when the Al^{3+} ions were initially added to both the copper and zinc suspensions. The $\bar{L}_{1.0}$ which remained unchanged indicates that addition of Al^{3+} ions did not have any effect on the size of

the particles. The slight increase in *m2* observed when Al^{3+} ions were initially added to the precipitate suspension, on the other hand, could be attributed to the possible formation of aluminium (III) hydroxy precipitate since the suspensions were conditioned around pH 5. The $\overline{L}_{1.0}$ and *m2* results for Ca^{2+} ions addition shown in Figure 6.7(C) and (D) were found to be consistent with the zeta potential results presented in Figure 6.6(B) and showed that the change in the concentration of the Ca^{2+} ions added to the precipitate suspensions resulted in a minimal change in the mean size and surface area of the particles. These results show that addition of trivalent cation to aqueous suspension of metal sulphide precipitates could be more effectively used to change the surface properties of colloidal particles produced by metal sulphide precipitation reactions.

6.3. Conclusions

The surface properties of particles produced by sulphide precipitation reactions were found to be influenced by suspension pH, ionic strength, excess sulphide concentration and addition of cations. An increase in suspension pH, from pH 6 to pH 11, resulted in an increase in the magnitude of the negative charge on the surface of the particles for both copper and zinc precipitates. The magnitude of the increase in negative surface charge was generally greater in the case of zinc, but this was reduced when the precipitate was suspended in a 100 mM background electrolyte solution, due to the compression of the electrical double layer. Below pH 6, the charge on the surface of zinc sulphide particles tended towards zero, with the point of zero charge around pH 3. For the copper precipitate, reducing the pH below pH 7 had little effect on the zeta potential, which remained between – 25 mV and – 30 mV.

Addition of a small amount of sulphide to the zinc precipitate suspension resulted in a significant decrease in the zeta potential of the particles, a slight decrease in the mean particle size, and an increase in the surface area of the particles. The magnitude of the negative zeta potential was reduced by ± – 10 mV when 100 mM background electrolyte solution was used. In the case of the copper precipitate, addition of a small amount of sulphide resulted in a slight decrease in zeta potential and an increase in mean particle size and surface area. An increase in surface area was attributed to the

University of Cape Town

formation of new copper sulphide particles due to the reaction between the added sulphide and the copper ions liberated from the copper hydroxysulphate component of the precipitate. Upon further sulphide addition, the magnitude of the negative zeta potential and the suspension pH were significantly increased. The increase in surface charge when sulphide was added to the suspension, in both cases, was attributed to adsorption of the negatively charged sulphide specie (i.e. HS^-) onto the surface of the particles.

The addition of a divalent cation (Ca^{2+}) to the suspension had little effect on the surface charge of the particles. However, addition of a small amount (0.5 mM) of Al^{3+} ions to the copper and zinc precipitate suspensions had a significant effect on the zeta potential of the particles. The zeta potential was changed from – 23 mV to – 5 mV for zinc and – 28 mV to – 10 mV for copper. Mean particles size and surface area of the suspended precipitate were not significantly affected by addition of cations.

The relatively small change in particle size and surface area, despite often significant changes in zeta potential, is attributed to the nature of the particles used in this study. The particles were recovered by freeze drying and the morphology of the particles was influenced by this process (Appendix E). However, the same phenomena observed in the experiments presented above would affect the particles in colloidal suspension. Therefore, any intervention which resulted in the zeta potential approaching zero would be expected to promote the flocculation and recovery of particles from colloidal suspension.

University of Cape Town

CHAPTER 7
CONCLUSIONS AND RECOMMENDATIONS

The study was motivated by the use of SRB mediated biological processes for production of bicarbonate alkalinity and sulphide, which could be used to neutralise acidic effluents and effect precipitation of metal ions as metal sulphides. The main objective of the study was to develop a clearer understanding into the relationship between operating conditions, process efficiency and particle characteristics. An original intention was to extend the approach of using a seeded fluidised bed reactor to manage the high levels of supersaturation associated with metal sulphide precipitation. To achieve these objectives, the characteristics of the particles produced during copper and zinc sulphide precipitation and the efficiency of the process were studied as a function of sulphide source, metal to sulphide molar ratio and operating pH. The options for downstream processing of the colloidal particles produced by metal sulphide precipitation reactions were also investigated by studying the effect of post-precipitation conditions on the surface properties of the particles.

University of Cape Town

Conclusions

From the results presented in this work, the following conclusions can be drawn:

- The origin of sulphide (biological or chemical) was found to have no significant effect on the mechanism involved in copper and zinc sulphide precipitation, which was dominated by primary nucleation. The presence of bicarbonate ions in solution during the precipitation process buffered the system against protons released during the reaction of HS^- and metal ions. However, the enhanced metal precipitation was obtained at the expense of particle characteristics, particularly in the case of copper. Very small copper sulphide particles were obtained when the precipitation process was conducted using low metal to sulphide molar ratio and the process efficiency was reduced as a result. This was mitigated to an extent by the presence of residual organic acids in the sulphate reduction digester overflow.

- Copper and zinc sulphide precipitation in a seeded fluidised bed reactor was found to be dominated by primary homogenous nucleation, with very little metal precipitation or particle aggregation taking place on the seeds, due to the very high levels of supersaturation accompanying the process. Most of the precipitated metal salt left the reactor in the effluent stream as fine particles.

- Conventional techniques (i.e. multiple reagent feed points and varying recirculation flow rates) used to manage high levels of supersaturation encountered during the precipitation of sparingly soluble salts were found to have no significant effect on process efficiency. This did not support the hypothesis that effective control of supersaturation in the fluidised bed reactor could lead to metal sulphide precipitates with good solid-liquid separation characteristics. The results were attributed to the fact that metal sulphides are substantially less soluble than metal salts (i.e. phosphates, carbonates, etc) used in previous studies. The rapid reaction kinetics, driven by the very high supersaturation, led to the formation of particles which were exposed to different chemical environments within the reactor.

- The heterogeneous nature of the environment in the fluidised bed reactor prompted the study of the precipitation process in a more homogeneous continuously stirred tank reactor (CSTR). The data showed that a pseudo-steady state, in terms of process efficiency, particle size and the charge on the surface of the particles, was attained after 30 minutes. The change in supersaturation, associated with the metal to sulphide molar ratio, and operating pH were found to significantly influence the particle characteristics and process efficiency. Under the conditions of high pH and excess sulphide, the process efficiency was high but a large number of very small, highly charged particles with poor solid-liquid separation characteristics were obtained, especially in the case of copper. The particle characteristics were improved when the precipitation process was conducted at low pH, but this was obtained at the expense of process efficiency. The results showed that the process efficiency was always high in the case of copper but the particle characteristics were worse than those obtained for zinc. The data suggest that the negatively charged sulphide specie (HS^- ions), which

University of Cape Town

adsorb onto the surface of the particles, play an important role in determining the surface characteristics and the nature of the particles. These results are in agreement with the hypothesis that surface properties of colloidal particles produced during metal sulphide precipitation processes are influenced by the conditions under which the particles are produced.

- The charge on the surface of colloidal particles produced by copper and zinc sulphide precipitation reactions was found to be influenced by the change in suspension pH, addition of sulphide and cations. A decrease in suspension pH and addition of cations decreased the surface charge while addition of sulphide, resulted in an increase in surface charge. Although the change in surface charge was significant, the change in mean particle size and surface area was minimal in all cases. This was attributed to the size and morphology of the precipitates, as a consequence of the technique used to recover and prepare them for the study. These results highlight the interventions that can be used to manipulate the charge on the surface of the colloidal metal sulphide particles and enhance particle flocculation and precipitate recovery if the conditions under which the precipitates are produced cannot be adequately managed.

The work presented here shows that the characteristics of the precipitates produced during metal sulphide precipitation process and the efficiency of the process are controlled by the operational conditions. The results of this study provide a deeper level of understanding into metal sulphide precipitation. They indicate that exposure to excess sulphide, whether due to stoichiometric excess or poor mixing at the reagent addition points, should be avoided as the adsorption of the negatively charged HS^- ions suppress particle aggregation, reducing precipitate recovery. The understanding of the difference in the mechanisms involved in copper and zinc sulphide precipitation highlights the problems involved in the processing of more sparingly soluble metal salts.

University of Cape Town

Recommendations

In view of the results and constraints encountered in this work, the following recommendations are suggested:

- The fundamental work in this thesis was carried out using chemically defined, synthetic solutions. In view of this, it is recommended that similar studies be conducted using real effluent and digester overflow to confirm the predictions of this work. Industrial effluents are typically complex and the extent to which the mechanisms identified in this work are affected by the complexity of the matrix should be quantified.

- Further studies are suggested to test the effect of downstream interventions, such as the ones used in this study, on mean particle size, surface area and settling characteristics of the precipitates. Such studies will help provide further evidence which show that the charge on the surface of colloidal particles produced by metal sulphide precipitation play an important role in particle aggregation and solid-liquid separation.

- The use of population balance models to predict the particle rate processes involved in metal sulphide precipitation have, thus far, not been particularly successful. Therefore, it is recommended that the surface chemical properties of the precipitates be considered when developing such models, since they have been shown to play an important role in particle aggregation.

University of Cape Town

REFRENCES

Aldaco, R., Irabien, A., Luis, P. (2005) Fluidized bed reactor for fluoride removal. *Chemical Engineering Journal*, 107, 113 – 117.

Al-Tarazi, M. (2004) Gas-Liquid Precipitation of Dissolved Heavy Metals Ions Using Hydrogen Sulphide Gas. PhD thesis, University of Twente, The Netherlands.

Al-Tarazi, M., Heesink, A. B. M., Azzam, M., Abu Yahya, S., Versteeg, G. F. (2004) Crystallization kinetics of ZnS precipitation: an experimental study using mixed-suspension mixed-product removal (MSMPR) method. *Crystal Research and Technology*, 39(3), 675 – 685.

Al-Tarazi, M., Heesink, A. B. M., Versteeg, G. F. (2004) Precipitation of metal sulphides using gaseous hydrogen sulphide: mathematical modelling. *Chemical Engineering Science*, 59, 235 – 246.

Al-Tarazi, M., Heesink, A. B. M., Versteeg, G. F. (2005) New method for determination of precipitation kinetics using a laminar jet reactor. *Chemical Engineering Science*, 60(3), 805 – 814.

American Public Health Association (APHA) (1975). Standard methods for the examination of water and wastewater. New York: APHA.

Amirtharajah, A. and Mills, K. M. (1982) Rapid-mix design for mechanisms of alum flocculation. *Journal of American Water Works Association*, 74(4), 210 – 216.

Baalousha, M. (2009) Aggregation and disaggregation of iron oxide nanoparticles: Influence of particle concentration, pH and natural organic matter. *Science of the Total Environment*, 407, 2093 – 2101.

Battistoni, P., Deangelis, A., Pavan, P., Prisclandaro, M., Cecchi, F. (2001) Phosphorus removal from a real anaerobic supernatant by struvite crystallization. *Water Research*, 35 (9), 2167 – 2178.

Bénet, N., Muhr, H., Plasari, E., Rousseaux, J. M. (2002) New technologies for precipitation of solid particles with controlled properties. *Powder Technology*, 128, 93 – 98.

Bhagat, M., Burgess, J. E., Antunes, A. P. M., Whiteley, C. G., Duncan, J. R. (2004) Precipitation of mixed metal residues from wastewater utilising biogenic sulphide. *Minerals Engineering*, 17, 925 – 932.

Bell, F. G., Bullock, S. E. T., Hallbich, T. F. J., Lindsay, P. (2001) Environmental

University of Cape Town

impacts associated with an abandoned mine in the Witbank Coalfield, South Africa. *International Journal of Coal Geology*, 45, 195 – 216.

Benner, S. G., Gould, W. D., Blowes, D. W. (2000) Microbial populations associated with the generation and treatment of acid mine drainage. *Chemical Geology*, 169, 435 – 448.

Berner, R. A. (1970) Sedimetary pyrite formation. *American Journal of Science*, 268, 1 – 23.

Bhattacharyya, D. and Ku, Y. (1984) Sulfide Precipitation of Heavy Metals: Effect of Complexing Agents. United States Environmental Protection Agency, EPA-600/S2-84-023, Cincinnati.

Bhattacharyya, D., Jumawan, A. B., Sun, G., Sund-Hagelberg, C., Schwitzgebel, K. (1981) Precipitation of heavy metals with sodium sulfide: Bench-scale and full-scale experimental results. *AIChE Symposium Series,* 77, 31 – 38.

Boonstra, J., van Lier, R., Janssen, G., Dijkman, H., Buisman, C. J. N. (1999) Biological treatment of acid mine drainage. Amsterdam: Elsevier.

Bosman, D. J. (1983) Lime treatment of acid mine water and associated solids/liquid separation. *Water Science and Technology*, 15, 71 – 84.

Bramley, A. S. and Hounslow, M. J. (1996) Aggregation during Precipitation from Solution: A Method for Extracting Rates from Experimental Data. *Journal of Colloid and Interface Science*, 183(1), 155 – 165.

Brown, M., Barley, B., Wood, H. (2002) Minewater treatment: technology, application and policy. London: IWA Publishing.

Brüser, E., Lens, P. N. L., Trüper, H. G. (2000) Environmental Technology to Treat Sulfur Pollution: Principles and Engineering. London: IWA Publishing.

Bryson, A. W. and Bijsterveld, C. H. (1991) Kinetics of the precipitation of manganese and cobalt sulphides in the purification of a manganese sulphate electrolyte. *Hydrometallurgy,* 27, 75 – 84.

Ciglenečki, I., Krznarić, D., Helz, G. R. (2005) Voltammetry of copper sulphide particles and nanoparticles: Investigation of the cluster hypothesis. *Environmental Science and Technology*, 39, 7492 – 7498.

Chang, I. S., Shin, P. K., Kim, B. H. (2000) Biological Treatment of Acid Mine Drainage under Sulphate Reducing Conditions with Solid Waste Materials as Substrate. *Water Research*, 34(4), 1269 – 1277.

Chiang, Y. L., Nathoo, J., Lewis, A. E. (2007) Investigating the control of manganese

University of Cape Town

sulphide precipitation. *The Journal of the South African Institute of Mining and Metallurgy*, 107, 1 – 6.

Christensen, B., Laake, M., Lien, T. (1996) Treatment of acid mine water by sulfate-reducing bacteria; results from a bench scale experiment. *Water Research*, 30, 1617 – 1624.

Claesson, P. M. and Christenson, H. K. (1988) Very long range attraction between uncharged hydrocarbon and flourocarbon surfaces in water. *Journal of Physical Chemistry*, 92, 160 – 165.

Clarke, P., Fornasiero, D., Ralston, J., Smart, R. St. C. (1995) A study of the removal of oxidation products from sulphide mineral surfaces. *Minerals Engineering*, 8(11), 1347 – 1357.

Cline, J. D. (1969) Spectrophotometric determination of hydrogen sulfide in natural waters. *Limnology and Oceanography*, 14, 454 – 458.

Cooney, M. J., Roschi, E., Marison, I. W., Comminelis, C. H., von Stockar, U. (1996) Physiological studies with the sulfate-reducing bacterium Desulfovibrio desulfuricans: Evaluation for use in a biofuel cell. *Enzyme and Microbial Technology*, 68, 838 – 845.

Coulton, R., Bullen, C., Hallet, C. (2003) The design and optimization of active mine water treatment plants. *Land Contamination and Reclamation*, 11(2), 273 – 279.

Deng, H., Chen, C., Peng, Q. Li, Y. (2006) Formation of transition-metal sulfide microspheres or microtubes. *Materials Chemistry and Physics*, 100(2/3), 224 – 229.

Dentel, S. Coagulation control in water treatment. *CRC Critical Reviews in Environmental Control*, 21, 41 – 135.

Derjaguin, B. V. and Landau, L. (1941) Theory of the stability of strongly charged lyophobic sols and of the adhesion of strongly charged particles in solution of electrolytes. *Acta Physicochimica URSS*, 14, 633 – 662.

Demopoulos, G. P. (2009) Aqueous precipitation and crystallization for the production of particulate solids with desired properties. *Hydrometallurgy*, 96, 199 – 214.

Djedidi, Z., Khaled, J. B., Cheikh, R. B., Blais, J., Mercier, G., Tyagi, R. D. (2009) Comparative study of dewatering characteristics of metal precipitates

University of Cape Town

generated during treatment of monometallic solutions. *Hydrometallurgy*, 95(1/2), 61 – 69.

Doerr, A. K., Tolan, M., Seydel, T., Press, W. (1998) The interface structure of thin liquid hexane films. *Journal of Chemical Physics*, 248, 263 – 268.

Duan, J. and Gregory, J. (1996) Influence of soluble silica on coagulation by aluminium sulphate. *Colloids and Surfaces A: Physicochemical and Engineering Aspects*, 107, 309 – 319.

Dvorak, D. H., Hedin, R. S., Edenborn, H. M., McIntire, P. E. (1992) Treatment of metal-contaminated water using bacterial sulfate reduction: results from pilot-scale reactors. *Biotechnology and Bioengineering*, 40, 609 – 616.

EarthLife Africa Jhb (2009) Acid mine drainage fact sheet.

Eigen, M. and Wilkins, R. G. (1965) The kinetics and mechanism of formation of metal complexes. In: Mechanisms of Inorganic Reactions. *ACS Symposium Series*, 49, 55 – 80.

Elimelech, M., Gregory, J., Jia, X., Williams, R. A. (1995) Particle deposition and aggregation: measurement, modelling and simulation. Woburn: Butterworth-Heinemann.

Esposito, G., Veeken, A., Weijma, J., Lens, P. N. L. (2006) Use of biogenic sulphide for ZnS precipitation. *Separation and Purification Technology*, 51(1), 31 – 39.

Fairthorne, G., Fornasiero, D., Ralston, J. (1997) Effect of oxidation on the collectorless flotation of chalcopyrite. *International Journal of Mineral Processing*, 49(1/2), 31 – 48.

Franke, J. and Mersmann, A. (1995) The influence of the operational conditions on the precipitation process. *Chemical Engineering Science*, 50(11), 1737 – 1753.

Fornasiero, D., Eijt, V., Ralston, J. (1992) An electrokinetic study of pyrite oxidation. *Colloids and Surfaces*, 62(1 – 2), 63 – 73.

Garrels, R. M. and Naeser, C. R. (1958) Equilibrium distribution of dissolved sulphur species in water at 25^0C and 1 atm total pressure. *Geochimica et Cosmochimica Acta*, 15(1 – 2), 113 – 130.

Gazea, B., Adam, K., Kontopoulos, A. (1996) A review of the passive systems for the treatment of acid mine drainage. *Minerals Engineering*, 9(1), 23 – 42.

Gibson, G. R. (1990) Physiology and ecology of sulphate-reducing bacteria. *Journal of Applied Bacteriology*, 59, 769 – 797.

Giggenbach, W. (1971) Optical spectra of highly alkaline solutions and the second

University of Cape Town

dissociation constant of hydrogen sulphide. *Inorganic Chemistry*, 10 (7), 1333 – 1338.

Gösele, W. and Kind, M. (1991) Study on the influence of mixing on the quality of continuous precipitating products. *Chemical Engineering Technology*, 63, 59 – 61.

Graveland, A., van Dijk, J. C., de Moel, P. J., Oomen, J. H. C. M. (1983) Developments in water softening by means of pellet reactors. *Journal American Water Works Association*, 75 (12), 619 – 662.

Guillard, D. and Lewis, A. E. (2001) Nickel Carbonate precipitation in a fluidised bed reactor. *Industrial and Engineering Chemistry Research*, 40(23), 5564 – 5569.

Hammack, R. W., Dvorak, D. H., Edenborn, H. M. (1993) The use of biogenic sulfide to selectively recover copper and zinc from severely contaminated mine drainage. In: *Biohydrometallurgical Technologies* (editors: Torma, A. E., Wey, J. E., Lakshmanan, V. L.). Warrendale: The Minerals, Metals & Materials Society, 631 – 639.

Hammack, R. W., Edenborn, H. M., Dvorak, D. H. (1994) Treatment of water from an open-pit copper mine using biogenic sulphide and limestone: a feasibility study. *Water Research*, 28, 2321 – 2329.

Hao, H. T. T., Liamlem, W., Annachhatre, A. P. (2007) Lead removal through biological sulfate reduction process. *Bioresource Technology*, 98, 2538 – 2548.

Harmandas, N. G. and Koutsoukos, P G. (1996) The formation of iron (II) sulfides in aqueous solutions. *Journal of Crystal Growth*, 167(3/4), 719 – 724.

Healy, T. W. and Moignard, M. S. (1976) A review of electrokinetic studies of metal sulphides. In: *Flotation: A. M. Gaudin Memorial Volume* (editor: Fuerstenau, M. C.), New York: American Institute of Mining, Metallurgical and Petroleum Engineers.

Hedin, R. S. (1997) Passive mine water treatment in the Eastern United States. In: *Mine Water Treatment Using Wetlands* (editor: Younger, P. L.). London: Chartered Institution of Water and Environment Management.

Higbie, R. (1935) The rate of absorption of a pure gas into a still liquid during a short time of exposure. *Transactions of AIChE*, 31, 365 – 389.

Hogg, R., (2000) Flocculation and dewatering. *International Journal of Mineral Processing*, 58, 223 – 236.

University of Cape Town

Hostomsky, J. and Jones, A. G. (1995). A penetration model of the gas–liquid reactive precipitation of calcium carbonate crystals. *Transactions of the Institution of Chemical Engineers*, 73(A), 241 – 245.

Hounslow, M. J, Ryall, R L., Marshall, V. R. (1988) A Discretized Population Balance for Nucleation, Growth and Aggregation. *AIChE Journal*, 34(11), 1821 – 1832.

Hounslow, M. J., Mumtaz, H. S., Collier, A. P., Barrick, J. P., Bramley, A. S. (1999) Aggregation during precipitation - putting the pieces of the puzzle together. *Industrial Crystallization*, 1 – 12.

Hounslow, M. J, Lewis, A. E., Sanders, S. J., Bondy, R. (2005) Generic Crystallizer Model: I. A Model Framework for Well-Mixed Compartment. *AIChE Journal*, 51(11), 2942 – 2955.

Hove, M., van Hille, R. P., Lewis, A. E. (2008) Mechanisms of formation of iron precipitates from ferrous solutions at high and low pH. *Chemical Engineering Science*, 63, 1626 – 1635.

Hove, M. (2008) The kinetics and mechanisms of the oxidation and precipitation of iron: The High Density Sludge Process (HDS). PhD thesis, University of Cape Town, South Africa.

Huismann, J. L., Schouten, G., Schultz, C. (2006) Biologically produced sulphide for purification of process streams, effluent treatment and recovery of metals in the metal and mining industry. *Hydrometallurgy*, 83, 106 – 113.

Hulbert, H. M. and Katz, S. (1964) Some Problems in Particle Technology: A Statistical Mechanical Formulation. *Chemical Engineering Science*, 19, 555 – 574.

Hulshoff Pol, L. W., Lens, P. N. L., Weijma, J., Stams, A. J. M. (2001) New developments in reactor and process technology for sulfate reduction. *Water Science and Technology*, 44, 67 – 76.

Hunter, R. J. (2001) Foundations of colloid science (second edition). New York: Oxford University Press Inc.

Israelachvili, J. N. and Pashley, R. M. (1984) Measurement of the hydrophobic interaction between two hydrophobic surfaces in aqueous electrolyte solutions. *Journal of Colloid and Interface Science*, 98, 500 – 514.

Jackson, E. (1986) Hydrometallurgical Extraction and Reclamation. Chichester: Ellis Horwood Limited.

University of Cape Town

Jandová, J., Lisá, K., Vranka, F. (2005) Separation of copper and cobalt-nickel concentrates during processing of manganese deep ocean nodule. *Hydrometallurgy*, 77, 75 – 79.

Jarvis, A. P. and Younger, P. L. (2000) Broadening the scope of mine water environmental impact assessment - a UK perspective. *Environmental Impact Assessment Reviews*, 20, 85 – 96.

Johnson, D. B. (2003) Chemical and microbiological characteristics of mineral spoils and drainage waters at abandoned coal and metal mines. *Water Air Soil Pollution: Focus*, 3, 47 – 66.

Johnson, D. B and Hallberg, K. B. (2005) Acid mine drainage remediation options: a review. *Science of the Total Environment*, 338, 3 – 14.

Johnson, D. B. (2006) Biohydrometallurgy and the environment: Intimate and important interplay. *Hydrometallurgy*, 83, 153 – 166.

Jones, A. J., Hostomsky, J., Li, Z. (1992) On the effect of liquid mixing rate on primary crystal size during the gas–liquid precipitation of calcium carbonate. *Chemical Engineering Science*; 47, 3817 – 3824.

Jones, A. G. (2002) Crystallization Process Systems. Oxford: Butterworth-Heinemann.

Jovanović, D. L., Validžić, I. Lj., Janković, I. A., Bibić, N., Nedeljković, J. M. (2007) Synthesis and characterisation of shaped ZnS nanocrystals in water in oil microemulsions. *Materials Letters*, 61, 4396 – 4399.

Kaksonen, A. H., Plumb, J. J., Robertson, W. J., Riekkola-Vanhanen, M., Franzmann, P. D., Puhakka, J. A. (2006) The performance, kinetics and microbiology of sulfidogenic fluidised-bed treatment of acidic metal- and sulfate-containing wastewater. *Hydrometallurgy*, 83, 204 – 213.

Karbanee, N., van Hille, R. P., Lewis, A. E. (2008) Controlled Nickel Sulfide Precipitation Using Gaseous Hydrogen Sulfide. *Industrial and Engineering Chemistry Research*, 47, 1596 – 1602.

Kaschiev, D. (2000) Nucleation: Basic theory with applications. Oxford: Butterworth-Heinemann.

Kim, B. R., Gaines, W. A., Szafranski, M. J., Bernath, E. F., Miles, A. M. (2002) Removal of Heavy Metals from Automotive Wastewater by Sulfide Precipitation. *Journal of Environmental Engineering*, 612 – 623.

Kind, M. (2002) Colloidal aspects of precipitation processes. *Chemical Engineering*

University of Cape Town

Science, 57, 4287 – 4293.

Kobayashi, M., Juillerat, F., Galleto, P., Bowen, P., Borkovec, M. (2005) Aggregation and Charging of Colloidal Silica Particles: Effect of Particle Size. *Langmuir*, 21, 5761 – 5769.

Kolthoff, I. M. and Moltzau, D. R. (1935) Induced precipitation and properties of metal sulphides. *Chemical Reviews*, 17, 293 – 325.

Kostenbader, N. and Haines, G. F. (1970) High density sludge treats acid mine drainage. *Coal Age*, 90 – 97.

Koumanakos, E., Dalas, E., Koutsoukos, P. G. (1990) The precipitation of cadmium sulphide in aqueous solutions. *Journal of the Chemical Society - Faraday Transactions*, 86(6), 973 – 977.

Ledin, M. and Pedersen, K. (1996) The environmental impact of mine wastes - roles of microorganisms and their significance in treatment if mine wastes. *Earth-Science Reviews*, 41, 67 – 108.

Lee, C., Yang, W., Hsieh, C. (2004) Removal of Cu (II) from aqueous solution in a fluidized-bed reactor. *Chemosphere*, 57, 1173 – 1180.

Leikin, S., Parsegian, V. A., Rau, D. C., Rand, R. P. (1993) Hydration forces. *Annual Review of Physical Chemistry*, 44, 369 – 95.

Letterman, R. D., Amirtharajah, A., O'Melia, C. R. (1999) Coagulation and flocculation. In: *Water Quality and Treatment* (editor: Letterman, R. D.). New York: McGraw-Hill.

Lewis, A. E. and Swaartbooi, A. (2006) Factors affecting metal removal in mixed sulphide precipitation. *Chemical Engineering and Technology*, 81(3/4), 197 – 204.

Lewis, A. E. and van Hille, R. P. (2006) An exploration into the metal sulphide precipitation method and its effect on metal sulphide removal. *Hydrometallurgy*, 81, 197 – 204.

Lewis, A. E., Nathoo, J., Mokone, T. P. (2008) Reactor design for metal precipitation in mine water treatment. Water Research Commission, Research report No. K5/1729, Pretoria, South Africa.

Licht, S., Forouzan, F., Longo, K. (1990) Differential densometric analysis of equilibria in highly concentrated media: Determination of the aqueous second dissociation constant of H_2S. *Analytical Chemistry* 62, 1356 – 1360.

Liang, Y., Hilal, N., Langston, P., Starov, V. (2007) Interaction forces between

University of Cape Town

colloidal particles in liquid: Theory and experiment. *Advances in Colloid and Interface Science*, 134/135, 151 – 166.

Lopez, O., Sanguinetti, D., Bratty, M., Kratochvil, D. (2009) Green technologies for sulphate and metal removal in mining and metallurgical effluents. *Enviromine 2009*, Santiago, Chile.

Luther, G. W. and Rickard, D. T. (2005) Metal sulfide cluster complexes and their biogeochemical importance in the environment. *Journal of Nanoparticle Research*, 7, 389 – 407.

Luther, G. W., Theberge, S. M., Rickard, D., Rowlands, C. C., Oldroyd, A. (2002) Aqueous Copper Sulfide Clusters as Intermediates during Copper Sulfide Formation. *Environmental Science and Technology*, 36, 394 – 402.

Luther, G. W., Theberge, S. M., Rickard, D. T. (1999) Evidence for aqueous clusters as intermediates during zinc sulfide formation. *Geochimica et Cosmochimica Acta*, 63(19/20), 3159 – 3169.

Mathew, S. K., Rajesh, N. P., Ichimura, M., Udayalakshmi (2008) Preparation and characterisation of copper sulphide precipitates by photochemical method. *Materials Letters*, 62(4/5), 591 – 593.

Mersmann, A. (2001) Fundamentals of Crystallization. New York: Marcel Dekker.

Meyer, B., Ward, K., Koshlap, K., Peter, L. (1983) Second dissociation constant of hydrogen sulfide. *Inorganic Chemistry*, 22, 2345 – 2346.

Micera, G. and Dessi, A. (1988) Chromium adsorption by plant roots and formation of long-lived Cr(v) species: An ecological hazard? *Journal of Inorganic Biochemistry*, 34(3), 157 – 166.

Migdisov, A. A., Williams-Jones, A. E., Lakshatanov, L. Z. and Alekhin, Y. (2001) Estimates of the second dissociation constant of H2S from the surface sulfidation of crystalline sulfur. *Geochimica et Cosmochimica Acta*, 66(10), 1713 – 1725.

Mishra, P. K. and Das, R. P. (1992) Kinetics of zinc and cobalt sulphide precipitation and its application in hydrometallurgical separation. *Hydrometallurgy*, 28(3), 373 – 379.

Mishra, K. K. and Kapoor, M. L. (1978). Kinetics of liquid-gas reactions through bubbles. *Hydrometallurgy*, 3, 75 – 83.

Moignard, M. S., James, R. O., Healey, T. W. (1977) Adsorption of calcium at the zinc sulphide-water interface. *Australian Journal of Chemistry*, 30(4),

University of Cape Town

733 – 740.

Mullin, J. W. (2001) Crystallization (fourth edition). Oxford: Butterworth-Heinemann.

Newell, A. J. H., Skinner, W. M., Bradshaw, D. J. (2007) Restoring the floatability of oxidised sulfides using sulfidisation. *International Journal of Mineral Processing*, 84, 108 – 117.

Nicolau, Y. F. and Menard, J. C. (1992) An electrochemistry study of ZnS and CdS surface chemistry. *Journal of Colloid and Interface Science*, 148, 552 – 570.

Nielsen, A. E. (1979) Industrial Crystallization. Amsterdam: Jong and Jancić.

Nielsen, A. E. (1964) Kinetics of precipitation. Oxford: Pergamon Press.

Ntuli, F. and Lewis, A. E. (2007) The influence of iron on the precipitation behaviour of nickel. *Chemical Engineering Science*, 62, 3756 – 3766.

OLI Systems Inc (2010) OLI Stream Analyzer, Version 3, New Jersey: Morris Plain.

Oryx Environmental & Jones and Wagener Consulting Engineers (2003) The Grootvlei Proprietary Mines Limited: Project to reduce and treat the volumes of water pumped from underground. Research report, Braamfontein, South Africa.

Oktaybaş, C., Açma, E., Arslan, C., Addemir, O. (1994). Kinetics of copper precipitation by H_2S from sulphate solutions. *Hydrometallurgy*, 35, 129 – 137.

Oyekola, O. O., van Hille, R. P., Harrison, S. T. L. (2009) Study of anaerobic lactate metabolism under biosulfidogenic conditions. *Water Research*, 43, 3345 – 3354.

Pattrick, R. A. D., Mosselmans, J. F. W., Charnock, J. M., England, K. E. R., Helz, G. R., Garner, C. D., Vaughan, D. J. (1997) The structure ofamorphous copper sulfide precipitates: an X-ray absorption study. *Geochimica et Cosmochimica Acta*, 61, 2023–2036.

Peters, R. W., Ku, Y., Chang, T. K. (1984) Heavy metal crystallization kinetics in an MSMPR crystallizer employing sulfide precipitation. *AIChE Symposium Series - Advances in Crystallization from Solutions*, 80, 55 – 75.

Rabinovich, Y. I. and Derjaguin, B. V. (1988) Interaction of hydrophobized filaments in aqueous electrolyte. *Colloids and Surfaces*, 30, 243 – 251.

Randolph, A. D. and Larson, M. A. (1962) Transient and Steady State Size Distributions in Continuous Mixed Suspension Crystallizers. *AIChE Journal*, 8(5), 639 – 645.

University of Cape Town

Randolph, A. D. and Larson, M. A. (1988) Theory of particulate processes (second edition). London: Academic Press.

Rhadika, V., Subramanian, S., Natarajan, K. A. (2006) Bioremediation of zinc using Desulfotomaculum nigrificans: Bioprecipitation and characterization studies. *Water Research*, 40, 3628 – 3636.

Ribet, I., Ptacek, C. J., Blowes, D. W., Jambor, J. L. (1995) The potential for metal release by reductive dissolution of weathered mine tailings. *Journal of Contaminant Hydrology*, 17, 239 – 273.

Richardson, J. F.; Haarker, J. H., Backhurst, J. R. (2002) Coulson and Richardson's Chemical Engineering: Particle Technology and Separation Processes, Oxford: Butterwoth-Heinemann.

Richens, D. T. (1997) The chemistry of aqua ions: Synthesis, structure and reactivity: A tour through the periodic table of the elements. New York: John Wiley.

Rickard, D. T. (1969) The chemistry of iron sulfide formation at low temperature. *Stockholm Contamination Geology*, 20, 67 – 95.

Rickard, D. T. (1989a) An apparatus for the study of fast precipitation reactions. *Minerals Magazine*, 53, 527 – 530.

Rickard, D. T. (1989b) Experimental concentration-time curves for the iron (II) sulfide precipitation in aqueous solutions and their interpretation. *Chemical Geology*, 78, 315 – 324.

Rickard, D. and Luther, G. W. (2006) Metal sulphide complexes and clusters. *Sulfide Mineralogy and Geochemistry*, 61, 421 – 504.

Rickard, D. (1995) Kinetics of FeS precipitation: Part 1. Competing reaction mechanisms. *Geochimica et Cosmochimica Acta*, 59(21), 4367 – 4379.

Rigopoulos, S. and Jones, A. G. (2001) Dynamic modelling of a bubble column for particle formation via a gas-liquid reaction. *Chemical Engineering Science*, 56, 6177 – 6184.

Rose, P., Pletschke, B., Whiteley, C. (2000) Complex organic carbon compounds as electron donors for sulphate reduction - the Rhodes 'Biosure' process in the treatment of mine drainage wastewater. *Proceedings of the Technology Transfer Workshop on Biological Sulphate Removal of the Anaerobic Process*, Pretoria, South Africa.

Rowley, M., Warkentin, D. D., Sicotte, V. (1997) Site demonstration of the biosulfide process at the former Brittania mine. Vancouver, British Columbia.

University of Cape Town

Rozan, T. F., Lassman, M. E., Ridge, D. P., Luther, G. W. (2000) Evidence for iron, copper and zinc complexation as multinuclear sulphide clusters in oxic rivers. *Nature*, 406, 879 – 882.

Sampaio, R. M. M., Timmers, R. A., Xu, Y., Keesman, K. J., Lens, P. N. L. (2009) Selective precipitation of Cu from Zn in a pS controlled continuously stirred tank reactor. *Journal of Hazardous Materials*, 165, 256 – 265.

Sastry, K. V. S. (1975) Similarity size distribution of agglomerates during their growth by coalescence in granulation or green pelletization. *International Journal of Mineral Processing*, 2, 187 – 203.

Seckler, M. M. (2004) Calcium phosphate precipitation in a fluidized bed. PhD Thesis, Delft University of Technology, The Netherlands.

Seckler, M. M., van Leeuwen, M. L. J., Bruinsma, O. S. L., van Rosmalen, G. M. (1996) Phosphate removal in a fluidized bed - II. Process of Optimization. *Water Research*, 30(7), 1589-1596.

Senanayake, G. (2009) A review of chloride assisted copper sulphide leaching by oxygenated sulphuric acid and mechanistic consideration. *Hydrometallurgy*, 98, 21 – 32.

Shea, D. and Helz, G. R. (1988) The solubility of copper in sulfidic waters: Sulfide and polysulfide complexes in equilibrium with covellite. *Geochimica et Cosmochimica Acta*, 52, 1815 – 1825.

Smoluchowski, M. V. (1917) Mathematical Theory of Kinetics of the Coagulation of Colloidal solutions. *Zeitschrift für Physikalische Chemie*, 92, 129 – 168.

Söhnel, O. and Garside, J. (1992) Precipitation: Basic Principles and Industrial Application. Oxford: Butterworth- Heinemann.

Steffen, R. K. (1989) Research on the contribution of mine dumps to the mineral pollution load in the Vaal Barrage. Water Research Comission, Research report No. 136/1/89, Pretoria, South Africa.

Stephens, H. and Cobble, J. (1971) Thermodynamic properties of the aqueous sulphide and bisulfide ions and the second ionization constant of hydrogen sulphide over extended temperatures. *Inorganic Chemistry*, 10, 918 – 921.

Stén, P. and Forsling, W. (2000) Precipitation of lead sulphide for surface chemical studies. *Colloids and surfaces A: Physicochemical and Engineering Aspects*, 172(1/3), 17 – 31.

University of Cape Town

Stumm, W. and Morgan, J. J. (1996) Aquatic Chemistry: Chemical Equilibria and Rates in Natural Waters (third edition). New York: John Wiley & Sons Inc.

Stumm, W. (1992) Chemistry of the solid-water interface: processes at the mineral-water and particle-water interface in natural systems. New York: John Wiley & Sons Inc.

Sukola, K., Wang, F., Tessier, A. (2005) Metal-sulfide species in oxic waters. *Analytica Chimica Acta*, 528(2), 183 – 195.

Tabak, H. H., Scharp, R., Burckle, J., Kawahara, F. K., Govind, R. (2003) Advances in biotreatment of acid mine drainage and biorecovery of metals: 1. Metal precipitation for recovery and recycle. *Biodegradation*, 14, 423 – 436.

Tang, H. X. and Stumm, W. (1987) The coagulating behaviours of Fe(III) polymeric species—I. Preformed polymers in various concentrations. *Water Research*, 21, 115 – 121.

Taty Costodes, V. C. and Lewis, A. E. (2006) Reactive crystallisation of nickel-hydroxy-carbonate in a fluidised bed reactor: 1. Fines production and column design. *Chemical Engineering Science*, 61, 1377 – 1385.

ter Maat, H., Al-Tarazi, M., Hogendoorn, J. A., Niederer, J. P. M., Versteeg, G. F. (2007) Theoretical and experimental study of the absorption rate of H_2S in $CuSO_4$ solutions. The effect of enhancement of mass transfer by a precipitation reaction. *Transactions of Institution of Chemical Engineers – Part A*, 85 (A1), 100 – 108.

Tokuda, H., Kuchar, D., Mihara, N., Kubota, M., Matsuda, H., Fukuta, T. (2008) Study of the reaction kinetics and selective precipitation of Cu, Zn, Ni and Sn with HsS in a single-metal and multi-metal systems. *Chemosphere*, 73, 1448 – 1452.

Torbacke, M., and Rasmuson, A. C. (2001) Influence of different scales of mixing in reaction crystallisation. *Chemical Engineering Science*, 56(7), 2459 – 2473.

Veeken, A. H. M. and Rulkens, W. H. (2003a) Innovative developments in the selective removal and reuse of heavy metals from wastewaters. *Water Science and Technology*, 47(10), 9 – 16.

Veeken, A. H. M., Akoto, L., Hulshoff Pol, L. W., Weijma, J. (2003b) Control of the sulfide concentration for optimal zinc removal by sulfide precipitation in a continuously stirred tank reactor. *Water Research*, 37, 3709 – 3717.

Verwey, E. J. W. and Overbeek, J. Th. G. (1948) Theory of the Stability of Lyophobic

University of Cape Town

Colloids. Amsterdam: Elsevier Publishing Company.

van Hille, R. P., Peterson, K. A., Lewis, A. E. (2005) Copper sulphide precipitation in a fluidised bed reactor. *Chemical Engineering Science*, 60, 2571 – 2578.

van Hille, R. P., Foster T., Storey, A., Duncan, J.; Lewis, A. E. (2004) Heavy metal precipitation by sulphide and bicarbonate: Evaluating methods to predict anaerobic digester overflow performance. *Proceedings of International Mine Water Association Conference*, Sun City, South Africa.

van Houten, B. H. G. W., Roest, K., Tzeneva, V. A., Dijkman, H., Smidt, H., Stams A. J. M. (2006) Occurrence of methanogenesis during start-up of a full-scale synthesis gas-fed reactor treating sulfate and metal-rich wastewater. *Water Research*, 40, 553 – 560.

Wachi, S. and Jones, A. G. (1991). Mass transfer with chemical reaction and precipitation. *Chemical Engineering Science*, 46, 1027 – 1033.

Wachi, S. and Jones, A. G. (1995). Aspects of gas–liquid reaction systems with precipitate particle formation. *Reviews in Chemical Engineering*, 11(1), 1 – 51.

Wagmam, D., Evans, W., Parker, V., Halow, L., Bailey, S., Schumm, R. (1968) Selected Values of 'thermodynamic Properties. Washington DC: US Government Printing Office.

Walmsley Environmental (1995) A preliminary assessment of the environmental, social, economic and financial implications of dewatering of East Rand Basin into the Blesbokspruit or alternately allowing it to flood. Department of Minerals and Energy Affairs, Research Report No. W147, South Africa.

Wang, D. S., Tang, H. X., Gregory, J. (2002) Relative importance of charge-neutralization and precipitation during coagulation with IPF-PACl: Effect of sulphate. *Environmental Science and Technology*, 36, 3866 – 3872.

Wang, Y., Zhou, W., Gao, B., Xu, X., Xu, G. (2009) The effect of total hardness on the coagulation performance of aluminium salts with different Al species. *Separation and Purification Technology*, 66, 457– 462.

Whittington-Jones, K., Molwantwa, J. B.; Rose, P. D. (2006) Enhanced hydrolysis of carbohydrates in primary sludge under biosulphidogenic conditions. *Water Research*, 40, 1577 – 1582.

Widdel, F. and Pfenning, N. (1988) Microbiology and ecology of sulfate- and sulfur-reducing bacteria. In: *Biology of anaerobic microorganisms* (editor: Zhender, J. B.). New York: Wiley and Sons.

University of Cape Town

Williams, R. and Labib, M. E. (1985) Zinc sulphide chemistry: An electrokinetic study. *Journal of Colloid and Surface Science*, 106, 252 – 254.

Wilms, D. and van Dijk, J. M. (1988) Recovery of nickel by crystallization of nickel carbonates in a fluidized-bed reactor. *VTT Symposium on Nonwaste Technology*. Espoo, Finland, 1 – 17.

World Health Organisation (WHO) (2006) Guidelines for drinking water quality. First Addendum to first edition Volume 1. Recommendations (third edition). Geneva: WHO.

Xiao, F., Ma, J., Yi, P., Ju-Chang Howard Huang, J. H. (2008) Effects of low temperature on coagulation of kaolinite suspensions. *Water Research*, 42, 2983 – 2992.

Yan. M., Wang, D., Yu, J., Ni, J., Edwards, M., Qu, J. (2008) Enhanced coagulation with polyaluminum chlorides: Role of pH/Alkalinity and speciation. *Chemosphere*, 71, 1665 – 1673

Younger, P. L., Banwart, S. A.; Hedin, R. S. (2002) Mine Water: Hydrology, Pollution and Remediation. Dordrecht: Kluver Academic Publishers.

Yu, C. J., Richter, A. G., Kmetko, J., Datta, A., Dutta, P. (2000) X-ray diffraction evidence of ordering in a normal liquid near the solid-liquid interface. *Europhysics Letters*, 50, 487 – 493.

Zhou, P., Huang, J., Li, A. W. F., Wei, S. (1999) Heavy metal removal from wastewater in fluidised bed reactor. *Water Research*, 33(8), 1918 – 1924.

University of Cape Town

APPENDICES

Appendix A

Raw data for the seeded fluidised bed reactor experiments reported in Chapter 4.

Table A0.1: Data for copper sulphide precipitation using two reagent feed points (2FP) configuration as function of time.

Time (minutes)	Cu^{2+} total (mg L^{-1})	Cu^{2+} disslved (mg/l)	Cu^{2+} in (mg L^{-1})	Conversion (%)	Removal efficiency (%)	Fines (%)	pH
0	169.90	169.90	169.90	0.00	0.00	0.00	4.52
30	46.01	38.15	66.66	42.77	30.98	11.79	7.60
90	42.73	35.85	63.93	43.92	33.16	10.76	7.52
150	40.89	34.42	62.39	44.83	34.46	10.37	8.15
270	41.77	34.50	63.13	45.35	33.83	11.52	7.83
360	41.44	33.93	62.85	46.01	34.07	11.95	7.88

Table A0.2: Steady state data for copper sulphide precipitation using two reagent feed points (2FP) configuration as a function of reactor height.

Reactor height (cm)	Cu^{2+} total (mg L^{-1})	Cu^{2+} dissolved (mg L^{-1})	Cu^{2+} in (mg L^{-1})	Conversion (%)	Removal efficiency (%)	Fines (%)	pH
0	169.90	161.60	161.60	0.00	0.00	0.00	4.52
30	50.34	46.24	68.88	32.87	26.92	5.95	7.06
70	41.47	33.13	61.49	46.12	32.56	13.56	7.85
110	41.54	32.93	61.55	46.50	32.51	13.99	7.94
160	41.77	34.50	61.74	44.12	32.35	11.77	7.83

Table A0.3: Data for copper sulphide precipitation using six reagent feed points (6FP) configuration as a function of time.

Time (minutes)	Cu^{2+} total (mg L^{-1})	Cu^{2+} disslved (mg L^{-1})	Cu^{2+} in (mg L^{-1})	Conversion (%)	Removal efficiency (%)	Fines (%)	pH
0	161.60	161.60	161.60	0.00	0.00	0.00	4.52
30	38.53	31.51	59.04	46.63	34.74	11.89	7.68
90	36.39	28.50	57.26	50.23	36.45	13.78	7.53
150	35.34	27.80	56.38	50.69	37.32	13.37	8.17
270	35.5	28.05	56.52	50.37	37.19	13.18	7.68
360	35.53	28.52	56.54	49.56	37.16	12.40	7.71

University of Cape Town

Table A0.4: Steady state data for copper sulphide precipitation using six reagent feed points (6FP) configuration as a function of reactor height.

	Cu^{2+} total (mg L^{-1})	Cu^{2+} dissolved (mg L^{-1})	Cu^{2+} in (mg L^{-1})	Conversion (%)	Removal efficiency (%)	Fines (%)	pH
0	161.60	161.60	161.60	0.00	0.00	0.00	4.52
30	40.36	16.54	60.57	72.69	33.36	39.33	7.10
70	37.22	28.87	57.95	50.18	35.77	14.41	7.57
110	35.86	26.69	56.82	53.02	36.88	16.14	7.78
160	35.5	28.05	56.52	50.37	37.19	13.18	7.68

Table A0.5: Data for zinc sulphide precipitation using two reagent feed points (2FP) configuration as a function of time.

Time (minutes)	Zn^{2+} total (mg L^{-1})	Zn^{2+} disslved (mg L^{-1})	Zn^{2+} in (mg L^{-1})	Conversion (%)	Removal efficiency (%)	Fines (%)	pH
0	161.60	161.60	161.60	0.00	0.00	0.00	5.52
30	52.97	0.07	71.08	99.90	25.47	74.43	7.36
90	134.33	0.08	138.88	99.94	3.27	96.67	7.33
150	97.97	0.08	108.58	99.93	9.77	90.16	7.29
270	99.99	0.42	110.26	99.62	9.31	90.31	7.40
360	118.17	0.22	125.41	99.82	5.77	94.05	7.50

Table A0.6: Steady state data for zinc sulphide precipitation using two reagent feed points (2FP) configuration as a function of reactor height.

Reactor height (cm)	Zn^{2+} total (mg L^{-1})	Zn^{2+} dissolved (mg L^{-1})	Zn^{2+} in (mg L^{-1})	Conversion (%)	Removal efficiency (%)	Fines (%)	pH
0	161.60	161.60	161.60	0.00	0.00	0.00	5.52
30	63.63	1.81	79.96	97.74	20.42	77.32	7.13
70	127.26	0.21	132.98	99.84	4.30	95.54	7.25
110	106.05	0.19	115.31	99.84	8.03	91.81	7.47
160	97.97	0.08	108.58	99.93	9.77	90.16	7.29

Table A0.7: Data for zinc sulphide precipitation using six reagent feed points (6FP) configuration as a function of time.

Time (minutes)	Zn^{2+} total (mg L^{-1})	Zn^{2+} disslved (mg L^{-1})	Zn^{2+} in (mg L^{-1})	Conversion (%)	Removal efficiency (%)	Fines (%)	pH
0	150.49	150.49	150.49	0.00	0.00	0.00	5.52
30	76.76	0.27	89.05	99.70	13.80	85.90	7.50
90	42.42	0.60	60.43	99.01	29.81	69.20	7.33
150	54.54	0.09	70.53	99.87	22.67	77.20	7.48
270	41.41	0.14	59.59	99.77	30.51	69.26	7.54
360	76.76	0.15	89.05	99.83	13.80	86.03	7.56

University of Cape Town

Table A0.8: Data for zinc sulphide precipitation using six reagent feed points (6FP) configuration as a function of reactor height.

Reactor height (cm)	Zn^{2+} total (mg L^{-1})	Zn^{2+} disslved (mg L^{-1})	Zn^{2+} in (mg L^{-1})	Conversion (%)	Removal efficiency (%)	Fines (%)	pH
0	150.49	150.49	150.49	0.00	0.00	0.00	5.52
30	86.86	43.32	97.47	55.55	10.88	44.67	6.33
70	44.44	1.14	62.12	98.16	28.46	69.71	7.03
110	65.95	0.24	80.04	99.70	17.60	82.10	7.40
160	54.54	0.09	70.53	99.87	22.67	77.20	7.48

The term Me^{2+}_{in} represent the actual amount of metal ions which react inside the reactor and it was calculated according to Equation A0.1

$$Me^{2+}{}_{in} = \frac{Q_{recycle} Me^{2+}{}_{out,total} + Q_{feed,Me^{2+}} Me^{2+}{}_{feed}}{Q_{total}} \quad \text{A0.1}$$

where $Q_{recycle}$ is the recycle flow rate (mL min^{-1}), Q_{total} is the total flow rate at the point of contact inside the reactor (mL min^{-1}), $Q_{feed,Me2+}$ is the flow rate of the metal solution (mL min^{-1}) and, $Me^{2+}{}_{out,total}$ and $Me^{2+}{}_{feed}$ represents the total metal concentration in the recycle stream and the concentration of the metal in the feed stream (mg L^{-1}), respectively.

University of Cape Town

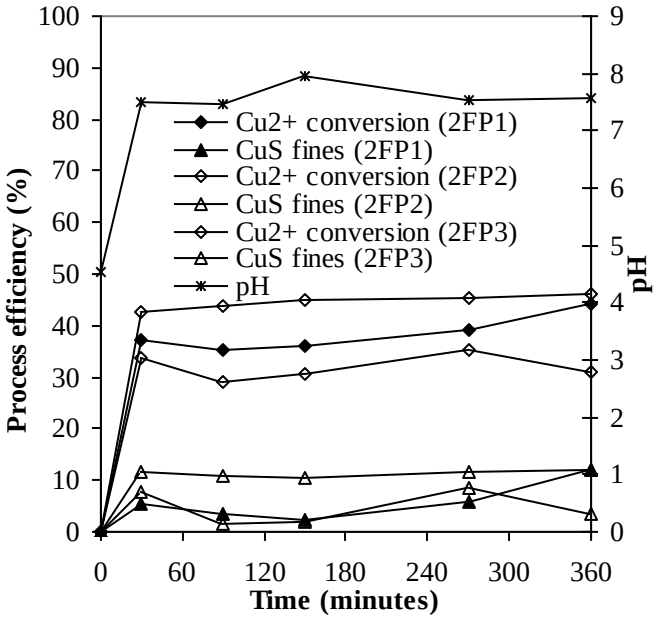

Figure A0.1: An example showing reproducibility and attainment of pseudo-steady state during metal sulphide precipitation in a seeded fluidised bed reactor.

University of Cape Town

Appendix B

Raw data for the induction time of zinc sulphide as mentioned in Chapter 4.

The induction time for the zinc sulphide precipitation reaction was measured by adding stoichiometric amount of standard sulphide solution (46.77 mM) to a zinc sulphate solution (7.6 mM Zn^{2+} ions) in a quartz flow cell connected to a UV/VIS spectrophotometer (Shimadzu). The change in absorbance due to the change in turbity as the particles nucleate from clear solution particle appearance was measured over time at 500 nm. Figure B0.1 shows the results obtained.

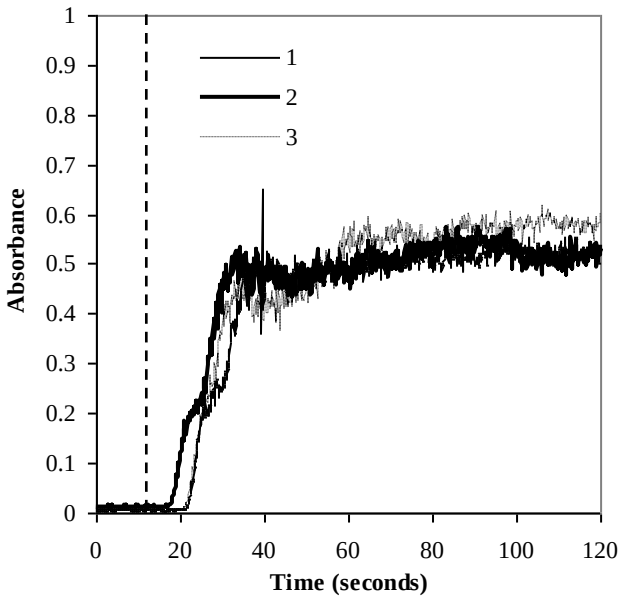

Figure B0.1: Induction time for zinc sulphide formation.

The dotted line in Figure B0.1 indicates the time (i.e. 15 seconds) when the sulphide was added to the zinc solution. It took around 5 seconds before the absorbance was changed due to the change in turbidity as the particles appeared from solution.

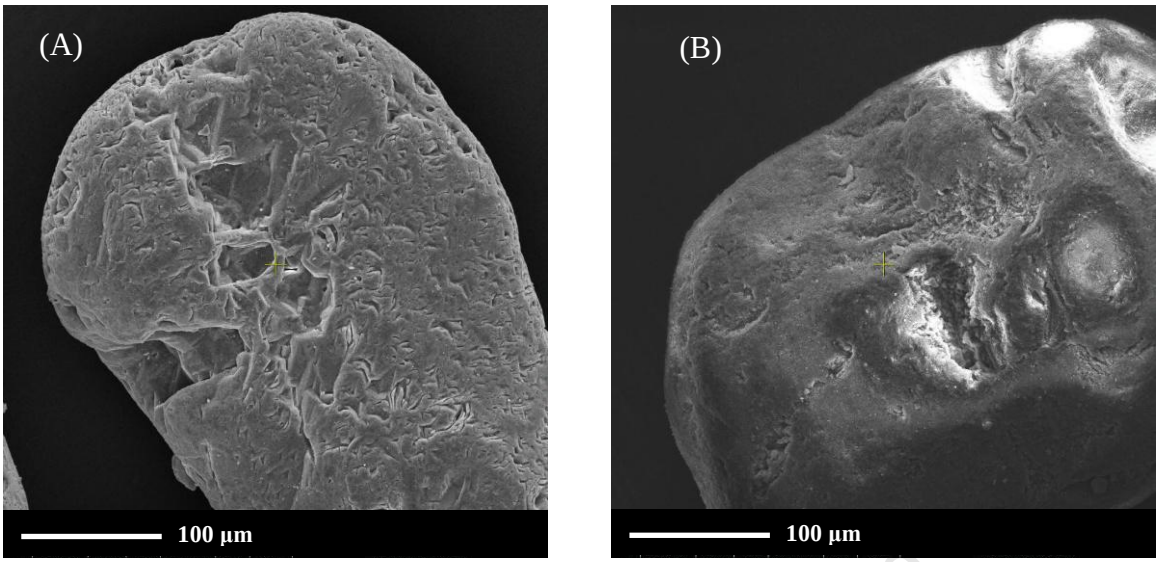

Figure B0.2: SEM micrographs of the seeds from FBR showing poor growth of (A) copper and (B) zinc sulphide onto the seed surfaces.

University of Cape Town

Appendix C

Raw data for particle size distribution measurements and the technique used to convert volume based distribution to number based distribution.

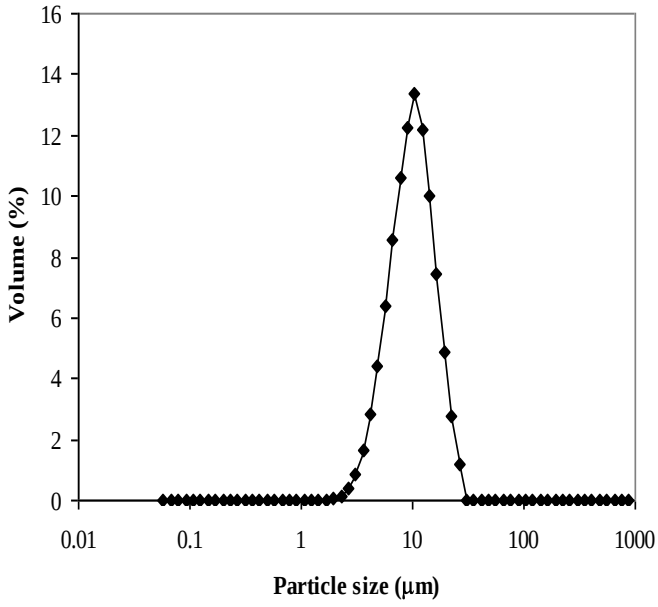

Figure C0.1: An example of a volume based particle size distribution from the Malvern Mastersizer

A technique based on the moment transformation of the number or population density function, n(L), described by Randolph and Larson (1988) was used to derive and describe PSD related information. In this technique, the distribution of discrete particles is simplified by the statistical density function called the number or population density. This function represent the number of particles in a given size range and it is described by.

$$n(L) = \frac{dN}{dL} \qquad \text{C0.1}$$

From a volume based histogram (*vol%* versus L_i), the density function is calculated according to,

$$n(L)dL = \sum_i \frac{vol\%_i \times conc(vol\%)}{100} \cdot \frac{1}{k_v \bar{L}^3} \qquad \text{C0.2}$$

where *i* indicates the size sub-range and the particle concentration is represented by *conc(vol%)*. A volume shape factor (k_v) equal to $\pi/6$ is used to take into account the sphericity of the particles.

The *j*th moment of the number density function with respect to its internal coordinate, *L*, is defined according to Equation C0.3

$$m_j = \int_0^\infty L^j n(L)dL \qquad j = 0, 1, 2, 3\ldots \qquad \text{C0.3}$$

From integration of Equation C0.3, the zeroth moment (*m0*), first moment (*m1*), second moment (*m2*) and third moment (*m3*) are obtained. The zeroth moment is equal to the total number of particles, and the first, second and third moments are proportional, respectively, to the total length, surface area and volume of the particulate matter (Randolph and Larson, 1988). This technique has been successfully used by Bramley et al (1996), Ntuli and Lewis (2007) and Hove et al (2008).

The number based mean size of the particles was determined from the zeroth and the first moment according to Equation C0.4

$$\bar{L}_{1.0} = \frac{m1}{m0} \qquad \text{C0.4}$$

University of Cape Town

Appendix D

Raw data for an investigation into the effect of processing conditions on particle characteristics presented in Chapter 5 showing attainment of steady state.

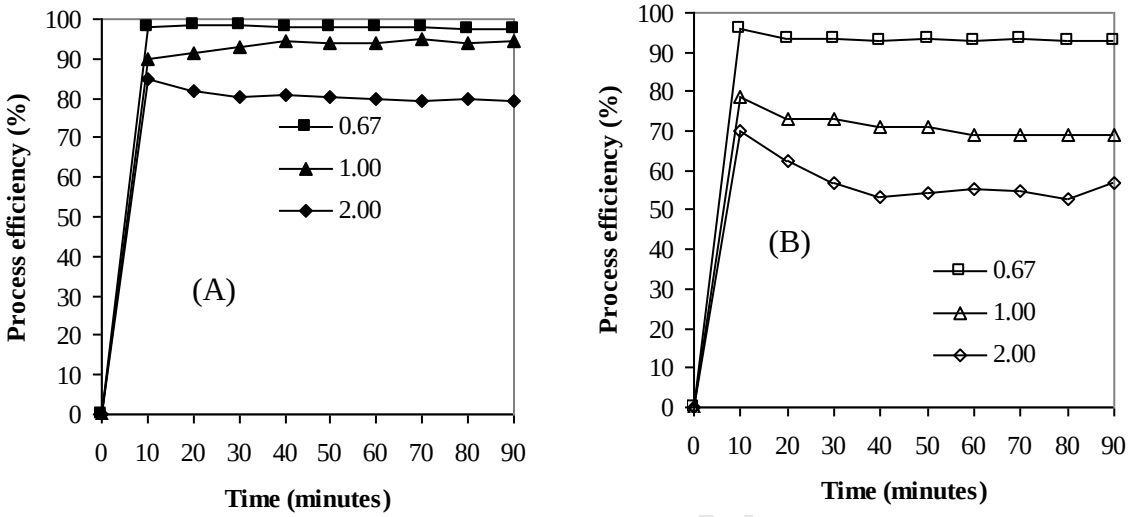

Figure D0.1: Change in process efficiency as a function of time for (A) copper and (B) zinc precipitates produced using different metal to sulphide molar ratios at pH 6.

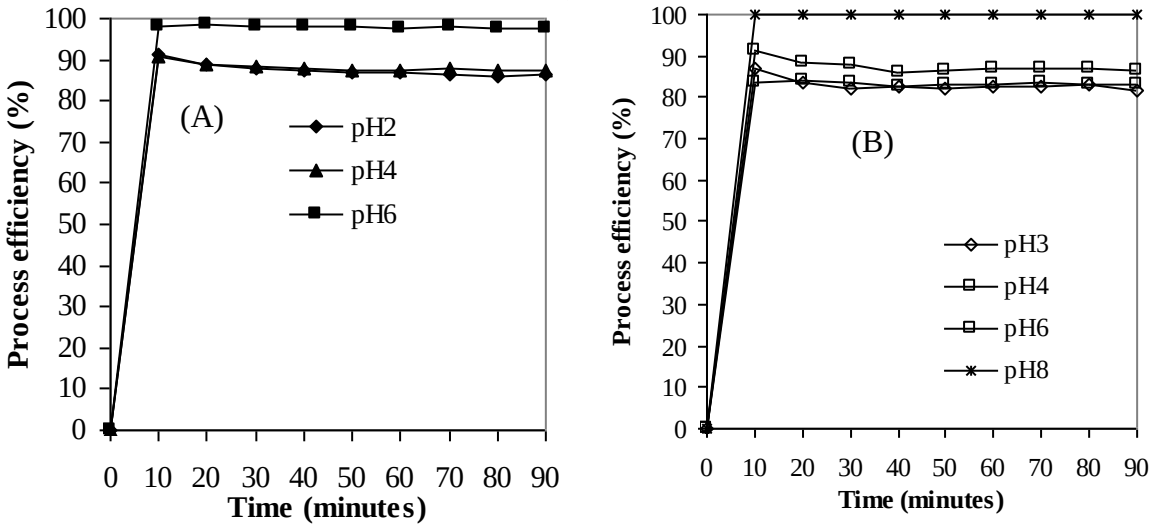

Figure D0.2: Change in process efficiency as a function of time for (A) copper and (B) zinc precipitates produced using metal to sulphide molar ratio of 0.67 under different operating pH conditions.

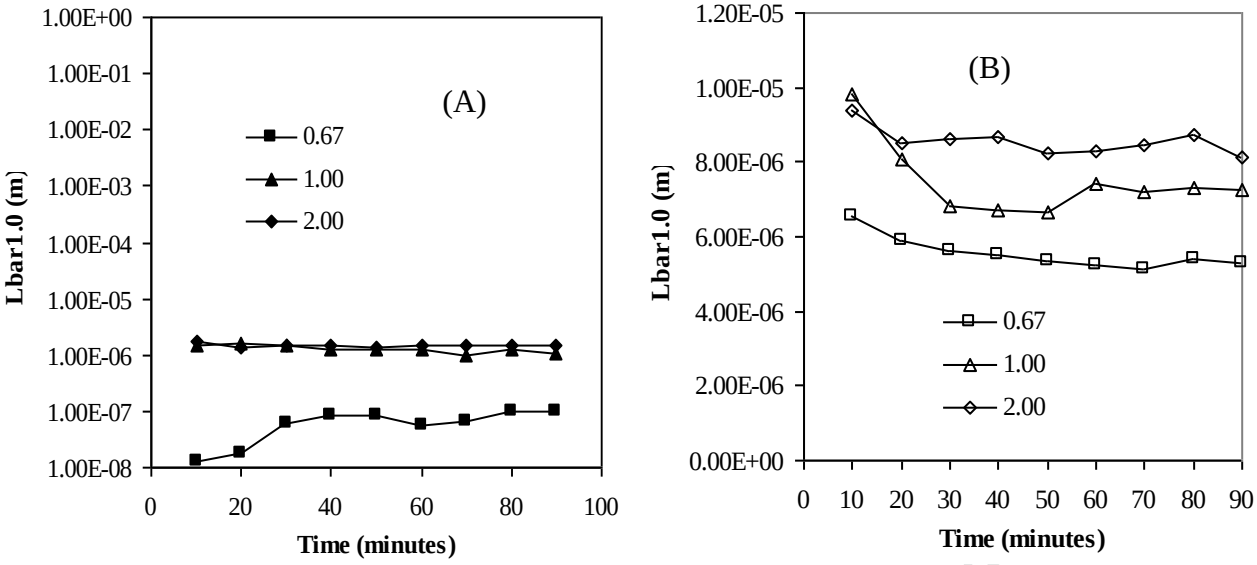

Figure D0.3:Change in number based mean size ($\overline{L_{1.0}}$) as a function of time for (A) copper and (B) zinc precipitates produced using different metal to sulphide molar ratios at pH 6.

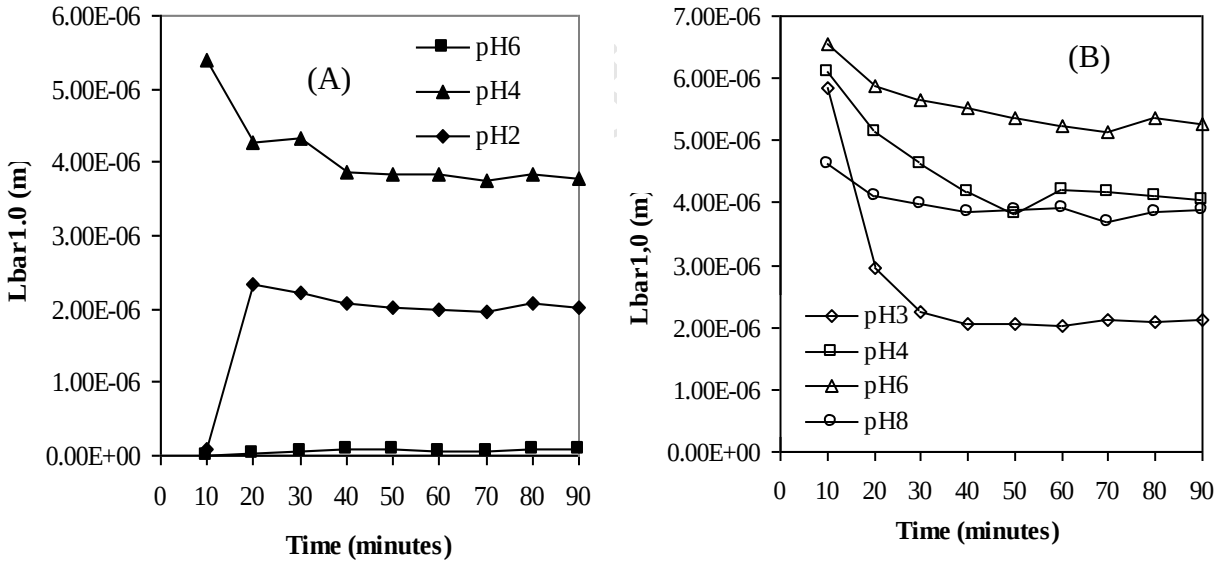

Figure D0.4: Change in number based mean size($\overline{L_{1.0}}$) as a function of time for (A) copper and (B) zinc precipitates produced using metal to sulphide molar ratio of 0.67 under different operating pH conditions.

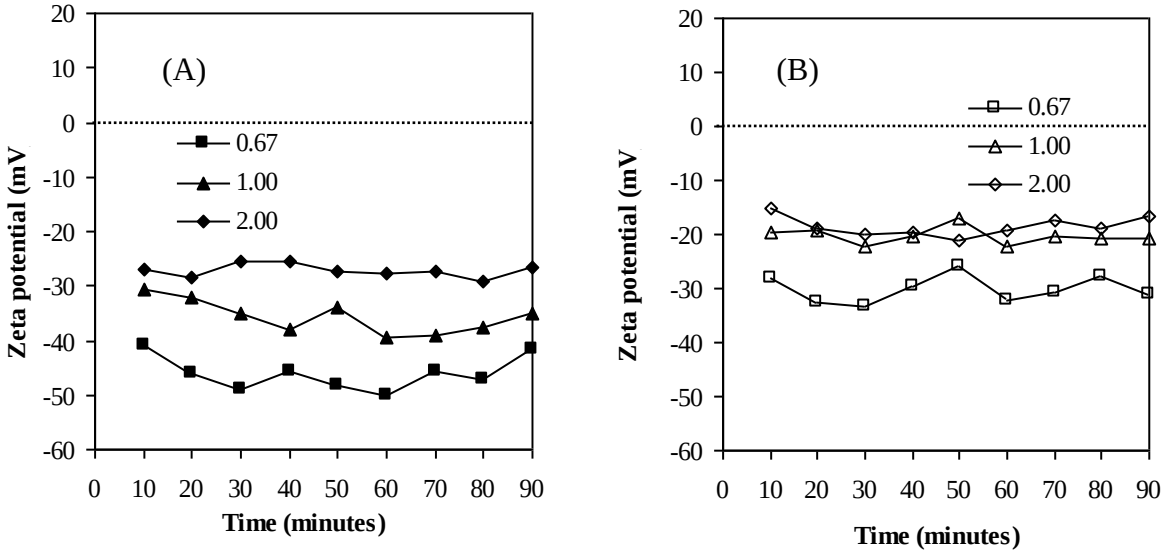

Figure D0.5: Change in zeta potential as a function of time for (A) copper and (B) zinc precipitates produced using different metal to sulphide molar ratios at pH 6.

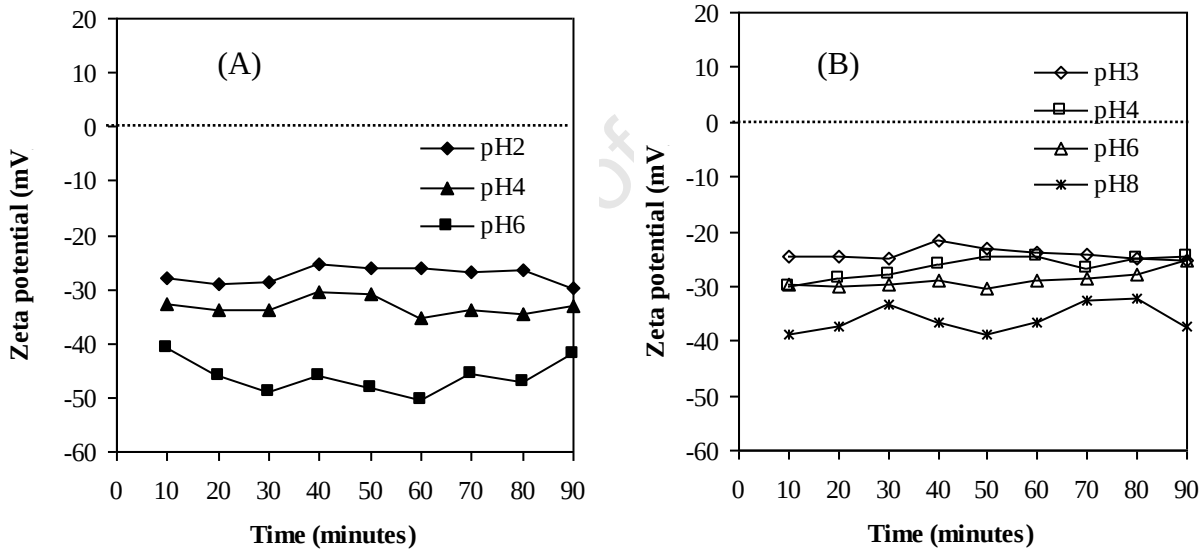

Figure D0.6: Change in zeta potential as a function of time for (A) copper and (B) zinc precipitates produced using metal to sulphide molar ratio of 0.67 under different operating pH conditions.

Table D0.1: An example of raw data for zeta potential measurements

Time (minutes)	ZP1 (mV)	ZP2 (mV)	ZP3 (mV)	ZP4 (mV)	ZP5 (mV)	Average (mV)	Standard deviation
10	-39.30	-42.00	-40.80	-40.90	-41.10	-40.82	1.11
20	-44.70	-45.50	-46.90	-47.00	-51.50	-47.12	1.12
30	-46.50	-50.60	-49.70	-49.60	-41.00	-47.48	1.79
40	-41.90	-44.50	-47.10	-49.90	-44.70	-45.62	3.43
50	-46.00	-49.50	-48.60	-48.30	-41.10	-46.70	1.49
60	-53.20	-50.80	-47.40	-49.60	-49.10	-50.02	2.42
70	-45.90	-45.80	-45.50	-45.50	-51.50	-46.84	0.21
80	-45.60	-47.60	-47.60	-47.40	-46.70	-46.98	0.97
90	-42.40	-40.40	-41.30	-43.10	-42.10	-41.86	1.19

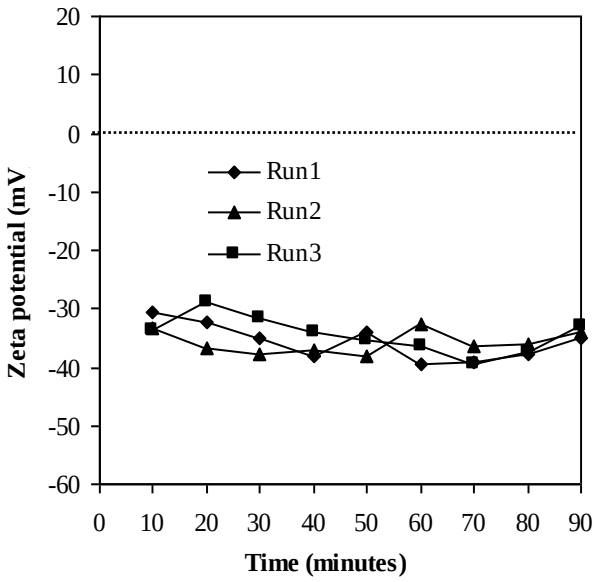

Figure D0.7: Reproducibility of the zeta potential measurements.

Appendix E

Raw data for an investigation in to the effect of operational parameter on surface properties of colloidal metal sulphide precipitates presented in Chapter 6

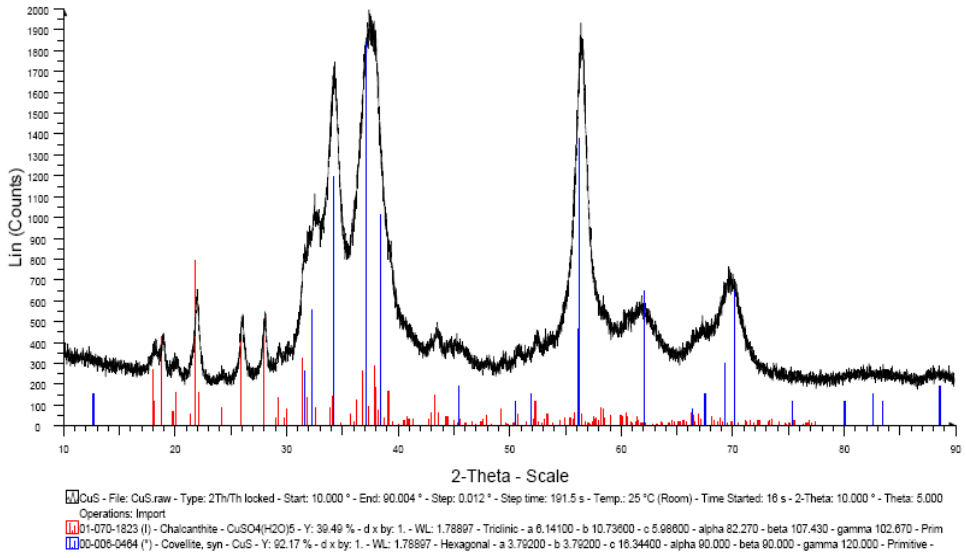

Figure E0.1: X-ray powder diffraction of the precipitate produced by copper sulphide precipitation at pH 4.5 showing the pattern for covellite and copper hydroxysulphate (chalcanthite).

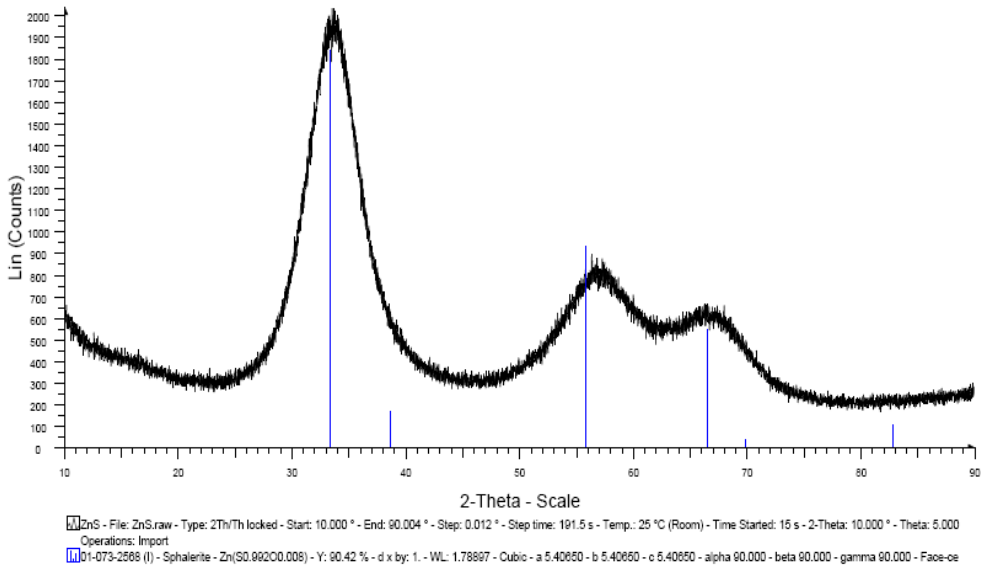

Figure E0.2: X-ray powder diffraction of the precipitate produced by zinc sulphide precipitation at pH 6.0 showing the pattern for sphalerite.

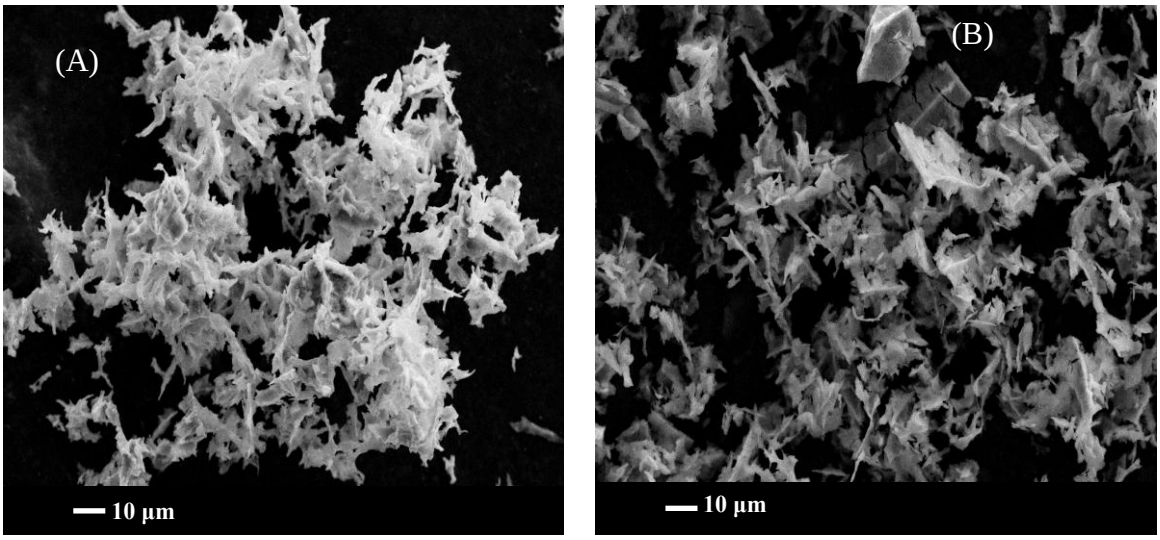

Figure E0.3: SEM micrograph of the precipitate produced from (A) copper and (B) zinc sulphide precipitation reactions

University of Cape Town

Appendix F

Method used for acid digestion:

A 10 mL mixture of 30% HCl and 40% HF in a 4:1 ratio was added to a 10 mL sample in a 250 mL flask. The flask was heated to boiling and 10 mL of 60% HNO_3 acid was subsequently added. After allowing the contents of the flask to boil until the volume was approximately 2 mL, a 5 mL of concentrated $HClO_4$ was added and the mixture boiled until the volume was again 2 mL. The contents of the flask were the quantitatively transferred to a 100 mL volumetric flask and the volume made up to 100 mL with Millipore water before filtering into a sample bottle using Whatman No.1 filter paper. The concentration of the metal ions in the filtrate was then measured using atomic absorption spectroscopy.

Calculation for alkalinity:

Total alkalinity as mg L^{-1} CaCO3 equivalents was calculated according to Equation F0.1:

$$C = \frac{A \times N \times 50000}{Samplevolume(mL)} \qquad \text{F0.1}$$

Where *A* is the volume of standard acid used (mL) and *N* is the normality of standard acid. Commercially available (Merck) 0.1 N H_2SO_4 was used as the reagent.

Total alkalinity as mg L^{-1} NaHCO3 equivalents was calculated according to:

$$D = C \times \frac{84}{50} \qquad \text{F0.2}$$

Molar concentration of bicarbonate = molar concentration *D* – molar concentration of sulphide estimated from analysis

University of Cape Town

Appendix G

Table G0.1: Characteristics of the seed material used in the fluidised bed reactor

Type	Silica sand grains(SiO_2)
Average particle size ($d50$)	250 μm
Bulk density (ρ_b)	1674 kg m^{-3}
Absolute density(ρ_a)	2650 kg m^{-3}
Porosity (ε)	0.375
Specific surface area (A_s)	0.2547 m^2 g^{-1}

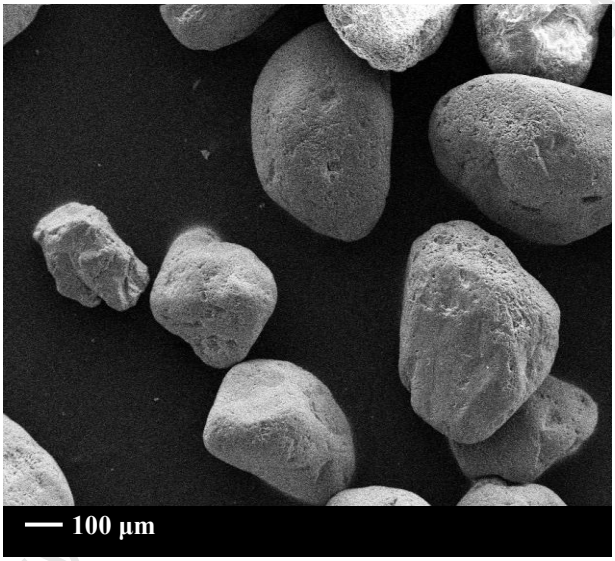

Figure G0.1: SEM micrograph of the seed material used in the fluidised bed reactor experiments

Appendix H

Fluidisation calculation

The fluidisation characteristics of the fluidised bed reactor were calculated using the Carman-Kozeny equation as given in Equation H0.1 (Richardson et al, 2002)

$$u_{mf} = 0.0055\left(\frac{e_{mf}^{\ 3}}{1-e_{mf}}\right)\frac{d^2(\rho_s-\rho)g}{\mu} \qquad \text{H0.1}$$

where u_{mf} is the minimum fluidisation velocity (m s^{-1}), e_{mf} is the voidage at minimum fluidisation, g is the acceleration due to gravity (m s^{-2}), ρ_s and ρ are the density of the particles and liquid respectively (kg m^{-3}), μ is the fluid viscosity (kg m^{-1} s^{-1}).

The pressure drop across the bed was calculated using Erqun equation as shown in Equation H0.2.

$$(1-e_{mf})(\rho_s-\rho) = 150\left(\frac{(1-e_{mf})^2}{e_{mf}^{\ 3}}\right)\left(\frac{\mu u_{mf}}{d^2}\right)+1.75\left(\frac{1-e_{mf}}{e_{mf}^{\ 3}}\right)\left(\frac{\rho u_{mf}^{\ 2}}{d}\right) \qquad \text{H0.2}$$

where d is diameter of the particles. The voidage of the reactor is calculated from the total volume of the bed and to the total volume of the particles inside the reactor according to Equation H0.3.

$$e_{mf} = \frac{\pi r^2 h - \left(\frac{m_s}{\rho_s}\right)}{\pi r^2 h} \qquad \text{H0.3}$$

where h is the height of the bed and m_s is the mass of the particles inside the reactor.

University of Cape Town

Appendix I

Visual MINTEQ is a thermodynamic chemical equilibrium software for the calculation of metal speciation, solubility equilibria and sorption for aqueous systems. It combines state-of-the-art descriptions of sorption and complexation reactions with easy-to-use menus and options for importing and exporting data from/to Excel.

An example showing Visual MinteQ outputs for copper sulphide precipitation in seeded fluidised bed. Predictions for metal to sulphide molar ratio of 1:1 and bircarbonate to sulphide ratio of 4:1

Table I0.1**:** Input parameters

Component	**mM**
Cu^{2+}	2.36
SO_4^{2-}	2.36
Na^{+}	14.16
H^{+}	9.44
CO_3^{2-}	9.44
S^{2-}	2.36

Table I0.2: Saturation indices pre-covellite precipitation

Mineral	**log IAP**	**Sat. index**	**Stoichiometry**							
Azurite	-10.67	6.73	3	Cu+2	2	H2O	-2	H+1	2	CO3-2
Brochantite	20.94	5.718	4	Cu+2	6	H2O	-6	H+1	1	SO4-2
Chalcanthite	-6.88	-4.24	1	Cu+2	1	SO4-2	5	H2O		
Covellite	-1.642	20.578	1	Cu+2	1	HS-1	-1	H+1		
Cu(OH)2(s)	9.273	-0.017	1	Cu+2	2	H2O	-2	H+1		
CuCO3(s)	-9.972	1.528	1	Cu+2	1	CO3-2				
CuOCuSO4(s)	2.393	-7.91	-2	H+1	2	Cu+2	1	H2O	1	SO4-2
CuSO4(s)	-6.88	-9.82	1	Cu+2	1	SO4-2				
Langite	20.94	3.451	-6	H+1	4	Cu+2	7	H2O	1	SO4-2
Malachite	-0.698	4.771	2	Cu+2	2	H2O	-2	H+1	1	CO3-2
Mirabilite	-6.691	-5.577	2	Na+1	1	SO4-2	10	H2O		
Natron	-9.783	-8.472	2	Na+1	1	CO3-2	10	H2O		
Tenorite(am)	9.273	0.783	1	Cu+2	1	H2O	-2	H+1		
Tenorite(c)	9.273	1.633	1	Cu+2	-2	H+1	1	H2O		
Thenardite	-6.691	-7.013	2	Na+1	1	SO4-2				
Thermonatrite	-9.783	-10.42	2	Na+1	1	CO3-2	1	H2O		

University of Cape Town

Table I0.3**:** Species distribution pre-precipitation

	Concentration	Activity	Log activity
CO3-2	1.8044E-06	1.0829E-06	-5.965
Cu(CO3)2-2	3.0531E-06	1.8323E-06	-5.737
Cu(OH)2 (aq)	1.1006E-07	1.1048E-07	-6.957
Cu(OH)3-	2.1303E-11	1.875E-11	-10.727
Cu(OH)4-2	1.1078E-17	6.6486E-18	-17.177
Cu+2	0.00016427	9.8587E-05	-4.006
Cu2(OH)2+2	9.8816E-06	5.9306E-06	-5.227
Cu2OH+3	2.6077E-08	8.2674E-09	-8.083
Cu2S3-2	0.00071228	0.00042748	-3.369
Cu3(OH)4+2	9.4211E-07	5.6542E-07	-6.248
CuCO3 (aq)	0.00062629	0.00062866	-3.202
CuHCO3+	0.000037421	3.2937E-05	-4.482
CuHSO4+	7.5075E-12	6.6079E-12	-11.18
CuOH+	0.000015559	1.3695E-05	-4.863
CuS(aq)	0.000036025	3.6162E-05	-4.442
CuSO4 (aq)	0.000030071	3.0185E-05	-4.52
H+1	2.6044E-07	2.2923E-07	-6.64
H2CO3* (aq)	0.0027196	0.0027298	-2.564
H2S (aq)	0.00012686	0.00012734	-3.895
HCO3-	0.0060159	0.005295	-2.276
HS-1	0.000060274	5.3052E-05	-4.275
HSO4-	3.4015E-08	2.9939E-08	-7.524
Na+1	0.014024	0.012344	-1.909
NaCO3-	2.8279E-07	2.4891E-07	-6.604
NaHCO3 (aq)	0.000032634	3.2757E-05	-4.485
NaOH (aq)	6.8004E-10	6.826E-10	-9.166
NaSO4-	0.000103	9.0659E-05	-4.043
OH-	4.9907E-08	4.3927E-08	-7.357
S-2	1.5352E-15	9.2135E-16	-15.036
SO4-2	0.0022269	0.0013365	-2.874

University of Cape Town

Table I0.4: Specie distribution post-precipitation

	Concentration	**Activity**	**Log activity**
CO3-2	2.8165E-06	1.7195E-06	-5.765
Cu(CO3)2-2	1.1689E-16	7.1362E-17	-16.147
Cu(OH)2 (aq)	3.1044E-18	3.1152E-18	-17.507
Cu(OH)3-	8.081E-22	7.1431E-22	-21.146
Cu(OH)4-2	5.6054E-28	3.4221E-28	-27.466
Cu+2	2.4945E-15	1.5229E-15	-14.817
Cu2(OH)2+2	4.2313E-27	2.5832E-27	-26.588
Cu2OH+3	8.0901E-30	2.6654E-30	-29.574
Cu2S3-2	8.349E-55	5.0971E-55	-54.293
Cu3(OH)4+2	1.1375E-38	6.9446E-39	-38.158
CuCO3 (aq)	1.5366E-14	1.542E-14	-13.812
CuHCO3+	6.76E-16	5.9755E-16	-15.224
CuHSO4+	8.7942E-23	7.7735E-23	-22.109
CuOH+	3.2334E-16	2.8581E-16	-15.544
CuS(aq)	9.5168E-26	9.5499E-26	-25.02
CuSO4 (aq)	4.7842E-16	4.8008E-16	-15.319
H+1	1.9181E-07	1.6955E-07	-6.771
H2CO3* (aq)	0.0023631	0.0023713	-2.625
H2S (aq)	1.1869E-14	1.191E-14	-13.924
HCO3-	0.0070351	0.0062186	-2.206
HS-1	7.5893E-15	6.7085E-15	-14.173
HSO4-	2.5794E-08	2.28E-08	-7.642
Na+1	0.014015	0.012388	-1.907
NaCO3-	4.4874E-07	3.9666E-07	-6.402
NaHCO3 (aq)	0.000038477	3.8611E-05	-4.413
NaOH (aq)	9.2239E-10	9.256E-10	-9.034
NaSO4-	0.00010598	9.3683E-05	-4.028
OH-	6.714E-08	5.9348E-08	-7.227
S-2	2.5801E-25	1.5752E-25	-24.803
SO4-2	0.002254	0.0013761	-2.861

University of Cape Town

Table I0.5: Saturation indices post-precipitation

Mineral	log IAP	Sat. index	Stoichiometry							
Azurite	-42.44	-25.04	3	Cu+2	2	H2O	-2	H+1	2	CO3-2
Brochantite	-21.508	-36.73	4	Cu+2	6	H2O	-6	H+1	1	SO4-2
Chalcanthite	-17.68	-15.04	1	Cu+2	1	SO4-2	5	H2O		
Covellite	-22.22	0	1	Cu+2	1	HS-1	-1	H+1	1	SO4-2
Cu(OH)2(s)	-1.277	-10.567	1	Cu+2	2	H2O	-2	H+1	2	CO3-2
CuCO3(s)	-20.582	-9.082	1	Cu+2	1	CO3-2				
CuOCuSO4(s)	-18.955	-29.258	-2	H+1	2	Cu+2	1	H2O	1	SO4-2
CuSO4(s)	-17.679	-20.618	1	Cu+2	1	SO4-2				
Langite	-21.509	-38.997	-6	H+1	4	Cu+2	7	H2O	1	SO4-2
Malachite	-21.858	-16.389	2	Cu+2	2	H2O	-2	H+1	1	CO3-2
Mirabilite	-6.678	-5.564	2	Na+1	1	SO4-2	10	H2O		
Natron	-9.582	-8.271	2	Na+1	1	CO3-2	10	H2O		
Tenorite(am)	-1.276	-9.766	1	Cu+2	1	H2O	-2	H+1		
Tenorite(c)	-1.276	-8.916	1	Cu+2	-2	H+1	1	H2O		
Thenardite	-6.675	-6.997	2	Na+1	1	SO4-2				
Thermonatrite	-9.579	-10.216	2	Na+1	1	CO3-2	1	H2O		

Table I0.6: Predicted precipitation efficiency

Component	Total dissolved	% dissolved	Total sorbed	% sorbed	Total precipitated	% precipitated
CO3-2	0.00944	100	0	0	0	0
Cu+2	1.9458E-14	0	0	0	0.00236	100
H+1	0.0118	100	0	0	0	0
HS-1	1.9458E-14	0	0	0	0.00236	100
Na+1	0.01416	100	0	0	0	0
SO4-2	0.00236	100	0	0	0	0

University of Cape Town